Not seeing the forest for the points:
Novel LiDAR metrics elucidate forest structure and increase LiDAR usability by managers

By

Heather Anuhea Kramer

A dissertation submitted in partial satisfaction of the requirements for the degree of

Doctor of Philosophy

in

Environmental Science, Policy, and Management

in the

Graduate Division

of the

University of California, Berkeley

Committee in charge:

Professor Scott L. Stephens, Co-Chair
Professor Nina Maggi Kelly, Co-Chair
Professor John D. Radke
Dr. Brandon Collins

Spring 2016

Abstract

Not seeing the forest for the points: Novel LiDAR metrics elucidate forest structure and increase LiDAR usability by managers

By

Heather Anuhea Kramer

Doctor of Philosophy in Environmental Science, Policy, and Management

University of California, Berkeley

Professor Scott Stephens, Co-Chair
Professor Nina Maggi Kelly, Co-Chair

Forest and fire ecology have long utilized remote sensing datasets to learn more about landscapes. Advances in gps spatial accuracy, GIS software capabilities, computing power, and remote sensing technology and software, as well as increases in the spatial and temporal resolution of remote sensing products, have made remote sensing a critical component of forest and fire ecology. Aerial light detection and ranging (LiDAR) is a fast-growing active remote-sensing technology that can be mined for detailed structural information about forests. These data are utilized in the fields of hydrology, forest ecology, silviculture, wildland fire ecology, wildlife ecology, and habitat modeling. LiDAR coverage has also become increasingly common, yet still contains much untapped potential.

Despite widespread research that derived copious valuable metrics from aerial LiDAR, few of these metrics are available to managers due to a significant knowledge and software barrier for LiDAR processing. Even when LiDAR is utilized to derive more complex metrics by scientists and LiDAR experts, metrics are often predictions of plot-based data across the landscape. While these metrics are useful, LiDAR can offer so much more. Because it holds information about forest structure in 3 dimensions, new metrics can be derived that capture the full complexity of forest structure.

I explore ways in which managers can use the plot network and data layers already available to them to derive large tree density, a metric that is critical for habitat modeling for many species, including the California spotted owl. I also explore the utility of LiDAR for estimating ladder fuels that carry fire from the ground into the canopy. Because there was no reliable method for quantifying these fuels, I also developed a plot-based methodology to collect these data. My dissertation work aims to increase LiDAR accessibility to managers and to develop new ways to use LiDAR to solve old problems. While there is much more work to be done, I am excited to share my work with LiDAR experts and forest managers, and hope that my

findings improve the way we use LiDAR, the way we manage forests, and the way that we model and manage for wildland fire.

Table of Contents

Table of figures and tables

Acknowledgements

My dissertation has been quite a process, and I wouldn't have made it through without the support of so many. I'd like to start by thanking my grandparents, who have always encouraged me to follow my dreams and for pursuing interests that trickled down to inspiring my choice of field. I especially thank my parents, Joan Canfield and William Kramer, for their love and continual support and encouragement through my whole life. I'm eternally grateful for the advice, encouragement, inspiration, and snacks from members of the Stephens lab; I couldn't have gotten through without you! I'd also like to thank Soren Berg for keeping me in the game, and Ramiro Cardona for giving me the energy to finish things up, as well as endless support and late-night meals.

I am sincerely grateful to my dissertation committee for their guidance, support, and helpful advice throughout the process. I'd like to especially thank Brandon Collins for continual support and encouragement, from start to finish.

Much thanks to everyone that helped me along the way, including staff on the Plumas National Forest, researchers at the Pacific Southwest Research Station, folks involved with the Western Klamath Restoration Partnership, Deer Creek Resources, and fantastic UC Berkeley undergraduate researchers.

I'd also like to thank all the amazing organizations and events that kept me excited to keep trucking, including the TNC TREX program, Berkeley SAFE, and Hideaway ranch, Mair, Alice, Dianne, Bud, Wizard, Tucker, and Silk.

Thank you all for your support through so many years!

Chapter 1: Introduction

Many areas of forest and fire ecology have begun to utilize LiDAR datasets to determine more about areas at the landscape scale (Bergen et al. 2009). With advances in gps spatial accuracy, GIS software capabilities, and computing power, these data are becoming a critical component of forest and fire ecology (Kelly and Di Tommaso 2015).

Aerial light detection and ranging (LiDAR) is an increasingly important, active remote-sensing technology that uses near infrared light to map the location of object "returns" in three dimensions (Lefsky et al. 2002). As a laser pulse is shot toward the ground from an aircraft, it travels down until it reflects off of an object, be it a tree, shrub, or the ground. The reflected pulse returns to the aircraft, and is recorded by instrumentation. The length of time between pulse emission and detection is used to calculate the distance traveled, using the speed of light. An inertial measurement unit in the airplane tracks the angle at which the pulse was shot, and high-accuracy gps is used in the aircraft to measure its location. All of these measures are used to calculate the positon, in three dimensions, where the reflection occurred. Because hundreds of thousands of pulses are shot every second, combined with multiple returns recorded for each pulse in multi-layered systems such as forests, a cloud of point returns can quickly be collected, often amounting to terabytes of data.

These clouds of points can then be mined for ecological information in forests (Kelly and Di Tommaso 2015), including: 1) ground elevation, from which a digital terrain model can be calculated (Lefsky et al. 2002), 2) canopy surface elevation, from which a model of canopy height can be calculated (Dubayah and Drake 2000), 3) canopy cover (Andersen et al. 2005), and 4) stand structure (Hall et al. 2005; Hudak et al. 2008; Kane et al. 2010). Other metrics can also be calculated with reasonable accuracy, including: 1) tree density (Næsset and Bjerknes 2001), 2) basal area (Hudak et al. 2006), 3) ladder fuels, i.e., canopy base height (Popescu and Zhao 2008) and surface fuels, i.e., surface fuel model (García et al. 2011b; Jakubowski et al. 2013b; Mutlu et al. 2008) used for fire modeling (González-Olabarria et al. 2012; Riaño 2003), 4) fuel bulk density (Erdody and Moskal 2010; Riaño et al. 2004a), 5) biomass (Popescu 2007), 6) carbon yields (Hyyppa et al. 2001), 7) forest productivity (Jensen et al. 2008; Morsdorf et al. 2006; Riaño et al. 2004b), and 8) shrub characteristics (Martinuzzi et al. 2009; Riaño et al. 2007; Wing et al. 2012). Work has also been done to segment the point cloud into individual trees to calculate specific metrics (Jakubowski et al. 2013a; Li et al. 2012; Popescu et al. 2003). With so many uses for these data, including hydrology, forest ecology, silviculture, wildland fire ecology, wildlife ecology, and habitat modeling, it is no surprise that interest in this remote sensing data source has grown significantly in the past two decades. Figure 1 shows the number of scientific publications that contain the words "LiDAR" and "forest" for each year since 1995.

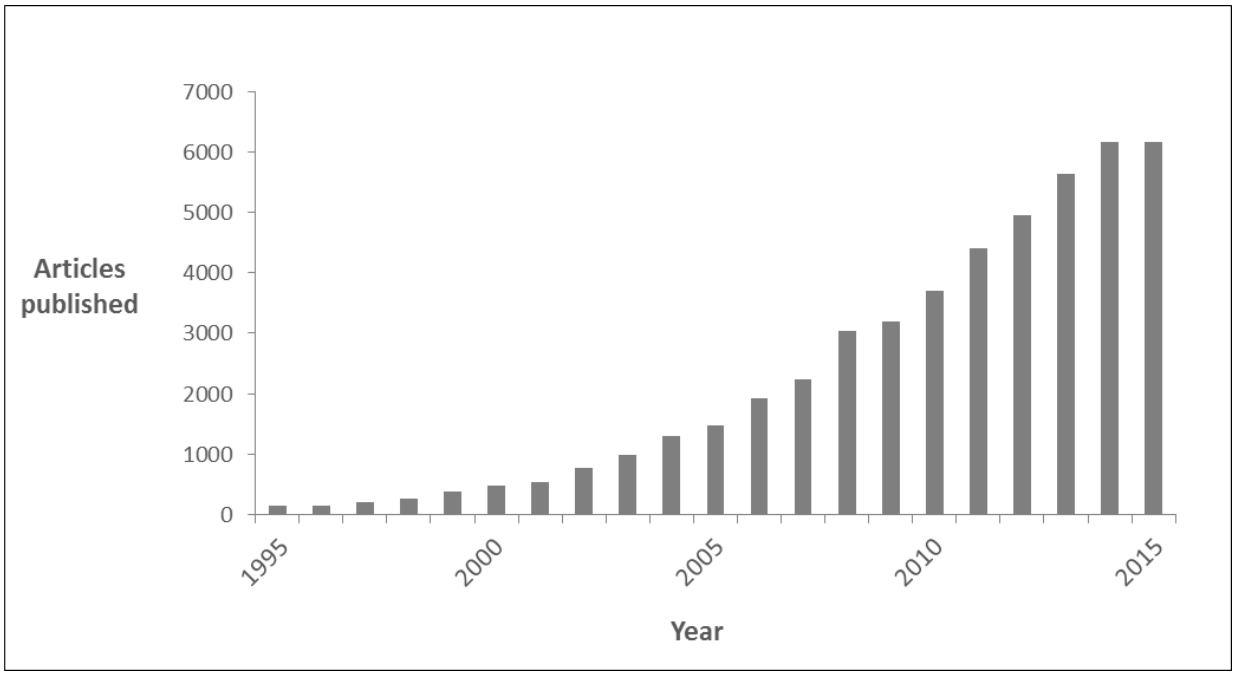

Figure 1. Bar graph showing the number of publications listed on Google Scholar that have "LiDAR" and "forest" in their bodies for each year since 1995.

LiDAR has become increasingly important to forest science in the past two decades. LiDAR coverage has also become increasingly common (Figure 1). For instance, many countries in Europe have flown wall-to-wall LiDAR coverage such as Denmark, Finland, the Netherlands, Slovenia, and Switzerland, and much of these data are made freely available for public download, representing an amazing public resource. In the US, many states now have complete LiDAR coverage, including CT, DE, IN, IA, LA, MN, NC, OH, and PA (Department of Commerce (DOC) et al. 2015).

There are also numerous websites that compile publicly available LiDAR data into an easily searchable online database that streamlines the downloading process (Department of Commerce (DOC) et al. 2015; OpenTopography 2016; U.S. Department of the Interior 2016).

Despite widespread research that derives copious valuable metrics from the aerial LiDAR point cloud, few products can be utilized by forest managers without a source of LiDAR expertise (Keane 2015; Thompkins 2013). Even when LiDAR is utilized to derive more complex metrics by scientists and LiDAR experts, metrics are often predictions of plot-based data across the landscape. While this use is admirable, LiDAR can offer so much more. Because it holds information about forest structure in three dimensions, new metrics can be derived that capture the full complexity of forest structure, which is a daunting task for a field crew to undertake on the ground, and therefore provides an entirely new perspective.

The contribution of my research is to:

1) Make LiDAR more accessible to managers by using creative metrics that do not rely on LiDAR processing beyond that completed by the vendor;
2) Utilize LiDAR to derive new metrics that elucidate forest structure in ways not possible with other forms of remote sensing.

Chapter 2: Accessible LiDAR: estimating large tree density for habitat identification

In my second chapter, I demonstrate a method whereby managers with only rudimentary knowledge of GIS software can derive a model predicting the density of large diameter trees. This is a simple metric to derive for those with LiDAR processing expertise, but has been inaccessible to managers, who do not have access to these tools or the knowledge to use them. Furthermore, areas with high numbers of large trees comprise critical habitat for many rare and endangered species, including the California spotted owl (*Strix occidentalis occidentalis*). I compare two predictive models of large tree density: 1) one derived from a suite of metrics derived from the LiDAR point cloud with proprietary, command-line software, and 2) another derived from only the canopy height model raster that is often delivered alongside the raw LiDAR data. I show that, in the case of my study area in Meadow Valley, CA, these two models are equivalent, suggesting that managers can make use of LiDAR data using only the canopy height model, a common raster deliverable.

There have also been multiple publications discussing the ideal setup for LiDAR ground-validation. While I do not dispute these guidelines, I show that the desired LiDAR-based products dictate the design of plots, and that a one-size-fits-all methodology is a dangerous one. Furthermore, I show that for metrics such as large tree density, managers may be able to utilize pre-established plot networks (strongly advised against by many LiDAR experts) to ground truth older LiDAR if their objectives are appropriate. This includes the acceptability of lower-precision plot centers if plots are large and forest data are not expected to be highly variable. While I do not advocate using less accurate gps technology for measuring new plots, it is important to acknowledge the usefulness historic plots could provide managers, especially to compare against historic LiDAR acquisitions where no new data are available.

Finally, I show that the large tree density calculated from the canopy height model is significantly higher around California spotted owl nest sites than randomly chosen sites. This metric is currently being utilized in the development of a California spotted owl habitat model that will be published within the year.

In my second chapter I explore ways to make LiDAR more accessible to managers, and evaluate methods of using LiDAR and ground-truthing data that are more likely to be available to managers. It is a shame that there is such an amazing source of information, but that few are able to utilize it on the ground for forest management.

Chapter 3: Quantifying Ladder Fuels: A New Approach Using LiDAR

In my third chapter (Kramer et al. 2014), I use LiDAR to explore a misrepresented variable in the world of fire ecology. Ladder fuels that form a bridge to carry fire from the surface of the ground into the forest canopy are critical for modeling wildland fire. However,

the norm has been to use a surrogate of canopy base height, and has been this way for decades. Despite the insensitivities of canopy base height to shrubs, small trees, and tree density, it remains a primary estimator of ladder fuels. Fuel model is also an indication of ladder fuels, but this metric is determined by expert opinion in the field, and has its own levels of inaccuracy. Because fire models use these and other challenging variables, they often employ adjustment factors to change the model prediction to something more reasonable, in the eyes of the modeler. This system is rife with problems, but continues to be the norm, even as new technologies arise.

LiDAR provides an excellent opportunity to explore new ways of measuring ladder fuels more quantitatively, yet few have pursued it. Many, however, have used LiDAR to predict canopy base height and fuel model, but with low success in natural systems. My third chapter explores whether LiDAR is able to differentiate between areas with low and high ladder fuels in Meadow Valley, CA. First I use fuel reduction as a surrogate for sparse ladder fuels and determine the best LiDAR-derived variable for differentiating between treated and untreated areas. Then I test whether this metric, relative 2-4 m cover, is significantly different between plots identified as having low or high levels of ladder fuel. I find that there is a significant difference, but am not able to develop a more quantitative relationship because the only established methodology that directly measures ladder fuels in the field is categorical.

Chapter 4: Estimating ladder fuels: a new approach by land and by air via LiDAR

In my fourth chapter, I develop a new, quantitative methodology for estimating the density of ladder fuels on the ground. This method utilizes multiple photographs per plot, and is useful not only for ladder fuel estimation, but also for monitoring plot change over time and establishing a visual for each plot. I pioneer this method in the Klamath mountains of CA, where there is a wide range of ladder fuel densities across the landscape. I derive a robust predictive model of ladder fuel density across the study area using LiDAR. Using these predictions, I identify areas with uncharacteristically dense patches of ladder fuels. Working with managers in the area, this map will help identify areas where fuel reduction is needed to reduce hazard from wildland fire, especially near communities and along evacuation corridors. It also shows areas near cultural sites that may pose a danger to site integrity due to an increased likelihood of crown fire. These data may also be used to identify areas near large legacy oaks, which are an important cultural resource in this area. Oaks in this area are already suppressed by dense conifers and threatened by Sudden Oak Death that is approaching the area.

Through my chapters, my goals have been to increase LiDAR accessibility to managers and to develop new ways to use LiDAR to solve old problems. While there is much more work to be done, I am excited to share my work with LiDAR experts and forest managers, and hope that my findings improve the way we use LiDAR, the way we manage forests, and the way that we model and manage for wildland fire.

Chapter 2: Accessible LiDAR: estimating large tree density for habitat identification

Abstract

Large trees are important to a wide variety of wildlife, including many species of conservation concern, such as the California spotted owl (*Strix occidentalis occidentalis*). Light detection and ranging (LiDAR) has been successfully utilized to identify the density of large diameter trees, either by segmenting the LiDAR point cloud into individual trees, or by building regression models between sometimes abstract variables extracted from the LiDAR point cloud and field data. Neither of these methods is easily accessible for the majority of land managers, and much available LiDAR data are being underutilized due to the steep learning curve required for advanced processing. This study derives a simple, yet effective method for estimating the density of large-stemmed trees from the LiDAR canopy height model, a standard raster product derived from the LiDAR point cloud that is often delivered with the LiDAR and is easy to process by personnel trained in geographic information systems (GIS). Ground plots needed to be large (1 ha) to build a robust model, but the spatial accuracy of plot center was less crucial to model accuracy. I also show that predicted large tree density is positively linked to California spotted owl nest sites.

1. Introduction

Large trees are critical components of many temperate forest ecosystems (Franklin et al. 2002). Large trees have features that directly provide habitat for wildlife (e.g., broken tops and cavities), in addition to indirectly providing habitat by contributing to greater complexity in forest structure. Both aspects of large trees have been shown to be important for wildlife species of conservation concern. Numerous studies have shown the California spotted owl's (*Strix occidentalis occidentalis*) (CSO) association with large, old-growth trees and structurally-complex stands used for nesting and roosting (Bias and Gutiérrez 1992; Gutiérrez et al. 1992; Keane 2014; Moen and Gutiérrez 1997). CSO populations are declining in the Sierra Nevada and they are currently under review for potential listing under the Endangered Species Act. Thus, information on the distribution and abundance of important large tree habitat elements and structurally-complex forest stands is needed to inform assessment and development of conservation strategies for CSOs, and more broadly, Sierra Nevada forest landscapes. In addition to CSOs, large tree habitat is important for numerous wildlife species including fishers (*Martes pennanti*), northern goshawks (*Accipiter gentilis*), woodpeckers, and others (Beier and Drennan 1997; Greenwald et al. 2005; Hollenbeck et al. 2011; Seavy et al. 2009; Zielinski 2014).

In the past, imagery from passive remote sensors, such as LANDSAT, was widely used to estimate the structure of forests (Forsman 1995; Hunter et al. 1995; McDermid et al. 2005; Moen and Gutiérrez 1997). LiDAR is a form of active remote sensing that is better able to detect the height of vegetation than passive remote sensing, and therefore may be a very useful tool for identifying wildlife habitat (Kelly and Di Tommaso 2015; Lefsky et al. 2002; Martinuzzi et al. 2009; Selvarajan et al. 2009; Vierling et al. 2008). This is particularly true in areas with tall (and likely large diameter) trees (Ackers et al. 2015; Bergen et al. 2009; García-Feced et al. 2011;

Wing et al. 2010). Ackers et al. (2015) found that LiDAR was a better predictor than LANDSAT of Spotted Owl habitat, which depended heavily on large tree density and overall canopy height (Ackers et al. 2015). Methods for estimating large tree density from LiDAR include individual tree segmentation and statistical modeling that utilizes one to many LiDAR-derived independent variables.

Tree segmentation algorithms segment the canopies of individual tree crowns from the LiDAR point cloud (Chen et al. 2006; Jakubowski et al. 2013a; Li et al. 2012; Popescu et al. 2003). This makes it possible to calculate the location of stems and accurately predict the number of large trees in a given area. Tree segmentation has been successfully implemented in some wildlife studies (García-Feced et al. 2011), and while it requires fairly simple LiDAR input, it necessitates complex algorithms to segment the crowns of all trees, calculate each stem's location and maximize crown height, back-calculate the diameter, and then calculate the density. Furthermore, this analysis also requires training data where all stems are mapped, which can be very labor intensive, especially for larger plots (>0.1 ha). Unfortunately, this workflow is not possible for most land managers due to the limited availability of a number of factors, including: 1) LiDAR with high point densities (due to funding limitations or age of LiDAR acquisition), 2) equipment, 3) personnel for fieldwork, 3) training in and access to tree segmentation software, and 4) time to carry out complex processing tasks.

Statistical models using LiDAR can be more abstract, and also accurately predict tree density (Hudak et al. 2006; Jakubowski et al. 2013c; Lee and Lucas 2007). While these models do not require the complex algorithms and high-density LiDAR needed by tree detection algorithms, they often utilize a suite of LiDAR-derived variables. These variables are not standard deliverables from LiDAR acquisitions, and typically require expertise of a LiDAR specialist. Furthermore, once a model is created, it can be hard to understand the ecological underpinnings, and the model must be re-evaluated when moving between different areas or forest types. Simpler models (e.g., fewer variables, less intensive statistics) are uncommon in LiDAR applications for natural resources.

In this study I explore regression-based approaches for accurately quantifying the density of large trees. While tree segmentation would be a more quantitative approach, I intentionally avoided it to investigate less demanding approaches in terms of LiDAR point density, field plots, processing hardware and software, and expertise of processing personnel. My specific research questions were: (1) When estimating large tree density from LiDAR, what is the difference in predictive accuracy between A) a multiple regression model comprised of many LiDAR-derived variables and B) a simple linear regression model derived from the canopy height model (CHM)? (2) Does plot size or plot center accuracy influence the strength of this relationship? and 3) Can the LiDAR-derived large tree density estimates be used to identify important structural habitat characteristics of California spotted owl (CSO) nest sites?

2. Methods

2.1 Study area

The study was conducted in the Meadow Valley area of the Plumas National Forest, which is in the northern Sierra Nevada of California (centered at 39°55′ North, 121°03′ West) (Figure 2). With a Mediterranean climate, most of its 1050 mm per year of precipitation falls during the winter (Ansley and Battles 1998). The 22,510 ha (55,623 ac) landscape is made up of

forest, montane chaparral, and meadows, and falls between 1050 m and 2150 m in elevation (Collins et al. 2013; Kramer et al. 2014). Mixed conifer tree species predominate, including ponderosa pine (*Pinus ponderosa*), Jeffrey pine (*Pinus jeffreyi*), sugar pine (*Pinus lambertiana*), Douglas-fir (*Pseudotsuga menziesii*), white fir (*Abies concolor*), incense-cedar (*Calocedrus decurrens*), and California black oak (*Quercus kelloggii*) (Barbour and Major 1995; Schoenherr 1992). At higher elevations, smaller pockets of red fir (*Abies magnifica*) and western white pine (*Pinus monticola*) can be found. Lower densities of lodgepole pine (*Pinus contorta*), western juniper (*Juniperus occidentalis*), California hazelnut (*Corylus cornuta*), dogwood (*Cornus spp*.), and willow (*Salix spp.*) also occur. Before fire suppression began in the early 1900s, the historic fire regime consisted of primarily low to moderate severity fires burning at 7–19-year intervals (Moody et al. 2006).

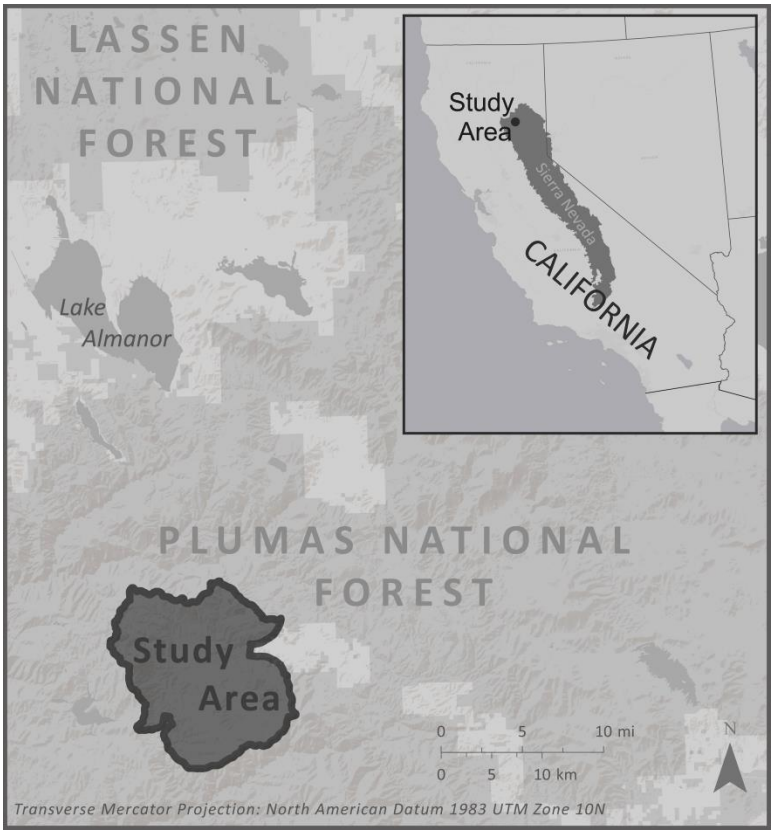

Figure 2. Meadow Valley study area on the Plumas National Forest, CA, measuring 22,510 ha.

Many different fuel reduction treatments were implemented across this landscape between 1999 and 2008 as part of the Herger-Feinstein Quincy Library Group Pilot Project (Herger and Feinstein 1998). The fuel treatments occurred across approximately 20% of the landscape and were intended to mitigate potential for uncharacteristically large and severe wildfire while conserving critical habitat for CSO and other species (Moghaddas et al. 2010). Multiple nesting sites of CSO have also been located and monitored across this study area (Stephens et al. 2014).

2.2 Field Data

The entire Meadow Valley study area was systematically surveyed for CSO nesting sites between 2002-2012 using standardized survey protocols to determine occupancy and reproductive status (Blakesley et al. 2010; Stephens et al. 2014). As part of these protocols efforts were made to locate the specific nest tree used by breeding owl pairs each year. A total of 13 CSO nest tree locations were documented and sampled using the standard FIA protocol described above. Field plots were sampled between 2004 and 2009. Plots were centered on all 13 known CSO nest trees within the study area, and at 132 CSO foraging locations. Foraging locations were estimated from 10 owls using standard radio-telemetry techniques (Kenward 2000; White and Garrott 1990); I conducted vegetation plots at a random subsample from 436 total foraging locations, with each owl sampled equally. In addition, any foraging location within a fuels treatment also received a vegetation plot. Error ellipses for radio-telemetry locations are dependent on distance to the animal, change in angle between bearings, and elapsed time between bearings; I sampled vegetation only at foraging locations in which the error ellipse was less than 1 ha, the size of the largest vegetation subplot (Gallagher 2010). A total of 145 plots were sampled (of which 134 were used for the study due to incomplete coverage by the LiDAR point cloud or inaccuracies between spatial and non-spatial datasets). Plot centers were recorded with a Trimble GeoExplorer3, with a reported accuracy of 2-5 m (actual accuracies for each plot were not recorded).

Standard FIA (Forest Inventory and Analysis) plot layout was implemented to collect plot and subplot data, but only a single subplot of each size was utilized to maintain subplot independence and control for slight inaccuracies in plot center coordinates due to lower accuracy GPS. These plots measured 1 ha (2.47 ac), $1/10^{th}$ ha (0.247 ac), and $1/60^{th}$ ha (0.041 ac), with plot radii of 56.41, 17.95, and 7.31 m (185.1, 58.9, and 24.0 ft), respectively, laid out concentrically around the recorded plot center. The plot and subplot arrangement that I used is illustrated in Figure 3. FIA protocol was used, but slightly modified for the largest, 1 ha plot size, to include the measurement of trees over 76 cm (30 in) in diameter at breast height (DBH), as opposed to the standard 81 cm (32 in) threshold. This change was implemented to reflect the harvesting regulations described in the US Forest Service 2001 Framework and the 2004 Sierra Nevada Forest Plan Amendment (US Forest Service 2001, 2004).

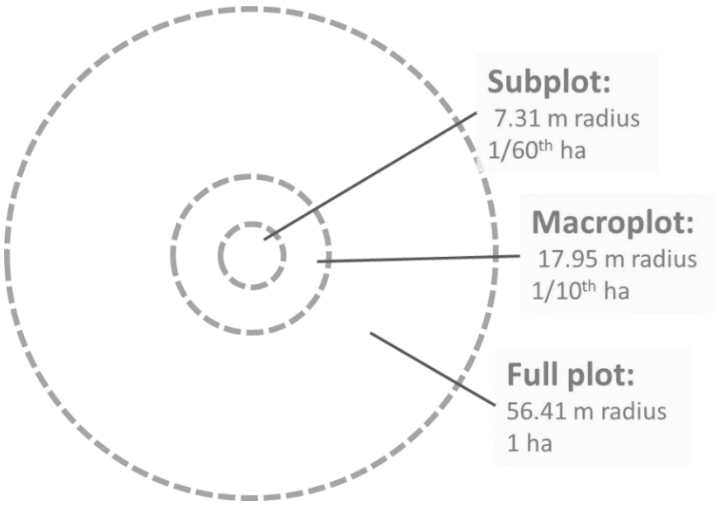

Figure 3. Layout of the 3 concentric plot sizes that were used for this study. Note that all standard FIA plots were collected, but only a single plot of each size was used to minimize spatial autocorrelation between macro- and sub-plots.

2.3 LiDAR Data and Processing

Watershed Sciences, Inc. collected aerial LiDAR over the Plumas and Lassen National Forests between July 31 and August 11, 2009. A Leica ALS50 Phase II laser system was used to collect LiDAR points utilizing a scan angle of ± 14° from nadir. A Leica RCD-105 39 megapixel digital camera was used to capture orthophotos, which were processed with Leica's Calibration Post Processing software v.1.0.4. IPASCO v.1.3 and the Leica Photogrammetry Suite v.9.2 were used to spatially place the photos. The vendor reported that average vertical and horizontal accuracy were 2.6 cm (1.02 in) and 7.2 cm (2.83 in), respectively, based on the mean divergence of points from ground survey point coordinates (3089 ground points were analyzed across four surveyed areas). An average point density of 4.68 points m-2 (0.43 points ft-2) was achieved. Although a variety of fuel reduction treatments were implemented on the landscape between field plot sampling and the LiDAR flight, no fuels were altered in the field plots.

The LiDAR point cloud was normalized and variables were extracted for each 1 ha plot using LasTools (Isenburg 2011). Variables included topography and forest structure (see Table A.1 in the appendix for detailed breakdown). The CHM was generated at 2 m resolution using Fusion(McGaughey 2012). ArcGIS was then used to clip the CHM to each plot area (1 ha, 1/10th ha, 1/60th ha) and analyze these for "% tall cover." The "% tall cover" variable describes the proportion of the plot area with a canopy height over a given breakpoint. Breakpoints tested ranged from 26 to 38 m, at 2 m intervals. Figure 4 shows the detailed work flow and illustrates how I used the LiDAR data to answer my key questions.

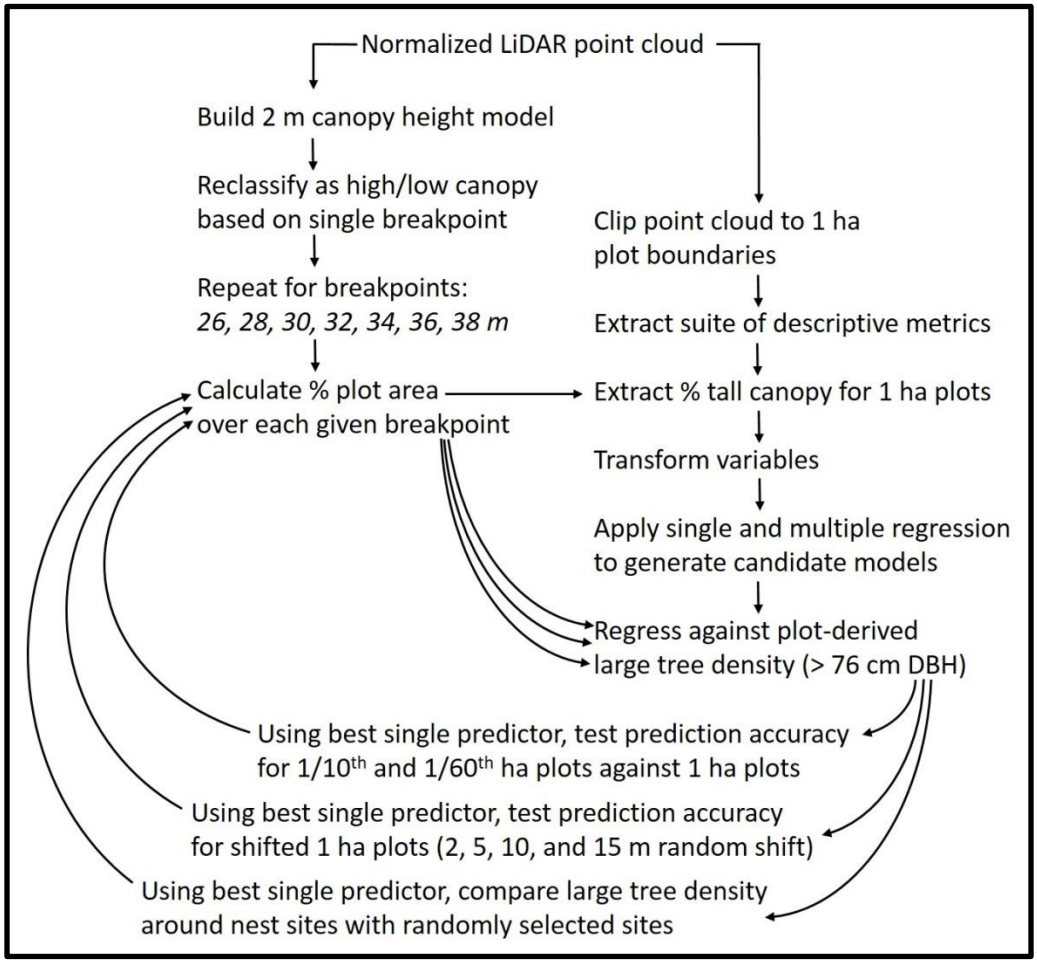

Figure 4. Project work flow used to analyze LiDAR and field data.

2.4 Statistical analysis

I used a combination of methods in the R software program (R Development Core Team 2008) to develop and evaluate linear models that estimated large diameter (> 76 cm (30 in) DBH) tree density from LiDAR, without the use of tree segmentation. I chose the threshold of > 76 cm (30 in) DBH to match the size threshold for trees collected in the largest, 1 ha plot size, as well as for both subplot sizes. This is also the maximum diameter limit guiding most forest management treatments specified in the 2001 Framework and the 2004 Sierra Nevada Forest Plan Amendment (US Forest Service 2001, 2004).

To avoid a non-normal response variable distribution according to the Shapiro-Wilk normality test (Shapiro and Wilk 1965), I transformed the field-based large tree count by taking its square root. I also used Q-Q plots to visually identify non-normal distributions of independent variables and bring their distributions closer to normality through transformation. A complete record of transformations is detailed in Table A.1. Applying these transformations increased the predictive ability of models and

eliminated model heteroscedasticity, tested with the Breusch-Pagan test in the car package of R (Breusch and Pagan 1979; Fox et al. 2009).

Once variables were transformed, I calculated the best simple linear regression model (the model with the highest R-sqared value), as well as the best multiple regression model. Because LiDAR-derived independent variables were highly correlated, an iterative model building approach was taken: 1) The best simple linear regression model was chosen based on the lowest AIC score using the leaps package in R (Lumley and Miller 2009). 2) Variables that were strongly correlated with the chosen independent variable (correlation >0.6 in either Pearson or Spearman correlations) were removed. 3) The process was repeated to find the next best independent variable. The final model was that with the lowest AIC and with all independent variables significant at $p<0.05$. I recorded both AIC values and the 10-fold cross-validation error, calculated with the CVTools package in R (Alfons 2012).

I also derived predictive models for large tree density for the $1/10^{th}$ ha (1,012m^2; 0.247 ac) and $1/60^{th}$ ha (168 m^2, 0.041 ac) plots using the above methodology in order to test whether plot size influences the strength of the relationship. I wanted to evaluate whether the most reliable predictor changed and by how much the correlation coefficient degraded as plot size was reduced, especially since the plot size recommended for aerial LiDAR validation ranges between 300 and 600 m^2 (0.074 and 0.15 ac) (Laes et al. 2011; Ruiz et al. 2014). Because larger plots have proportionally less edge per unit area, and a number of factors at plot edge can influence the relationship between canopy structure and the number of stems within the plot area, I predict that model accuracy will be greatly decreased for smaller plots. Some of these factors are illustrated by Figure 5, where 2 nearly identical plots have very different stem counts due to leaning stems, stems near the plot edge, and trees with uneven crowns.

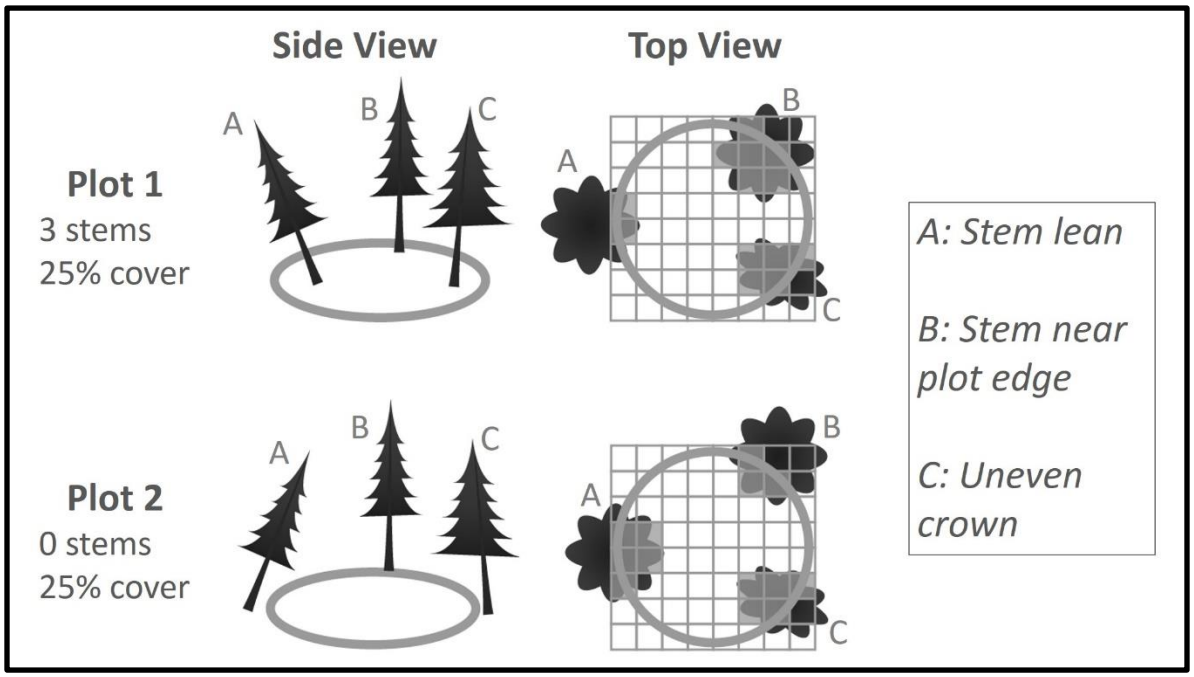

Figure 5. Plots 1 and 2 show 25% cover, but plot 1 contains 3 stems, while plot 2 contains none. Three tree characteristics that can lead to model inaccuracies, if they occur near the plot edge, are: A) stem lean, B) stem near plot boundary, C) uneven crown.

Based on evaluation of model performance at the 1/60th ha, 1/10th ha, and 1 ha plot scales (see Results), I chose the simple linear regression model and the 1 ha plot for further analysis. This model was preferable since it had the highest adjusted R-squared value, uses the CHM (a commonly derived LiDAR product) as its base for prediction, and is simple enough to make logical sense for its predictions.

To address whether plot center accuracy influences the strength of this relationship, I shifted all 1 ha plots in a random direction (illustrated in Figure 6) and recalculated the model coefficients, as well as the correlation coefficient. I repeated this shift and recalculation 100 times, and performed the analysis at shift distances of 2, 5, 10, and 15 m. For each shift distance, I compared the distribution of values for the model coefficients and correlation coefficient. I chose these distances because they are common values for the horizontal accuracy of many mid-range GPS units that are commonly used by a non-LiDAR-specific field crew when recording plot centers.

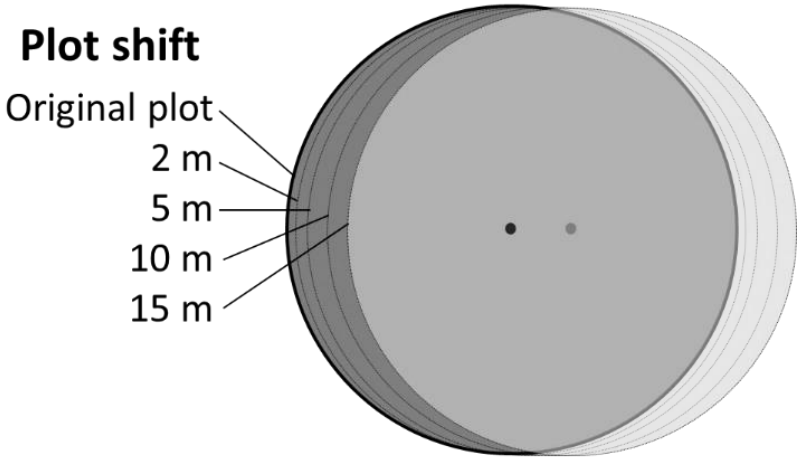

Figure 6. Illustration of plot center shift of 2, 5, 10, and 15 m. The black dot and dark circle represent the original plot center and area, respectively, while the lighter dot and circle represent the location of the 15 m shifted plot. Other shifts are shown as outlines. At 15 m, this shift represents a highly inaccurate GPS point, yet with the 1 ha plot size, over 83% of the original plot is contained by the shifted plot.

Large tree density centered on CSO nest trees was examined at multiple scales to evaluate the potential utility of using this variable to quantify habitat associations. Large tree density across the Meadow Valley study area was estimated and mapped using a single-regression model. Large tree density was extracted from this layer for areas within 50, 100, 500, and 1000 m of nest trees and at 100 randomly chosen points on the landscape for comparison. T-tests were used to compare large tree density between owl and random sites at each spatial scale.

3. Results

3.1 Large diameter tree density

Due to high collinearity between independent variables, combined with these variables quickly becoming insignificant to the model at the $p<0.05$ level, the multiple linear regression only contained two independent variables and was only slightly better able to predict large tree density, as shown in Table 1. Equation 1 shows the best single regression linear model, where the independent variable was the percent of the plot area where the CHM was over 32 m (CHM32). Equation 2 shows the best multiple linear regression model, where the independent variables included CHM32 and the variance of point heights above 2 m (VAR).

*Sqrt(Trees ha-1) = 1.10+0.817*sqrt(CHM32 meters)* **Eqn. 1**

*Sqrt(Trees ha-1) = 2.37+0.786*sqrt(CHM32)-0.909*(log(VAR)+1)* **Eqn. 2**

Variables included in model	AIC	10-fold cross-validation error *	Adjusted R-squared
CHM32	347	0.88	0. 77
CHM32, VAR	344	0.87	0. 77

Table 1. Model statistics are reported for the best single and multiple linear regression models. These include the predictor variables, AIC score, cross-validation error, and adjusted R-squared value for each model. CHM32 refers to the relative percent of plot area where the CHM is over 32 m; VAR refers to variance among point heights. **The cross-validation error is reported for the square root of trees ha-1.*

Both models had very similar AIC and cross-validated prediction error (Table 1). Both models had a cross-validation error below a single tree per ha, which is accurate enough to be highly useful for managers.

3.2 Importance of plot size

Of the three plot sizes evalauted, the 1 ha plot was the best predictor of large tree density, with a model adjusted R-squared of 0.77 (Table 1). Model prediction accuracy decreased as plot size shrank. Even plots 1/10th ha in size (considered large by most managers and field crews) were poor predictors of large tree density, with the best model producing an adjusted R-squared of only 0.54 compared with 0.77 for the 1 ha plot. Even so, large tree density in both the 1 ha and 1/10th ha plots was best predicted by a CHM-derived variable. The best independent variable for each plot size, as well as coefficient of determination for each model for 1/10th and 1/60th ha plots are reported in Table 2. Note that while multiple regression was attempted, no variables beyond the first were significant.

	Plot area	Explanatory variable	Adjusted R-squared	p-value
Subplot	1/60th ha	COV32-34	0.21	< 0.01
Macroplot	1/10th ha	CHM34	0.54	< 0.01

Table 2. Each plot area is shown with its corresponding best linear model, showing the model variables, adjusted R-squared value, and p-value for that model. COV32-34 represents the relative percent cover of all LiDAR returns between 32 and 34 m. CHM34 refers to the relative percent of plot area where the CHM is over 34 m.

To help explain the difference in model accuracy, Table 3 details the average number of large diameter trees, as well as the proportional amount of edge to area, for the three plot sizes. These factors were likely both contributors to the poor predictive power of models built using smaller plot sizes. Table 3 shows that 1/60th and 1/10th ha plots had less than ½ and 2 large trees per plot, respectively, making prediction inherently difficult. Furthermore, the large ratio of plot edge to plot area likely contributed to model inaccuracy as well, with 1/60th ha plots having 8 times as much relative edge than 1 ha plots (Table 3).

Plot area	Average large trees per plot	Radius (m)	Circumference (m)	Area (ha)	Edge:Area
1/60th ha	0.47	7.31	45	0.016	0.273
1/10th ha	1.74	17.95	112	0.101	0.111
1 ha	15.56	56.41	354	0.999	0.035

Table 3. Each plot size is shown with the average number of large (>76 cm (30 in) DBH) trees, as well as the radius, circumference, and area of each plot size and the ratio of edge to area. A lower edge to area ratio indicates less edge effect. Note that the 1/60th ha plot has almost 8 times as much relative edge as the 1 ha plot.

3.3 Importance of plot center accuracy

Plot centers were shifted up to 15 m, but none of these shifts dramatically changed the linear model accuracy or coefficient values. Boxplots displaying the model fit and coefficients are shown in Figure 7. Adjusted R-squared ranged between 0.72 and 0.78 for models built with shifted plot centers (the non-shifted model had an adjusted R-squared value of 0.77). Values for slope and intercept varied between 1.06 and 1.22, and 0.78 and 0.84, respectively (unshifted model values were 1.10 and 0.82, respectively).

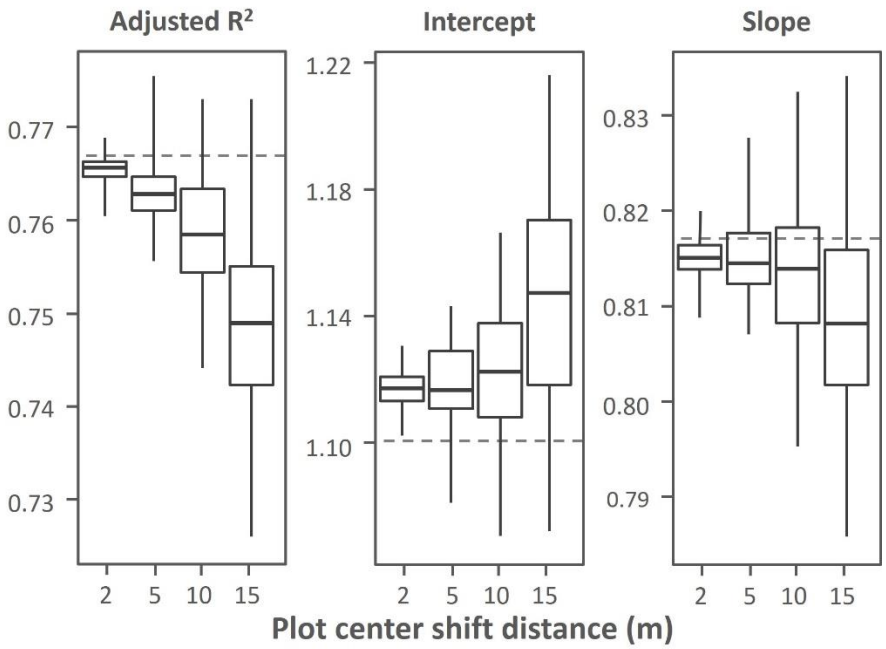

Figure 7. The distribution of model values (R-squared, as well as the slope and intercept of the model), and how these changed on the 1 ha plot size as the coordinates of plot center were shifted 2, 5, 10, and 15 m in a random direction (n=100). Original model values are shown as a grey dashed line.

3.4 Large trees around nest sites

Large diameter tree density was modeled for the entire study area and is shown with thirteen CSO nest sites in Figure 8. Smaller buffers around nest trees had a disproportionately high density of large trees, which dropped off gradually as the search radius from the nest tree increased, illustrated in Figure 9. Within 50 m of nest trees, compared to random locations, large tree densities were significantly different, with 31 versus 12 trees ha-1, respectively. Area near nest sites remained significantly different from random at distances of 50, 100, and 500 m. Only at a buffer distance of 1 km was large tree density no longer significantly different between CSO nest sites and random locations.

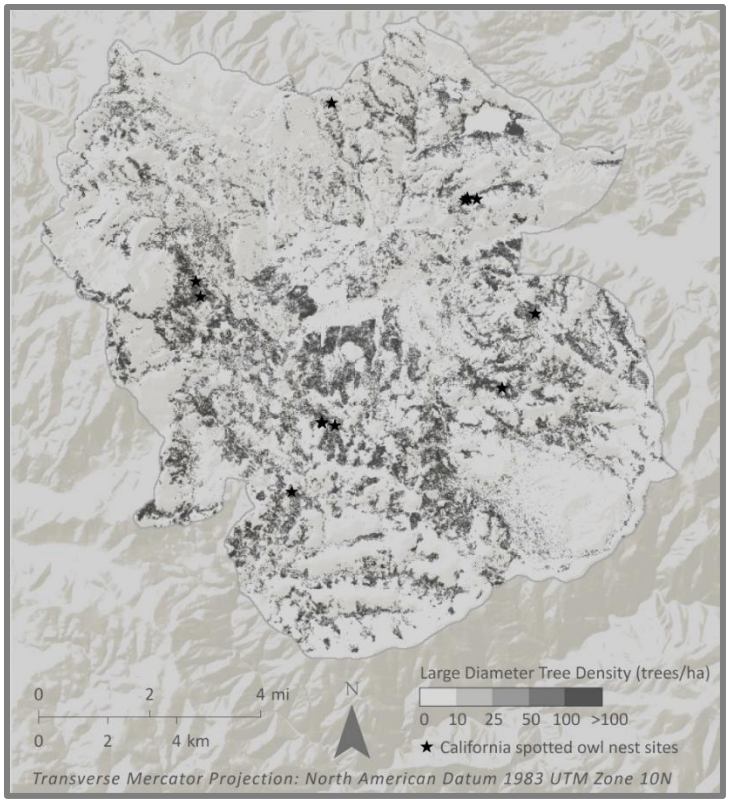

Figure 8. Study area, showing large (over 76 cm (30 in) DBH) tree density and California spotted owl nest sites. Large tree density was derived from the canopy height model via single linear regression.

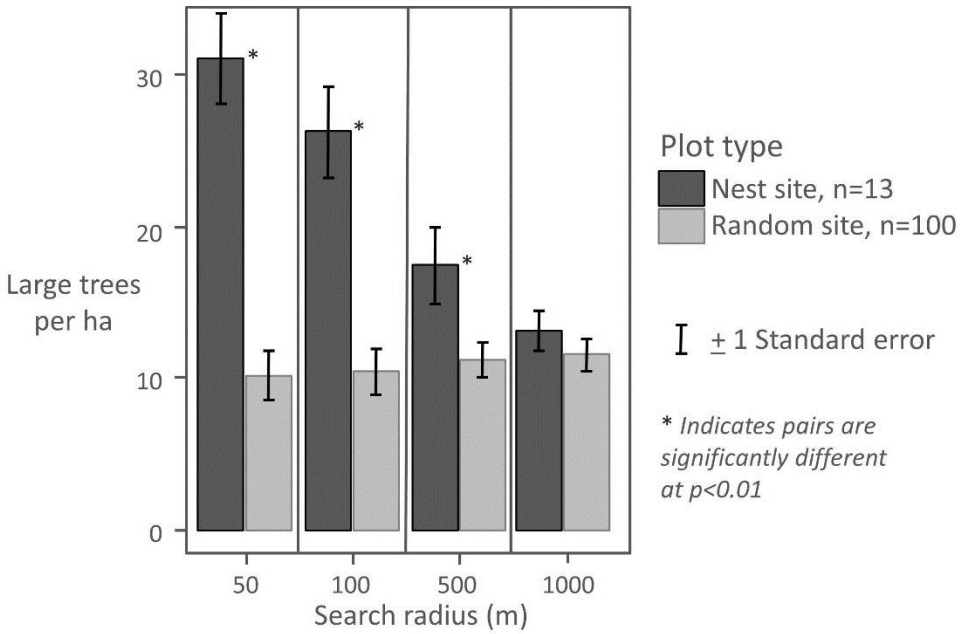

Figure 9. Large (over 76 cm (30 in) DBH) tree density near thirteen California spotted owl nest sites and 100 random sites over a range of search radii is shown. Plots with significantly different distributions (at $p < 0.01$) of large tree density are indicated by "*". Large tree density was derived from the canopy height model via single linear regression.

4. Discussion

Large trees are a critical habitat component for several wildlife species of concern and are presently lacking in many western forests relative to historical forest conditions (Franklin and Johnson 2012). In the case of the CSO, reductions in the number of large trees and structurally-complex older forest stands due to past forest management may be a contributing factor to current CSO population declines. Further, recent studies have documented high rates of large tree mortality due to interacting effects of drought, climate change, wildfire and insect activity (Dolanc et al. 2014; Knapp et al. 2013; Lutz et al. 2009). Thus, estimating large tree distribution and abundance is important for identifying and managing large tree habitat elements and older-forest stands important to CSOs and other associated species. I show that aerial LiDAR can be successfully utilized to estimate the density of large trees. Both multiple and simple linear models accurately predicted the density of trees over 76 cm (30 in) DBH across 1 ha plot areas. However, the strength of this relationship decreased as plot size shrank to $1/10^{th}$ ha and $1/60^{th}$ ha, indicating that the plot size should be at least 1ha when using the CHM to predict the density of large trees. I suspect that much of this difference in model accuracy was due to edge effect, illustrated by Figure 5, and small sample size for smaller plots. Other factors that can decrease the accuracy of this estimate include trees that have non-standard crown:DBH relationships, including individuals with damaged crowns, sheared branches, or broken tops, and species with different ratios of crown area:stem diameter.

I also show that while the accuracy of plot center slightly decreases the model's accuracy with 1 ha plots and marginally changes its coefficients, the model is still strong (adjusted R-squared never dropped below 0.72) with shifts in plot center of up to 15 m. This is likely due to the fact that with such a large plot size, much of the original plot area is included in the sampled LiDAR (83% of the original 1 ha plot is retained when the center is shifted 15 m). This indicates that for variables such as large tree density, which require large plots to accurately measure, a highly accurate (sub-meter) plot center may not be necessary. While most long-term plot networks do not utilize plot sizes as large as 1 ha, this study stands as a reminder that some datasets can still be useful to LiDAR validation, despite having less than ideal accuracy for plot centers.

Recently, many researchers have focused on producing a standardized LiDAR plot protocol (Laes et al. 2011; Ruiz et al. 2014), where recommended plot sizes range between 300 and 600 m^2 and nothing less than a mapping grade GPS is required. While this is an excellent step toward helping managers best prepare for maximizing the utility of new LiDAR acquisitions, it may also lead managers to assume that plots collected

outside of these standards are useless for LiDAR analysis. This study suggests that these protocols might be less rigid for a variable such as large diameter tree density, where much larger plots are necessary to develop a robust predictive model. I suspect that this would also be the case for forest attributes such as basal area and biomass, where accurately quantifying the density of large diameter trees at a broad scale is critical to forming an accurate relationship between LiDAR estimates (based on forest structure) and stem attributes. I advise managers and researchers to critically examine the scale of the variable in which they are interested before deciding on an ideal plot design.

This was an observational study based on one location, albeit a relatively large area, introducing the potential for locational bias in the analysis. Furthermore, because the study area is a single sample of the landscape, results from this study should be carefully applied to other areas, and may require additional ground-truth analysis based on large plots from the new area. Regarding the plots themselves, placement was designed and implemented to sample CSO use areas and may not be representative of the entire landscape. Furthermore, plot center accuracy was not high by current standards (likely below 2 m, but possibly up to 5 m). However, the analysis showed that slight shifts in plot center did not influence results, so model inaccuracy from this source should be minimal.

Because this canopy-height derived variable identifies the area of tall canopy, it assumes a link between canopy area and tree density, as well as a link between stem diameter and tree height. This means that the statistical model likely is unable to capture large trees when a significant portion of the tree tops are broken. However, to the extent that broken-top trees are still emergent in the dominant tree canopy or these large broken-top trees are often found near other large-diameter individuals without broken tops, the model would be expected to predict an accurate large tree density. Because tree species differ in the relationship between canopy height, canopy volume, and stem diameter, this model will need to be evaluated and perhaps re-calibrated based on local knowledge of tree species and crown extents. However, for the purpose of a general prediction, this basic model performed surprisingly well, and is a simple and relatively accurate method for managers and researchers to evaluate large diameter stem density across the landscape in Sierra Nevada mixed conifer forests.

4.1 Future Research

Additional studies to augment this research include carrying out similar analyses in different forest types. I suspect that these results will perform best in forests where the majority of large trees are coniferous, since these are identified by the CHM. Because of the variable quality of LiDAR available to land managers, investigation of the necessary point density to make accurate predictions is also essential.

My work indicates that estimation of large tree density via LiDAR-derived CHM could be a useful method for identifying CSO nesting habitat. I encourage wildlife researchers to investigate the usefulness or improvement of this variable for modeling

wildlife habitat for species associated with large tree habitat elements or forest stands with high densities of large trees, such as the CSO.

My results show that older plots, which may not be ideal for traditional LiDAR-based derivations due to imprecise data or inaccurate plot center coordinates, could still be useful for other variables. I encourage others to explore their plot data and think critically about what can be compared to available LiDAR data.

4.2 Immediate implications for managers

Forest managers are challenged by the need to identify and manage large tree habitat across the Sierra Nevada. Information needs may range from identifying individual large trees that function as an important nesting/den habitat element within an area of generally younger, smaller forest, to identifying forest stands or patches with high densities of large trees across a landscape. I encourage thoughtful implementation of my methods to identify large trees and assess large tree density across landscapes. Such information on distribution and abundance of large trees can be used to identify areas of importance to associated wildlife species, such as the CSO, and to inform forest management options. Further, little to no information exists on large tree densities across the Sierra Nevada, thus estimates of large tree density may be an important variable to incorporate into models of wildlife habitat. However, site productivity, dominant tree species composition, and management history are linked to the specific CHM threshold that is most appropriate, and I caution users to test multiple CHM cutoffs before finalizing their model. In other Sierra mixed conifer forests, I encourage managers with access to a LiDAR-derived CHM and a network of FIA plots that include the 1 ha plot size to derive a similar equation to predict the density of large trees. This would be a relatively simple project for anyone familiar with GIS and statistics, and could result in a highly useful layer for managers and wildlife ecologists .

5. Conclusions

Based on my method, managers can use the CHM, a common LiDAR deliverable, to accurately estimate large tree density, even when only lower density LiDAR (inappropriate for tree segmentation) is available. This can be accomplished without any specific LiDAR processing hardware, software, or expertise, and does not require any LiDAR-specific plot protocol. This method demonstrates an excellent method for managers to put their LiDAR to practical use, although there are a few caveats.

I also show that older data traditionally labeled as “unusable” for LiDAR comparison, due to inaccurate plot center GPS coordinates, can provide valuable information for certain LiDAR-derived variables. For plots such as these to be successfully compared to LiDAR data, either 1) plots must be large enough to minimize GPS inaccuracy or 2) the variable must vary at a larger spatial scale than the potential inaccuracy of plot center.

Estimates of large tree density across the Sierra Nevada are lacking. Such information is needed to inform development of conservation and restoration strategies

for CSOs and Sierra Nevada landscapes. My methods provide an approach for generating this information in areas where LiDAR data are available.

Acknowledgements

Thanks to my co-authors Brandon Collins, Claire Gallagher, John Keane, Scott Stephens, and Maggi Kelly. I thank the Plumas National Forest for allowing us to use their LiDAR dataset. Thanks also to Robert McGaughey for assisting us with the LiDAR-processing program, FUSION. Much thanks to Martin Isenburg and LAStools, as well as the LASmoons grant, for use of the software program, LAStools. Marek Jakubowski contributed valuable advice on LiDAR processing methodology. Joan Canfield contributed comments that improved this paper. This material is based upon work supported by the Pacific Southwest Research Station, USDA Forest Service, and the National Science Foundation Graduate Research Fellowship Program under Grant No. DGE 1106400.

Chapter 3: Quantifying ladder fuels: A new approach using LiDAR

Abstract

I investigated the relationship between LiDAR and ladder fuels in the northern Sierra Nevada, California USA. Ladder fuels are often targeted in hazardous fuel reduction treatments due to their role in propagating fire from the forest floor to tree crowns. Despite their importance, ladder fuels are difficult to quantify. One common approach is to calculate canopy base height, but this has many potential sources of error. LiDAR is a candidate to better characterize ladder fuels, but has only been used to address this question peripherally and in only a few instances. After establishing that landscape fuel treatments reduced canopy and ladder fuels at the site, I tested which LiDAR-derived metrics best differentiated treated from untreated areas. The percent cover between 2 and 4 m had the most explanatory power to distinguish treated from untreated pixels across a range of spatial scales. When compared to independent plot-based measures of ladder fuel classes, this metric differentiated between high and low levels of ladder fuels. These findings point to several immediate applications for land managers and suggest numerous new avenues of study that could lead to possible improvements in the way that I model wildfire behavior across forested landscapes in the US.

1. Introduction

Past land management practices, including wildfire suppression, extensive timber harvesting, and grazing have left many dry western US forests prone to greater extents of high severity fire than occurred historically (Hessburg et al. 2005). In addition to being ecologically detrimental, the contemporary patterns of high severity fire put lives, property, and natural resources in danger (Husari et al. 2006a). Fuel reduction treatments are often used to mitigate fire hazards in strategic areas to help decrease the risk of harming these assets (Agee and Skinner 2005). These treatments have been shown to be effective in ameliorating fire behavior and reducing tree mortality through both modeled simulations (Johnson et al. 2011; Stephens et al. 2009) and when encountered by real wildfires (Agee and Skinner 2005; Ecological Restoration Institute 2013; Finney et al. 2005; Moghaddas and Craggs 2007; Pollet and Omi 2002; Raymond and Peterson 2005; Safford et al. 2009; Safford et al. 2012; Strom and Fulé 2007). Recent studies suggest the duration for reduction in potential fire behavior and effects, or treatment longevity, can exist for up to 8-15 years in the Sierra Nevada (Chiono et al. 2012; Stephens et al. 2012). Some have argued that fuel reduction treatments are the most cost-effective solution in the face of our current fire suppression expenditures because treating the forest will keep fire in check more economically than suppression alone (Snider et al. 2006).

Fuel reduction treatments in the Sierra Nevada have multiple effects on fuel structure, reducing surface fuels, ladder fuels, and canopy continuity while maintaining large, fire-resistant trees (Agee and Skinner 2005; Stephens et al. 2009). Treatments utilize different methods to accomplish these changes: prescribed burning, hand-thinning (generally targets trees under 30 cm in diameter at breast height (dbh), mastication (targets understory trees and shrubs), mechanical harvesting (thin from below, targeting trees up to 76 cm dbh), and

sometimes a combination of these. Each treatment type addresses a different subset of these effects, but the one common outcome is reduced ladder fuels. The extent of many contemporary fires is forcing land managers to coordinate fuel reduction treatments across landscapes to collectively reduce fire spread and intensity (Collins and Stephens 2010). Knowing the current state of fuels across landscapes is critical for planning this type of fuel treatment network, which requires accurate maps of surface, ladder, and canopy fuels.

Ladder fuels are difficult to measure in the field, and few studies have attempted to develop an explicit, field-based measurement procedure (but see (Menning and Stephens 2007; Prichard et al. 2013; Wright et al. 2007)). Instead, canopy base height (CBH) and a fuel model (sometimes with an adjustment of fire behavior) are used as a surrogate for ladder fuels (Scott and Reinhardt 2001). CBH is defined as the point above which there is a given mass of fuel per unit volume to carry the fire upward. In theory, CBH and the fuel model should account for ladder fuels, but in practice, CBH is poorly defined, hard to measure in the field, and is only complicated by ladder fuels that can be too small in diameter to include in the plot sample, but still contribute to the fire's ability to crown (Hall and Burke 2006; Rebain 2010 (revised December 18, 2012); Scott and Reinhardt 2001). While the general definition of CBH is agreed upon, the threshold of fuel per unit volume is arbitrary; the most agreed-upon value is 0.012 kg m^{-3} (Reinhardt et al. 2006a), but other thresholds have been used (Fernandes 2009; Mitsopoulos and Dimitrakopoulos 2007; Ottmar et al. 1998; Sando and Wick 1972).

CBH is often derived allometrically from plot tree lists, but has also been calculated through intensive sampling (Reinhardt et al. 2006b), introducing potential errors when moving from the plot to the scale of the landscape. Some allometric equations only require species and dbh, though most also include some combination of tree height, crown length (or height to live crown base), and crown ratio or width (Brown 1978; Brown and Johnston 1976; Cruz et al. 2003; Sando and Wick 1972; Wilson and Baker 1998). Equations developed for northern boreal plantations only required stand height and density to predict the canopy base height (McAlpine and Hobbs 1994), while in the Aleppo pine (*Pinus halepensis* Mill.) forests of Greece, no satisfactory equation could be derived from basic stand measurements (Mitsopoulos and Dimitrakopoulos 2014). Other methods for calculating CBH have been implemented: Wilson and Baker (Wilson and Baker 1998) controlled for the variability of multilayered stands by taking the midpoint of minimum and average height to live crown base as the CBH. Cruz, Alexander, and Wakimoto (Cruz et al. 2004) introduced the concept of the fuel strata gap, which accounts for the vertical gap in fuels, as an alternative to CBH. CBH has been criticized for its arbitrary threshold and insensitivity to tree density when used to calculate a torching index for the "Fire and Fuels Extension" of the Forest Vegetation Simulator software (Rebain 2010 (revised December 18, 2012)). Because of this concern, an alternative measurement was created that could estimate torching without being so dependent on CBH (Rebain 2010 (revised December 18, 2012)). Even so, CBH remains a highly influential variable in many wildfire models used today (Hall and Burke 2006).

Terrestrial LiDAR has been used to estimate canopy height, canopy cover, CBH, and fuel strata gap on the plot scale (García et al. 2011a). Airborne LiDAR is already available to many National Forests and National Parks, and has been used to specifically derive fire model inputs

(Andersen et al. 2005; Erdody and Moskal 2010; Jakubowski et al. 2013b), but the concerns about using CBH in place of a more direct measure of ladder fuels remain. One study in the Pinelands of New Jersey that examined the link between airborne LiDAR and shrub biomass (Skowronski et al. 2007) suggests airborne LiDAR as a potential candidate for estimating shrubby ladder fuels, noting that normalized cover between 1 and 4 m can distinguish recently burned sites where biomass and cover are lower. Clark et al. (Clark et al. 2009) used this same metric to directly equate to ladder fuels. Wing et al. (Wing et al. 2012) derived relative understory vegetation cover in northern California using airborne LiDAR with calibrated return intensities. While these studies were carried out in a different forest type, they suggest a starting-point for estimating ladder fuels in mixed conifer stands. These studies indicate the potential for developing a LiDAR-derived metric to better account for ladder fuels. This would be a useful asset, especially because of the potential for high spatial resolution over large areas.

The primary questions addressed by this study were (1) Can a LiDAR-derived metric (or set of metrics) differentiate between treated and untreated areas? and (2) Does this metric (or set of metrics) correspond with field observations of ladder hazard? I explored some metric assumptions, compared the metric(s) to plot-based ladder fuel measurements, and visually assessed the validity of my conclusions from transects showing LiDAR points, aerial images, and treatment boundaries. I seek to robustly estimate ladder fuels and provide an alternative to the much-criticized surrogate (CBH).

2. Methods

2.1 Study Area

Meadow Valley is located in the northern Sierra Nevada of California in the Plumas National Forest (centered at 39^{o} 55' North, 121^{o} 03' West) (Figure 10). It has a Mediterranean climate with most of its 1,050 mm $year^{-1}$ of precipitation falling in the winter months (Ansley and Battles 1998). The 22,500 ha landscape ranges from 1,050 m to 2,150 m in elevation and is made up of forest, montane chaparral, and meadows. Tree species are primarily mixed conifer, including ponderosa pine (*Pinus ponderosa*), Jeffrey pine (*Pinus jeffreyi*), sugar pine (*Pinus lambertiana*), Douglas-fir (*Pseudotsuga menziesii*), white fir (*Abies concolor*), incense-cedar (*Calocedrus decurrens*), and California black oak (*Quercus kelloggii*) (Barbour and Major 1995; Schoenherr 1992). Smaller pockets of red fir (*Abies magnifica*) and western white pine (*Pinus monticola*) are found at higher elevations, and lodgepole pine (*Pinus contorta*), western juniper (*Juniperus occidentalis*), California hazelnut (*Corylus cornuta*), dogwood (*Cornus* spp.), and willow (*Salix* spp.) also occur at lower densities. The historic fire regime before fire suppression began in the early 1900s consisted of low to moderate severity fires burning at 7-19 year intervals (Moody et al. 2006).

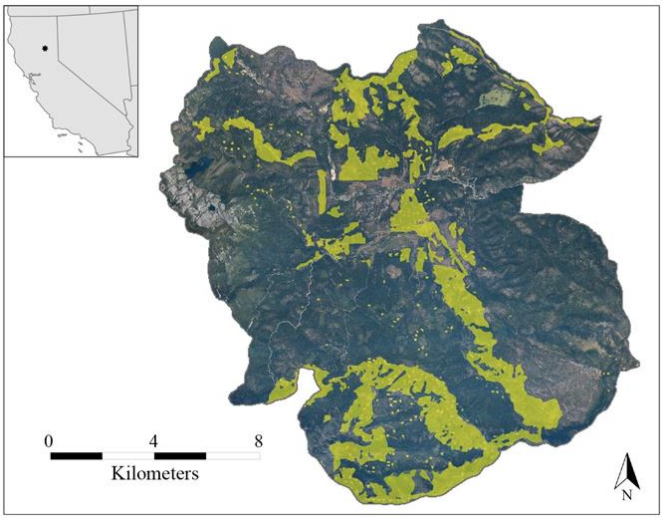

Figure 10. Meadow Valley study area, showing areas with fuel reduction (in yellow) between 1999 and 2008.

Recent fire activity has caused a rising concern about community safety and forest conservation, which spurred enactment of the Herger-Feinstein Quincy Library Group Pilot Project. The goals of the project were to maintain forest health, reduce potential for high severity fire, and conserve wildlife habitat, while maintaining the local economy (USDA Forest Service Plumas National Forest 2003). To reduce fire risk, a major objective was to increase the CBH from 1.2-2.4 m (pre-treatment) to at least 7.6 m (post-treatment), necessitating the removal of many small and medium trees (ladder fuels) (USDA Forest Service Plumas National Forest 2003).

The above project implemented a variety of treatment types across the landscape to address its goals, resulting in a network of treatments that span a range of treatment intensities, types, and ages. Treatments can be classified into five types: (1) hand-thinning (chainsaw) and pile-burning trees <30 cm dbh; (2) rotary drum mastication of shrubs and small trees, with shredded debris left on-site; (3) prescription burning under moderate weather conditions; (4) mechanical thinning of trees <51 cm dbh, or <76 cm dbh, depending on silvicultural prescription, which, for some areas, was followed by prescription burning; and (5) group selection silviculture that removed all conifers <76 cm dbh (USDA Forest Service Plumas National Forest 2003). Reported treatments covered 3,999 ha, or 17% of the total study area (see Figure 10 for spatial arrangement) and were implemented primarily between 2003 and 2008 (10% of treatments were completed between 1999 and 2002). Treatment longevity has been estimated to be between 8 and 15 years in similar areas (Chiono et al. 2012; Stephens et al. 2012), so I was confident in including treatments up to 10 years old in the study sample.

A treatment polygon layer was assembled by the Herger-Feinstein Quincy Library Group monitoring team (Team 2011), where treatments were represented spatially and described in detail. Areas were removed from analysis if they were unforested, had an incomplete

treatment as of August 2009, or were treated extremely lightly (treatments designed for stream corridors that created negligible visual change (Collins 2013) or heavily (as was the case for group selection cuts). A buffer of 30 m to either side of all treatment boundaries was also excluded to account for inaccurately mapped treatment edges. This decreased the area of analysis from 22,510 ha to 17,800 ha, with 11% of that area treated (Figure 10).

2.2 Field Data

I took advantage of two existing field datasets. One focused on treated areas, referred to as treatment plots; the other captured the range of vegetation/fuel conditions across the landscape, referred to as landscape plots. Treatment plots consisted of data collected prior to and following fuel reduction treatments, which were used to quantify change in ladder and canopy fuels. For this assessment, I relied on CBH to represent ladder fuels, and canopy cover and bulk density to represent canopy fuels. While these metrics, particularly CBH, are problematic for the reasons discussed above, they provided the best estimate feasible from the field. The intent was not to develop a direct relationship between CBH and LiDAR, but rather to confirm that the treatments did reduce ladder and canopy fuels.

Treatment plots were established in areas planned for treatment, prior to treatment implementation, located across a range of topographic settings and treatment types. A total of 72 plots were established; 26 were excluded because they were either located in areas never treated (16), had undergone group selection silviculture (3), or had poor consistency between measurements (abundant new large and small trees appearing in the plot after treatment) (7). Treatment plots were sampled 1-3 years before treatment (sampled between 2002 and 2007), and again 1 year after treatment (sampled between 2004 and 2009). Treatment plots measured 50 m by 20 m (0.1 ha), and sampling involved measuring large trees (≥76.2 cm dbh) across the entire plot, medium-large trees (40.6-76.1 cm dbh) on the center half of the plot, medium-small trees (12.7-40.5 cm dbh) on the center quarter of the plot, and small trees (2.5-12.6 cm dbh) on 5 subplots (each 16 m^2) along the plot centerline. Tree measurements included height, crown base height, and dbh. The Forest Vegetation Simulator (FVS) (Dixon 2002) was used to calculate the stand-level metrics shown in Table 4 to quantify treatment change. This demonstrated that treatments were effective in reducing cover and density and increased canopy base height by removing mostly small and medium sized trees.

	Pre-treatment (St. error)	**Post-treatment (St. error)**	**Percent of original**
Tree density (trees ha^{-1})	1045 (111)	412 (63)	40
Basal area (m^2 ha^{-1})	43 (3)	29 (3)	67
Canopy base height (m)	3.0 (0.4)	6.7 (0.1)	223
Canopy bulk density (kg m^{-3})	0.18 (.01)	0.09 (.01)	51
Canopy cover (%)	58 (3)	41 (3)	71

Table 4. Forest characteristics before and after treatment in Meadow Valley. Plots (46) were measured before and after treatment, metrics were calculated with FVS (Dixon 2002), and the resultant change is shown. Ladder fuel reduction is indicated by 1) an increase in CBH and 2) a large reduction in trees ha^{-1} paired with a relatively smaller reduction in basal area (many trees were removed, but most were small).

Landscape plots were a second field data collection effort, utilizing methodology outlined by Menning and Stephens (Menning and Stephens 2007). These data were used to independently validate that the LiDAR metric correlated with ladder fuels. Landscape plots were sampled within and outside the Meadow Valley study area between 2004 and 2006. Plot locations were chosen randomly from the stratified landscape. Stratifications encompassed 4 categories (3 topographic and 1 biotic), each classified into 3-6 levels. Categories included slope (3 levels: >15%, 15-30%, >30%), elevation (3 levels: <1,400 m, 1,400-1,600 m, >1,600 m), aspect (4 levels: N, E, S, W), and dominant vegetation (6 levels based on the California Wildlife Habitat Relationship classes derived from interpreted aerial images) (VESTRA 2003). Plots were circular, with a fixed radius of 12.6 m, representing an area of 0.05 ha. Plot centers were recorded with Trimble's GeoXT global positioning system (GPS) and differentially corrected. To calculate ladder fuels, each plot was divided into 4 equal quadrants, and the ladder fuel class (A, B, C, D, or E, described in Table 5) was assessed visually and recorded for each quadrant (see (Menning and Stephens 2007)). Fuel classes were determined by a combination of vertical fuel continuity (vertical gap greater than vs. less than 2 m) and the presence of low aerial fuels (e.g. high shrubs (>2m), small trees, and low branches). Canopy cover was also assessed at each plot using the number of hits from a sight-tube along two 12-m transects (1 sample m^{-1}).

Class	Clumped low aerial fuels	Vertical gaps <2m
A	yes	yes
B	yes	no
C	no	yes
D	no	no
E	no forest	no forest

Table 5. Ladder fuel hazard assessment classes (Menning and Stephens 2007).

There were 140 plots within the study area that were forested and either untreated or completely treated when field work began in spring 2004. Variability among plots was high, with only 28 plots (20%) falling into clearly low (all quadrants were class D) or high (all quadrants were class A) levels of ladder fuels. I defined a more inclusive classification method to preserve sample size (73 plots; 52% of the original 140) while maintaining a robust designation of low and high ladder fuel plots. Because vertical fuel continuity corresponds more closely to the traditional definition of ladder fuels, I assigned a high ladder fuel class to plots

where there was high vertical continuity (gaps were small), regardless of the presence of low aerial fuel. However, I maintained the definition for low ladder fuels in its purest form: large gaps and no low aerial fuels. Each plot (of 4 subplots) was classified as having high ladder fuels if it had at least 2 subplots of class A or C (gaps <2 m), and no subplots of class D (no low fuel; gaps >2 m). Plots were classified as having low ladder fuels if at least 2 subplots were class D (no low fuel; gaps >2 m) and no subplots were class A or C (gaps <2 m). While I realize that this approach is somewhat subjective, I wanted to avoid an excessive reduction in sample size when classifying the plots. The majority of the plots did not intersect treatments, though 8 had been lightly treated between 1999 and 2004. For this delineation, only half of the plots were classified as having either low or high ladder fuels, demonstrating the high variability of ladder fuels within each plot, and to an even greater degree across the landscape.

2.3 LiDAR Data and Processing

LiDAR was flown between July 31 and August 11, 2009, by Watershed Sciences for the Plumas and Lassen National Forests. A Leica ALS50 Phase II laser system was used with a scan angle of $\pm 14^{o}$ from nadir to collect LiDAR points. Orthophotos were also taken with a Leica RCD-105 39 megapixel digital camera and processed with Leica's Calibration Post Processing software. Photos were spatially placed using IPASCO and the Leica Photogrammetry Suite. The average point density was 4.68 points m^{-2}. The vendor reported average vertical and horizontal accuracy were 2.6 cm and 7.2 cm, respectively, based on the mean divergence of points from ground survey point coordinates (3,089 ground points were analyzed across 4 surveyed areas).

Fusion software (McGaughey 2012) was used to extract LiDAR-derived metrics for analysis at a scale of 30 m to determine whether a metric (or set of metrics) could differentiate between treated and untreated areas. I chose this spatial scale because it is common for many datasets used by land managers, including Landsat and LANDFIRE. Fusion software was used to extract a total of 53 different metrics accounting for topography (5) and forest structure (48) (McGaughey 2012) (described in detail in table A.2 in the appendix). I also added 6 additional strata layers (2-4 m, 4-8 m, 8-16 m, 16-32 m, 32-48 m, and >48 m) that accounted for the relative cover in a layer based on hits within and below that layer, as described by Skowronski et al. (Skowronski et al. 2007) and Kane et al. (Kane et al. 2013). No points below 2 m were used as the primary metric due to the potential error in differentiating ground points from vegetation, following Kane et al. (Kane et al. 2013) (though point counts below 2 m were used to calibrate the strata layers described above).

I clipped the LiDAR pointcloud to the plot boundaries (plot center with a 12.6 m radius) and calculated the average value of the LiDAR-derived metric(s) within that area to determine whether this metric (or set of metrics) corresponded with field observations of ladder hazard.

2.4 Workflow

My workflow, shown in Figure 11, illustrates how I used the 2 sets of field data, airborne LiDAR, and spatial data denoting fuel reduction treatment boundaries to address my research questions.

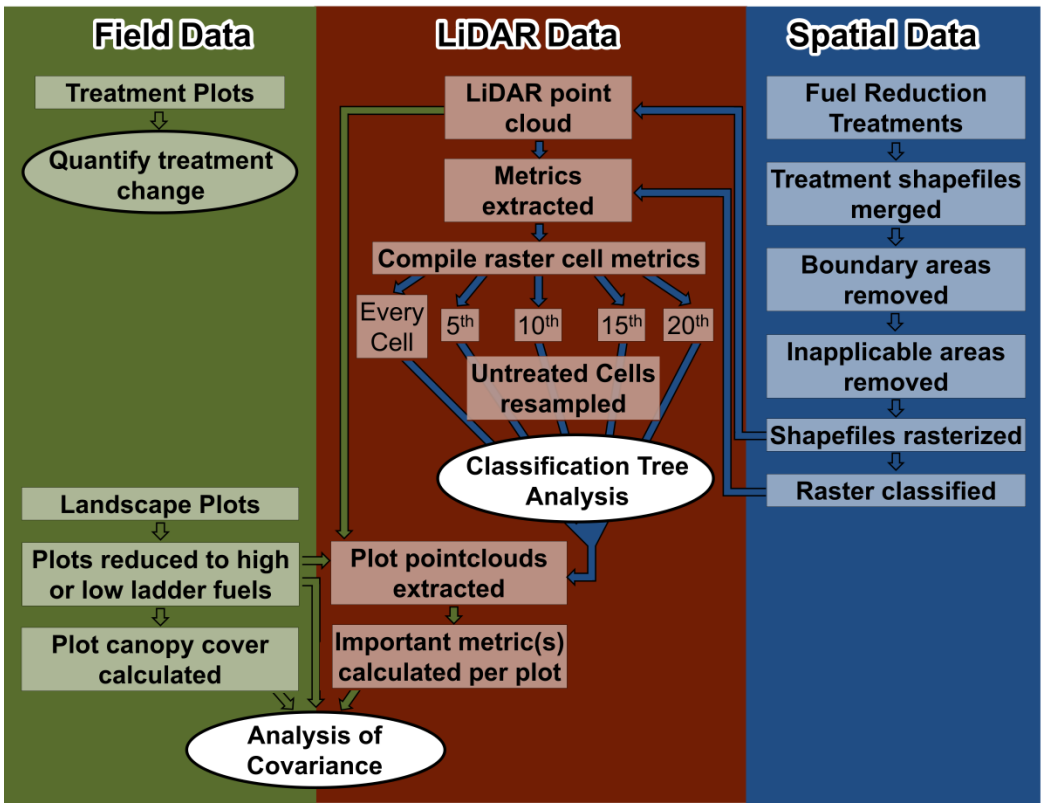

Figure 11. Project work flow, including all data sources and methods. Analysis products are shown in ovals. Data sources and intermediate steps are shown in rectangles.

2.5 Statistical Analysis

I used classification tree analysis to determine whether a LiDAR-derived metric (or set of metrics) could differentiate between treated and untreated areas. The classification trees identified LiDAR-derived metrics that helped explain the difference between treated and untreated pixels (Figure 12). Classification trees explain the variation of a categorical response variable by splitting the sample one or more times into relatively homogeneous groups with respect to the response variable. Each split breaks the data into 2 nodes based on an explanatory variable and a break point (if the value for the explanatory variable is greater than the breakpoint, that data point goes into one node, and if not, it goes to the other node). A model is chosen that fits the data, but also minimizes the number of splits. A classification tree approach was chosen rather than standard linear regression because the response variable was categorical (treated or untreated), and I was interested in considering all potential explanatory variables (many of which were correlated) but identifying only those important for differentiating between treated and untreated areas (De'ath and Fabricius 2000). I was not trying to build a predictive model (already pursued by many, with varying degrees of success (Andersen et al. 2005; Erdody and Moskal 2010; Jakubowski et al. 2013b)), but simply

identifying factors that would merit further investigation, and believed that exploring the data with classification trees was the most straightforward and understandable approach.

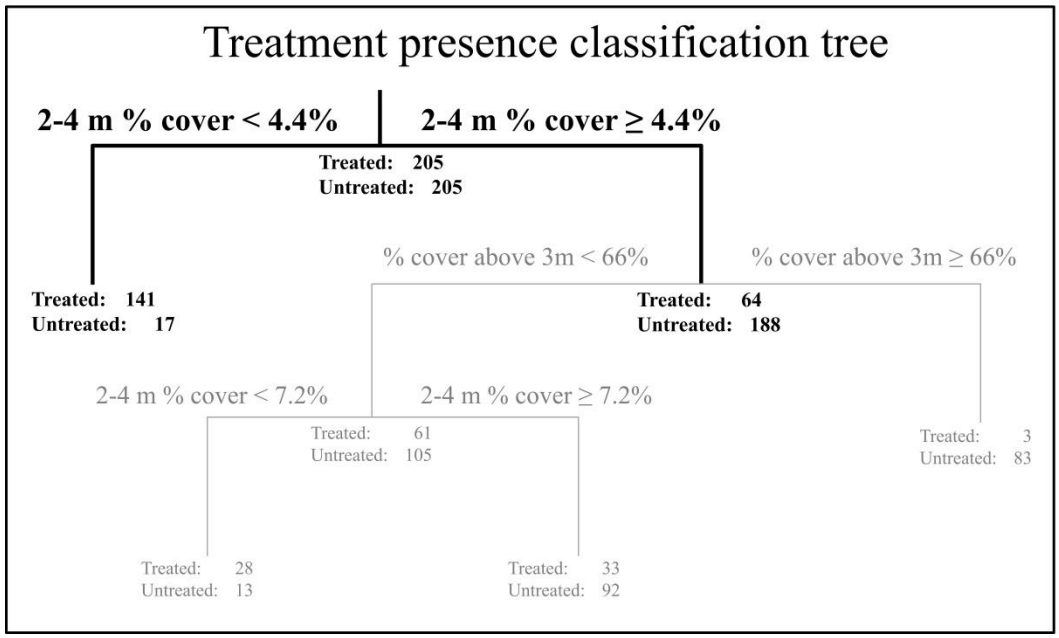

Figure 12. An example classification tree differentiating between treated and untreated cells at a sampling density of every 10th cell is shown. Pruned nodes are greyed out. The only break metric in this classification was 2-4 m cover, with a break point of 4.4%. Misclassification for the pruned tree can be calculated as the number of samples wrongly classified (17+64) / the total number of samples (410) = 19%. Because there are an equal number of treated and untreated samples, the null model misclassification rate is 205/410 = 50%.

To account for spatial autocorrelation and the robustness of the classification tree, 30 m cells were sampled at densities of every cell (0 m apart) and 5, 10, 15, and 20-cell spacing (120, 270, 420, and 570 m apart). Because only 11% of the sample area was treated, untreated cells were resampled for even representation of treated and untreated area.

For each cell density, the classification tree algorithm was implemented in R (R Core Team 2014) using the rpart algorithm to build a model that best differentiated between treated and untreated cells using the LiDAR-derived response variables. Each tree was pruned to the fewest nodes with cross-validation error within 1 standard deviation of the lowest cross-validated error. The goal of this analysis was to reveal the metric or set of metrics best able to differentiate between the treated and untreated landscape.

To determine whether this metric (or set of metrics) corresponded with field observations of ladder hazard, I tested the predictive power of the metric(s) revealed by part 1 against the only established method for quantifying ladder fuels (known to us), developed by

Menning and Stephens (Menning and Stephens 2007). I ran an analysis of covariance between ladder fuel class (using the high vs. low designations described above), the metric value, the field-calculated canopy cover, and an interaction term between the metric and canopy cover. The purpose of this test was two-fold: 1) explore the potential bias of cover to the LiDAR-derived measure of ladder fuels based on the possibility of differential point penetration; and 2) evaluate the relationship between the LiDAR-derived metric and the plot-based measure of ladder fuels. The potential bias (1) would be disproved if there was no significant contribution of either canopy cover or the interaction between canopy cover and the LiDAR metric to the estimation of ladder fuels. The relationship between ladder fuel and the metric (2) would be revealed through the significance of the LiDAR metric in the model. If significant, this test would show that the LiDAR-derived metric could predict at least some aspect of ladder fuels.

To visually confirm the results, I created 8 transect images of the LiDAR where it crossed a treatment boundary, paired with the orthophoto collected with the LiDAR, as well as the reported treatment boundary. Transects were 300 m long and 10 m wide. Transect locations were chosen where the treatment boundary appeared to agree well with the metric estimate and where the metric changed as it crossed from treated to untreated. This was typical of most, but not all treatments. Although this test is not a random sample, I was interested in investigating the LiDAR point distribution in the cases identified by the statistical analysis where the metric changed. While this test was qualitative, it provided an opportunity to visually assess the results.

3. Results

Classification tree results at all spatial scales pointed to a single, most important variable: the relative percent cover between 2 and 4 m, referred to subsequently as "2-4 m cover" (Table 6). A sample classification tree is shown in Figure 12 to illustrate tree structure, pruning, and misclassification rate calculations. The misclassification rate at all spatial scales was low for models built with just a single split (between 17 and 21% misclassification compared to the null model's 50%), showing that model fit was good. The classification tree analysis of the full landscape was the only model that had more than one split. Additional splits further defined treated pixels as having slope $<22^{o}$ and cover (percentage of point heights above 3 meters) <70%, yet only and improved the misclassification rate by 2%, pointing to 2-4 m cover as the primary metric of interest for the second stage of the analysis. Figure 13 shows the levels of 2-4 m cover across the landscape and confirms that a low break point between 3% and 8% (the range suggested by the break points in Table 6) was a good indicator of treatment.

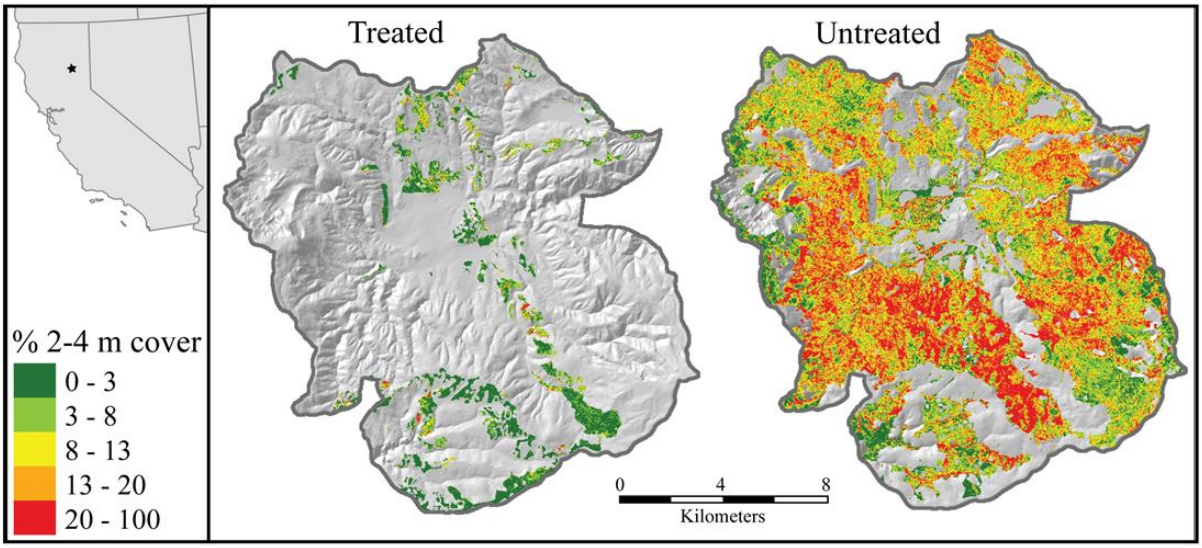

Figure 13. Meadow Valley study area, showing areas with fuel reduction and those with no treatment after 1999. Green to red color scale indicates the relative percentage of 2-4 m cover across the analyzed treated (left) and untreated (right) landscape.

Sampling method ***(sample size)***	**Break metric**	**Break point**	**% misclassification**
Every cell* *(43,542)*	% 2-4 m cover	6.3	20
Every 5th cell *(1,718)*	% 2-4 m cover	6.1	20
Every 10th cell *(410)*	% 2-4 m cover	4.4	19
Every 15th cell *(216)*	% 2-4 m cover	7.5	17
Every 20th cell *(96)*	% 2-4 m cover	3.4	21

Table 6. Results from classification tree analyses at a range of spatial sampling scales, describing the break point metric, the break point value, and the misclassification rate for the pruned tree (compared to 50% misclassification in the null model). **Only one pruned classification tree (every cell) had more than one break. In this case, the full model had 3 breaks (in order, these breaks were 2-4 m cover, slope in degrees, and percentage of point heights above 3 meters, with breakpoints at 6.3%, 22^{o}, and 70%, respectively), with a misclassification rate of 18% (compared to 20% using only the first break).*

To ensure that canopy cover was not biasing the LiDAR results (by not allowing enough pulse penetration through the canopy to obtain a robust estimate), I tested whether high vs.

low ladder fuels (measured on the ground) were affected by plot-derived canopy cover, 2-4 m cover, or the interaction between the two using an analysis of covariance. I found that ladder fuels were not significantly influenced by either canopy cover or the interaction between canopy cover and 2-4 m cover, while they were significantly influenced by 2-4 m cover alone ($p < 0.05$, $n=73$). The distribution of 2-4 m cover across high and low levels of ladder fuels is shown in Figure 14. This model used only 2-4 m cover as a predictor for plot-derived ladder fuel and the split occurred at 5.3%, squarely within the range suggested by the break points in Table 6.

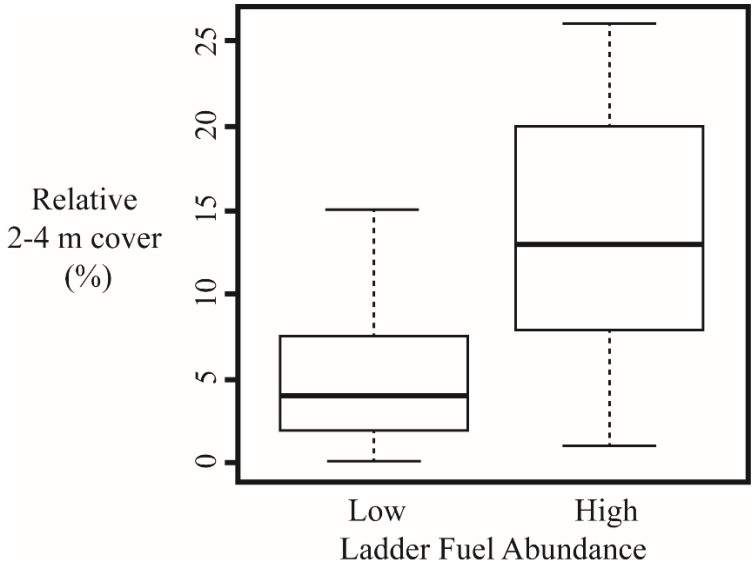

Figure 14. Box and whisker plot of the distribution of LiDAR-derived relative percentage of 2-4 m cover within plots having low and high ladder fuel abundance as derived from field plots using the methods of Menning and Stephens (Menning and Stephens 2007) ($n=73$). Distributions were significantly different ($p<0.001$). Median 2-4 m cover in high ladder fuel plots was 13.0%, while it was 4.0% in low ladder fuel plots. **Outliers are not shown to simplify viewing.*

In the analysis, I came upon a few areas that appeared uncharacteristic of the general trend (identified as treated, but whose 2-4 m cover was an outlier among the treated polygons). While this brings into question the validity of the treatment boundaries I used to analyze the data, the area of these anomalies was small compared to the overall study area. I communicated with the Plumas National Forest (USFS) office and obtained specific details on these areas to determine the exact treatment history (Thompkins 2013). All cases revealed that the unit in question was either: 1) untreated at the time of the LiDAR flight (i.e. the date of completion was misreported in the database), 2) contained a riparian or other sensitive area (which, by law, could not be treated, but was included as treated in the dataset), 3) appeared to have poorly mapped boundaries beyond the 30 m buffer I created to mitigate for these, or 4)

had variable treatment effects throughout treatment units (as was the case with some burned units). Inaccurate treatment boundaries are an issue land managers must deal with on a regular basis, but this research shows a potential alternative method for checking treatment boundaries against those reported, and could prove to be a valuable asset.

4. Discussion

Fuel treatments are critical to mitigating fire risk and target surface, ladder, and sometimes canopy fuels. Ladder fuels are not directly measured in the field, however, and the derived proxy of CBH is used in place of a better metric. CBH is an extremely influential metric for crown fire initiation models (Hall and Burke 2006), yet represents ladder fuels poorly (Scott and Reinhardt 2001). Furthermore, since CBH is derived allometrically using tree lists, it is generally associated with a high degree of spatial error (Jakubowski et al. 2013b). The dependence on such a tenuous variable makes output from fire models more uncertain than would be desired. This uncertainty has even driven the development of more unconventional measures of fire behavior that depend on more direct plot-derived data rather than CBH (e.g., P-torch as used in the Fire and Fuels Extension to the Forest Vegetation Simulator; (Rebain 2010 (revised December 18, 2012))).

Methods to directly quantify ladder fuels using a key in the field are rare (Menning and Stephens 2007; Prichard et al. 2013; Wright et al. 2007). Menning and Stephens' approach was semi-qualitative, and classified ladder fuels into one of 5 types, which proved to be highly variable even within the 4 adjacent subplots (Menning and Stephens 2007). Subplot variability suggests that upscaling plot-based measures to the stand scale (as done to populate a landscape from plots for a 2-dimensional fire model) may be inaccurate and points to the necessity for a remote-sensing derived, landscape-scale ladder fuel metric that quantifies heterogeneity within stands. My work demonstrates the potential application of LiDAR for quantifying ladder fuels, which has already been used to describe forest structure beneath the canopy (Kane et al. 2010; Kane et al. 2013; Kane et al.). Despite my fairly successful findings, questions concerning appropriate measurement scale and ladder fuel variability and clumpiness still need to be addressed.

4.1 Relationship between treatments, LiDAR, and ladder fuels

On a 17,800 ha landscape, 11% of which had undergone fuel reduction that effectively reduced ladder fuels and slightly reduced canopy fuels (Table 4), 2-4 m cover proved to be the LiDAR-derived metric with the most explanatory power to differentiate between treated and untreated areas (Figure 13). The model accurately predicted fuel treatment presence vs. absence for 79 – 83% of the analyzed pixels across a range of sampling densities, with break points ranging between 3.4% and 7.5% (Table 6). While this model was not a perfect fit, my objective was not to build a model that could determine the location of fuel reduction treatments, but rather, to select candidate variables for further testing. When compared to an independent, field-designated assessment of ladder fuel, the distribution of 2-4 m cover was significantly different between plots with high and low quantities of ladder fuel (Figure 14). The break point identified by this analysis was 5.3%, which falls squarely within the range suggested

by my first test. Images supported the conclusion that the ladder fuels that could not be seen from the air or easily extrapolated from plot-based measures could be estimated from LiDAR. Inasmuch as CBH can be compared with the 2-4 m cover LiDAR metric, average pre-treatment CBH in treatment plot tree lists was 3.0 m (Table 4), which is within the 2 to 4 m range. This convergence suggests this metric may be indicating a vital height range to monitor when considering ladder fuels. Furthermore, studies in the Pinelands of New Jersey have suggested a very similar metric that correlates with shrub biomass that has been equated to ladder fuels (Clark et al. 2009; Skowronski et al. 2007).

Figure 15 shows two of the transect images that I created to visually assess the relationship between 2-4 m cover and fuel treatment. These images are representative of those I created, and were chosen to depict a range of conditions. Both images show a distinct difference in 2-4 m cover across the treatment boundary. The top image shows an area with heavy cover (LiDAR-derived cover varied from 48 to 78% along the transect) as well as a portion of dense shrubs on the far right. There is a potential instance of LiDAR hits not penetrating the canopy just to the right of the treatment boundary, but overall, the point penetration is adequate. The bottom image shows an area with lighter cover (cover varied between 18 and 61% along the transect); the treatment is hard to discern from the aerial image alone, but quite apparent from the LiDAR's 2-4 m point density.

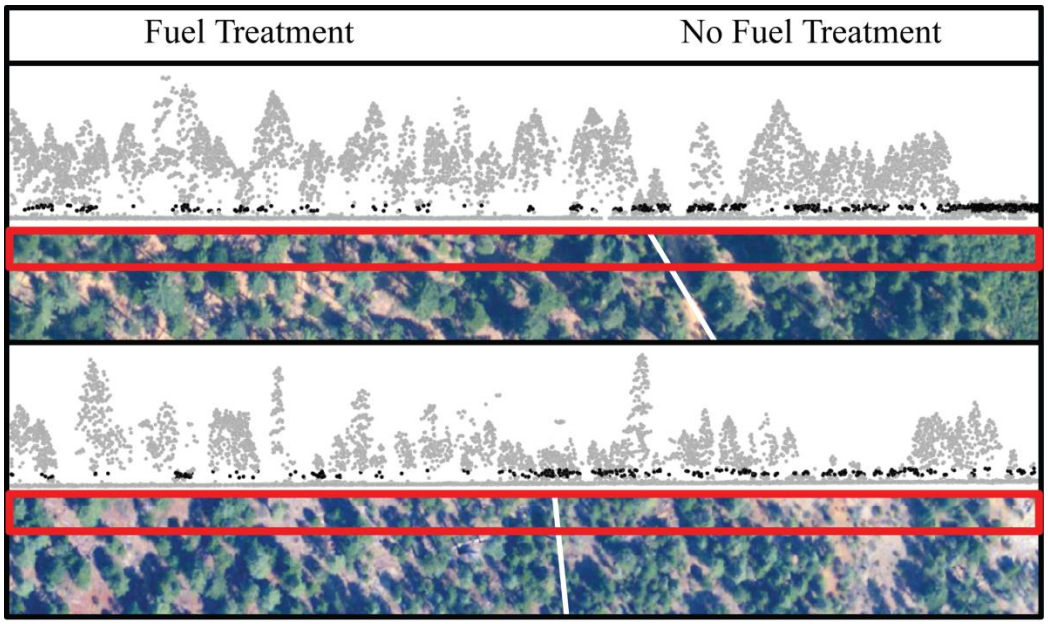

Figure 15. Two pairs of transect images, each showing a 300 m by 10 m transect of LiDAR points across a treatment boundary, paired with the corresponding aerial image. The LiDAR has been transformed to show an even ground elevation and points 2-4 m from the ground are shown in black. The aerial image shows the transect outlined in red and the treatment boundary in white. Transects were chosen to present different levels of canopy density (cover varied between

48 and 78% in the upper image pair and 18 and 61% in the lower pair) and the visual ambiguity of treatments in the aerial image (treatment is apparent in the aerial image of the upper transect, but difficult to discern from the aerial image of the lower transect).

This study is exploratory, however, and has a number of limitations. This research was done post hoc, leaving a greater chance for type I error (finding a relationship where one does not actually exist). The study utilized a single study area, necessitating further work to validate the findings beyond this area before they should be used operationally. I also utilized a non-conventional, two-step process to reach my conclusions, potentially introducing additional sources of error. I used fuel reduction treatment as a proxy for ladder fuels in order to narrow down the pool of LiDAR metrics to those that likely related to ladder fuels. The pool of LiDAR metrics did not include strata below 2m in height due to increased noise in the dataset (Kane et al. 2013) and fuels below 2 m generally being classified as surface fuel characteristics, leaving out this measure of fuel hazard. The analysis used only one statistical model (classification trees), which converged on a single metric: 2-4 m cover. Comparison with measurements of the fuel treatments themselves revealed that these treatments were targeting fuels in the 2-4 m range, suggesting that the classification tree analysis may have been biased toward the 2-4 m range. This metric does not include any information about fuels outside of the 2-4 m range, or describe the relative clumping of fuels within that range. The final test compared the single LiDAR-derived metric (2-4 m cover) to a simplified categorical classification (with its own inherent biases) of ladder fuels.

Nevertheless, this study suggests that ladder fuels can be at least partially accounted for by LiDAR, opening many avenues of further study. For instance, some studies have shown the utility of voxels (or "volume elements" rather than "picture elements" or pixels) (Popescu and Zhao 2008; Wang et al. 2008) for modeling LiDAR density and forest structure, including canopy base height (e.g. (Popescu and Zhao 2008)). This newer data representation might lend itself well to the characterization of 18D forest structure, and in particular, ladder fuels. Additionally, there has been recent work examining tradeoffs between LiDAR point density and forest metric accuracy (e.g. (Jakubowski et al. 2013c)), but no work to date on this and other scaling questions with respect to ladder fuels. Finally, better characterization of ladder fuels could add new information and a new analytical dimension to fire behavior and effects models, particularly those that deal with three-dimensional fire behavior (e.g. FIRETEC-HIGRAD; (Linn et al. 2002)), and should be investigated.

4.2 Immediate Management Implications

On landscapes similar to Meadow Valley, with similar treatment types and ages, LiDAR-derived 2-4 m cover could be used by managers as an aid in confirming and updating reported treatment boundaries. The analysis revealed a number of areas where treatment boundaries appeared inaccurate. Managers must deal with such errors, large and small, on a regular basis, as well as consider the impact of potentially inaccurate treatment boundaries on modeled fire

behavior and fire suppression planning. A raster layer describing 2-4 m cover differentiated between treated and untreated areas (Figure 12) and could inform managers of areas needing a follow-up visit to re-evaluate treatment boundaries.

My research also suggests the utility of the 2-4 m cover metric for landscape assessment. While it was not my goal to create an absolute metric for ladder fuels, 2-4 m cover could be used as a proxy for the relative abundance of ladder fuel across a landscape. Managers could use this to identify areas with high levels of ladder fuels and potentially target them for treatment, especially when affected by other high-hazard conditions. Because most treatments target ladder fuels more than canopy fuels, this metric could also be extremely useful for highlighting areas where treatments could make the greatest positive change to ladder fuel levels (i.e., if an area with heavy ladder fuels is targeted for treatment, that treatment will likely reduce fuels more effectively than an area with lighter ladder fuels and similar surface fuel and topographic characteristics). Similarly, managers could deprioritize areas with relatively lower levels of ladder fuels or implement treatments that target other fuel pools (e.g. prescribed fire to reduce surface fuels). Planning prescribed burns in areas with lower ladder fuel hazard would be advantageous due to potentially reduced risk of escape.

4.3 Long-term Uses of this Research to Managers

With further research, perhaps a more quantitative LiDAR-derived measure of ladder fuels could be developed. Compared to CBH, this measure would be more direct and would likely be more spatially accurate across landscapes and applicable across forest types. Furthermore, because this measure would be derived from LiDAR, it could be estimated across the whole landscape, instead of being limited to the plot and then scaled up. This would not only yield a superior product, but would maintain the spatial heterogeneity of fuels, a factor that researchers recognize as increasingly important to consider when modeling fire (Stephens et al. 2008).

If such a metric for ladder fuels was incorporated into fire models to replace CBH, crown fire predictive models could be improved (Cruz and Alexander 2010). CBH is difficult to both measure and use, yet it has remained a vital component of fire models because no alternative measure exists. This research demonstrates the potential of a LiDAR-derived measure of ladder fuels that would be a more direct metric and could account for finer scale spatial heterogeneity across the landscape.

5. Conclusion

LiDAR has great potential to characterize aspects of forest structure important to understanding fire behavior. As wildfire danger grows, we should better utilize LiDAR datasets, collected for public lands across the US, in support of fire management. This study suggests a simple metric that can be used to quantify the presence of ladder fuels in forests across large areas and demonstrates several valuable immediate uses of this metric for land managers: 1) confirm and update boundaries of fuel treatments similar to those examined; 2) estimate relative ladder fuel abundance across the landscape and target high ladder areas for treatment.

LiDAR data provides an opportunity to augment traditional measures of forest structure currently used as inputs to fire behavior models by offering spatially explicit quantification of fire-relevant canopy metrics. Previous studies have focused on extracting inputs for fire models from LiDAR (such as deriving CBH and canopy bulk density) (Andersen et al. 2005; Erdody and Moskal 2010; Jakubowski et al. 2013b), but perhaps future research could focus on LiDAR metrics that specifically target ladder fuels and more direct measures of structure that can be validated quantitatively, without the use of allometric equations. Rather than using LiDAR to predict an allometrically derived fire modeling input, this study presents an alternate perspective: to use LiDAR to directly quantify ladder fuels. Such new applications of LiDAR could fundamentally alter the way we assess crown fire potential across landscapes and apply fuel treatments to mitigate that risk.

Acknowledgements

Thanks to my co-authors Brandon Collins, Maggi Kelly, and Scott Stephens. I thank the Plumas National Forest for allowing us to use their LiDAR dataset. Thanks to Bridget Tracey, Nick Delaney, and the Treated Stand Structure Monitoring crew for collecting field data. I especially thank the Plumas National Forest's silviculturist, Ryan Tompkins, for assisting with questions about specific treatments. Thanks also to Van Kane for early advice on planning the aim of this project and, in conjunction with Robert McGaughey, assisting us with the LiDAR-processing program, FUSION. Joan Canfield and anonymous editors contributed comments that improved this paper. This material is based upon work supported by the National Science Foundation Graduate Research Fellowship Program under Grant No. DGE 1106400. Thanks also to the Berkeley Research Impact Initiative grant, sponsored by the UC Berkeley library, for covering publication fees.

Chapter 4: Estimating ladder fuels: a new approach combining field photography with LiDAR

Abstract

Forests historically associated with frequent fire have changed dramatically due to fire suppression and past harvesting over the last century. The buildup of ladder fuels, which carry fire from the surface of the forest floor to tree crowns, is one of the critical changes, and it has contributed to uncharacteristically large and severe fires. The abundance of ladder fuels makes it difficult to return these forests to their natural fire regime or to meet management objectives. Despite the importance of ladder fuels, methods for quantifying them are limited and imprecise. LiDAR (Light Detection and Ranging), a form of active remote sensing, is able to estimate many aspects of forest structure across a landscape. This study investigates a new method for quantifying ladder fuel density in the field (using photographs with a calibration banner) and remotely (using LiDAR data). I apply these new techniques in the Klamath Mountains of Northern California to predict ladder fuel levels across the study area. My results demonstrate a new utility of LiDAR data to identify fire hazard and areas in need of fuels reduction.

1. Introduction

Remote sensing has been key to many areas of environmental science, and wildland fire is no exception (Arroyo et al. 2008; Dubayah and Drake 2000; Hyyppa et al. 2000; Lefsky et al. 2002). Wildland fires consume homes, endanger lives, and consume a large number of taxpayer dollars every year (Husari et al. 2006b; US Forest Service 2015). During the past century, many forests in the Western United States have undergone unprecedented change in forest structure and fire behavior due to forest and fire management practices, including resource extraction and fire suppression (Hessburg et al. 2005). One dramatic change in Western forests that historically experienced frequent, low- to moderate-severity fire has been the infilling of ladder fuels that help facilitate the movement of fire from the surface of the ground to tree canopies (Hessburg et al. 2005; Skinner et al. 2006).

The Landsat program has informed the study of wildland fire severity, and analysis of Landsat imagery has shown that recent fires have produced a disproportionately large amount of high severity fire (where over 90% of trees are killed) (Miller et al. 2009). These altered contemporary fire patterns are due to a number of factors, but considerable increases in surface and ladder fuels play an important role (Agee and Skinner 2005). Increases in ladder fuels in particular allow fire to readily transition into overstory tree crowns by providing greater vertical fuel continuity and preheating canopy fuels that have not yet ignited (Menning and Stephens 2007). Additionally, dense ladder fuels can make suppression more difficult and increase wildland firefighter exposure to hazardous conditions by inhibiting escape to safety zones when fire behavior shifts unexpectedly (Hirsch and Martell 1996). In addition to the biophysical influences of ladder fuels on fire behavior and fire management, they can also

reduce habitat quality through decreasing accessibility and foraging efficiency for wildlife and tribal subsistence gathering (Norgaard 2014).

Despite the importance of ladder fuels to fire behavior, effects, and firefighter safety, they have not been directly quantified except in a few cases (Menning and Stephens 2007; Prichard et al. 2013; Wright et al. 2007), all of which are sampled on the ground, with no remote sensing component. Because ladder fuels are below the canopy, passive remote sensing platforms are not able to capture their composition, except in very thin-canopied forests. In most cases, a surrogate for ladder fuels is used, which is comprised of a combination of canopy base height (CBH) and fuel model (sometimes with an adjustment of fire behavior) (Scott and Reinhardt 2001). CBH is the height above which there is enough fuel per unit volume to carry the fire upward. The most common value for this threshold is 0.012 kg m^{-3} (Reinhardt et al. 2006a), but other thresholds have been suggested and used (Fernandes 2009; Mitsopoulos and Dimitrakopoulos 2007; Ottmar et al. 1998; Sando and Wick 1972).

In addition to a variable fuel threshold, estimations for CBH are commonly based on allometric equations, moving them further from a reliable direct measurement. Although active remote sensing platforms have been used to estimate CBH in a number of studies, the allometric derivation makes CBH an inherently difficult measure to estimate from remote sensing (Andersen et al. 2005; Erdody and Moskal 2010; Jakubowski et al. 2013b). The allometric equations upon which CBH is derived use a combination of the following inputs: species, dbh, tree height, crown length (or height to live crown base), and crown ratio or width (Brown 1978; Brown and Johnston 1976; Cruz et al. 2003; Sando and Wick 1972; Wilson and Baker 1998). While these allometric equations are likely appropriate for plantations with uniform conditions (Andersen et al. 2005; Dean et al. 2009; McAlpine and Hobbs 1994), they are unlikely to maintain accuracy in more natural stands because they often ignore small-diameter trees and shrubs that are critical components of ladder fuels (Hall et al. 2005; Rebain 2010 (revised December 18, 2012); Scott and Reinhardt 2001). This was also the case in Greece, where no satisfactory equation for CBH in Aleppo pine (*Pinus halepensis* Mill.) forests could be derived from basic stand measurements (Mitsopoulos and Dimitrakopoulos 2014). Alternatives to the standard methods to measure CBH include Wilson and Baker (1998), who estimated the CBH as the midpoint of minimum and average height to live crown base in multilayered stands ; and Cruz, Alexander, and Wakimoto (2004) characterized the vertical gap in fuels as an alternative to CBH, and called their new metric the fuel strata gap. Due to CBH's arbitrary threshold and insensitivity to tree density, an alternate method was developed to estimate the torching index in the Fire and Fuels Extension of the Forest Vegetation Simulator (Rebain 2010 (revised December 18, 2012)). Despite these inaccuracies, most wildland fire behavior and effects models still rely heavily on CBH (Hall and Burke 2006).

Menning and Stephens (2007) recognized the need for a more robust measure of ladder fuels, and developed a categorical system for identifying ladder fuels in forested systems as one of four classes. Kramer et al. (2014) relate the ground plot measurements from Menning and Stephens (2007) to aerial light detection and ranging (LiDAR), showing that LiDAR is able to differentiate between areas with dense and sparse ladder fuels. However, because the categorical, ground-based measures only span four structural distributions to describe every

configuration of ladder fuels, relationships could not be built to more specifically estimate these fuels.

Aerial LiDAR is an active remote sensing technology that has been used to accurately estimate multiple aspects of forest structure, and presents an excellent data source from which to derive ladder fuel density (Coops et al. 2007a; García et al. 2011a; Kane et al. 2010; Kelly and Di Tommaso 2015; Lefsky et al. 2002). LiDAR has even been used to calculate metrics similar to ladder fuels, such as understory vegetation cover (Wing et al. 2012) and shrub biomass (Skowronski et al. 2007), although both of these studies necessitated intense sampling efforts, and neither captured the density and vertical continuity of ladder fuels as a whole.

Here I develop a ground-based methodology that provides more precise, quantitative estimates than the categorical system derived by Menning and Stephens (2007) , yet does not require the extensive field data collection efforts required by others (Menning and Stephens 2007; Skowronski et al. 2007; Wing et al. 2012). I then investigate whether LiDAR can predict this metric. Specifically, my main research questions for this project are: 1) Does the photo-banner methodology adequately sample ladder fuel density within each plot? And 2) How robustly can aerial LiDAR predict these estimates of ladder fuel density across a range of conditions?

2. Methods

This study is part of the Western Klamath Restoration Partnership, and utilizes the pre-established focal areas identified by that project. This partnership includes federal, state, local, community, and indigenous groups, as well as non-profits. The objective of the partnership is, in part, "to develop collaborative fire management practices," which necessitates an assessment of fuel conditions across the landscape (Harling and Tripp 2014).

2.1 Study area

The Klamath River Basin is located in Northern California, and includes diverse land ownership and management. The 2,622 ha (6,480 ac) study area is located between Orleans, CA and Happy Camp, CA, centered at 41.5^{o} North, 123.5^{o} West (Figure 16). While LiDAR was collected over a 14,323 ha (35,394 ac) area, four focal areas are utilized by the overarching project, limiting the study area to 2,622 ha. Topography is steep and complex, with elevation in the study area ranging between 160 and 520 m. Canopy cover ranged between 0 and 100%, but was often quite dense, averaging 90% across the study area (derived from the proportion of LiDAR first returns over 1.37 m).

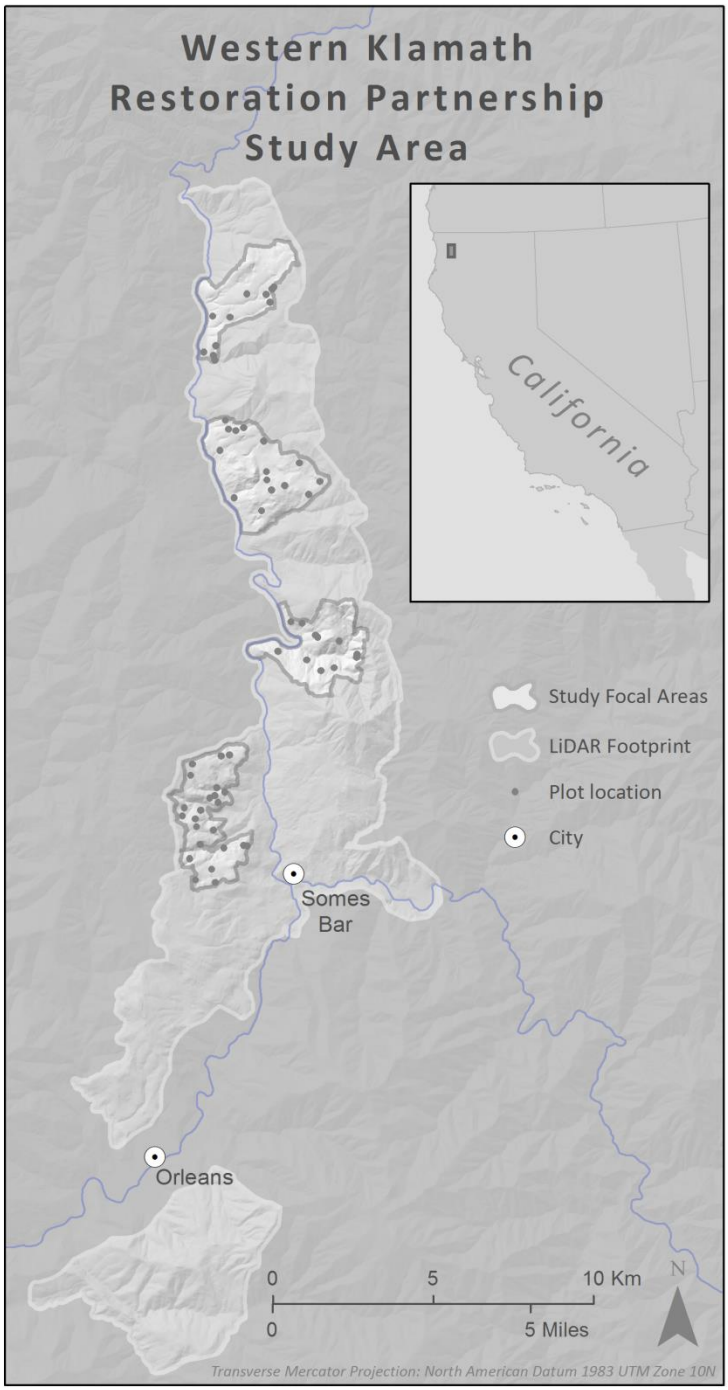

Figure 16. Klamath River study area between Orleans and Happy Camp, CA. Within the 14,323 ha LiDAR footprint, four focal areas, totaling 2,622 ha (6,480 ac), were chosen to sample the forest.

The Klamath has a Mediterranean climate: hot, dry summers, and cool, wet winters, although there is substantial variability across the region (Skinner et al. 2006; Taylor and

Skinner 1998). Normal daily maximum and minimum temperatures range between 11 and 35 degrees C, and between 1 and 11 degrees C, respectively (Skinner et al. 2006). The majority of precipitation falls during the winter months, with an average of 143 cm every year (Skinner et al. 2006). The Klamath includes the highest diversity of conifer forests in North America (Cheng 2004). The study area contains areas of forest, shrub, and meadow, with the dominant tree species being tanoak (*Notholithocarpus densiflorus*) and Douglas-fir (*Psedotsuga menziesii*). It is also common to find pacific madrone (*Arbutus menziesii*) and canyon live oak (*Quercus chrysolepis*). The study area also includes rarer abundance of golden chinquapin (*Chrysolepis chrysophylla*), California black oak (*Quercus kelloggi*), California bay (*Umbellularia californica*), pacific dogwood (*Cornus nuttallii*), big-leaf maple (*Acer macrophyllum*), ponderosa pine (*Pinus ponderosa*), red alder (*Alnus rubra*), and sugar pine (*Pinus lambertiana*). Many of these tree species, such as California bay and multiple species of oak, are important sources for tribal gatherers, both historically and in the present (Davis and Hendryx 2004). The diversity of oaks present in this system also provide important habitat for many species (Skinner et al. 2006).

Fire has long been an important part of the Klamath, with many ignitions coming from lightning strikes (Skinner et al. 2006) as well as the indigenous people (Lake 2013). Before the 1900s, fires were ignited and managed by indigenous tribes, ranchers, and foresters, maintaining a frequent, mixed severity fire regime (Lake 2013; Skinner et al. 2006; Whittaker 1960). In 1911, fires were discouraged by the Weeks Act, and by the 1920s, fires were actively suppressed in accessible areas, with remote fires remaining unchecked until 1945, with the advent of enhanced firefighting equipment (Skinner et al. 2006). Since the implementation of fire suppression, fire frequency decreased dramatically, resulting in a sharp decrease in annual area burned (Miller et al. 2012; Skinner et al. 2006; Taylor and Skinner 1998).

The change in fire frequency also led to a change in forest structure, with oaks becoming overtopped, and meadows getting encroached upon by conifers. This resulted in a decrease in forest complexity, with denser, more homogenous forests, and smaller forest openings (Skinner 1995; Taylor and Skinner 1998).

2.3 Field Data

Field plots were established and measured during the summer of 2015. Plot locations were chosen based on a stratified random sample, which sorted stands in the four focal areas by 1) management history - heavily managed plantations versus less managed or natural, identified by the CalVeg database (USDA Forest Service - Pacific Southwest Region - Remote Sensing Lab 2010); 2) insolation - high versus low, with a cutoff of 1,175,000 watt-hours per square meter; and 3) stand size – small and large for managed stands with a quadratic mean diameter break at 25 cm; small, medium, and large for less managed stands, with breakpoints at 30 cm and 61 cm, respectively. This yielded 10 different strata combinations, or stand types. More common stand types were assigned more plots, but rare types still contained at least three plots. Plot locations were limited to areas with <45% slope, between 25 m and 200 m from the nearest road, at least 25 m from all stand boundaries (where forest type changes), and with at least 100 m between plots. These limits were established to ensure the safety of the

field crew and reduce travel time to plots to maximize plots collected. Sixty plots were established and measured during the 2015 field season.

Plot centers were recorded with a Trimble Geo 7X with a Tempest antenna. One thousand points per plot were collected, followed by differential correction with a PDOP filter of 4. This resulted in plot center coordinates with an average horizontal precision of 87 cm. While the positional accuracies of the differential GPS and of the LiDAR data are high (sub-meter), their additive error creates an inconsistent misalignment between the two datasets. Because the accuracy of the predictive models relies heavily on the ground data lining up with LiDAR, I tested and adjusted plot center coordinates using mapped tall tree crowns. The distance and azimuth from plot center were measured to at least five tall, dominant conifers whose crowns reached above the main canopy and therefore would be apparent in the LiDAR canopy height model (CHM). Many of these identification trees fall outside the plot boundary. The distances to trees were measured using a TruPulse 360 laser rangefinder with an average error of +/- 30 cm, thus the local accuracy of the stem map's geometry far exceeds the accuracy of the GPS or the LiDAR measurements. The stem maps—plot centers and locations of non-leaning trees—were incorporated into a GIS based on the plot centers' GPS positions, and then compared to the CHM generated by the LiDAR point cloud. All tree characteristics recorded in the field, including a unique ID number, tree height, species, DBH, and lean, were added to the GIS to help with the CHM comparison. The CHM was generated at 25 cm pixel resolution to correct for possible GPS-LiDAR misalignment.

In general, the tree positions in the CHM were close to the tree positions derived from the GPS; however, in a number of instances, the tree configuration apparent in the CHM was clearly different than the ground data. Plot locations were only shifted if an improved location fit was apparent. The combination of individual plot center and trees associated with that plot were moved manually and as a unit. Only x-y shift was applied (no stretching or warping) until the new fit between GPS trees and the CHM was optimal. I cross-checked the alignment of the shifted plot using tree heights as measured on the ground vs. the local maxima of the LiDAR-derived CHM. Table A.3 shows the horizontal precision reported for each plot, as well as the distance of plot shift. Of the 60 plots, 45 were shifted an average of 3.3 m. The average shift distance for all plots, including those that were unshifted, was 2.5 m. Figure 17 shows an example case of plot shifting. In this example, some trees and part of the unshifted plot fall on the road, whereas trees in the shifted plot line up with the LiDAR-derived canopy height model. Each plot center was intentionally located at least 25 m from roads, proving that the plot center as measured by the GPS does not line up with the LiDAR data. Had the unshifted plot been used, model accuracy would have been reduced due to the inclusion of road in the LiDAR point cloud.

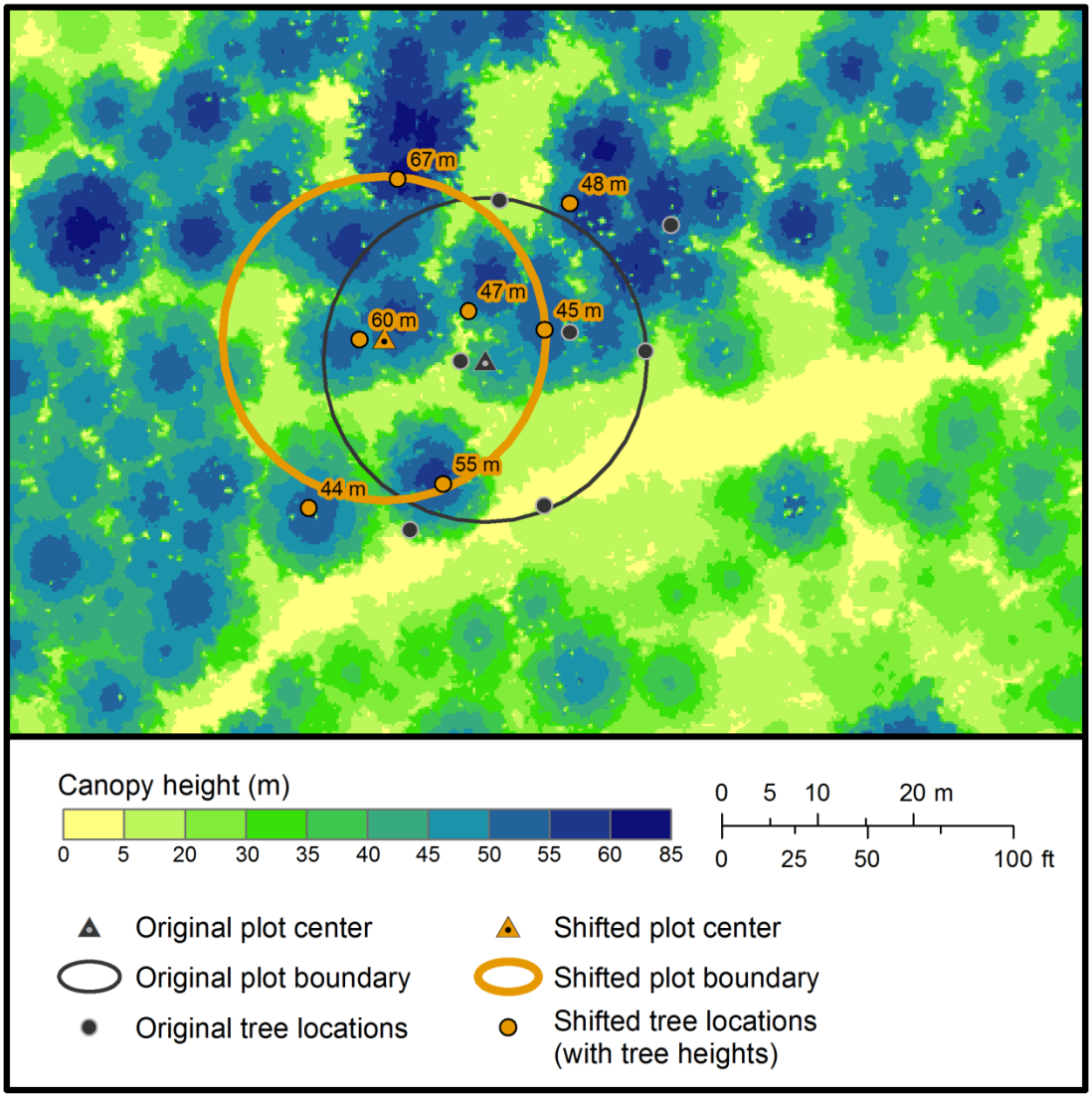

Figure 17. The original plot location and new, shifted plot location are shown with the locations of mapped tall trees in relation to plot center. Tree heights are shown with the shifted tree locations.

Plots used a 16.93 m radius to produce a plot area of 900 m^2. While a suite of measurements was taken at each plot, the only measures used by this study were a set of 4 photographs. A banner, measuring 4 m tall x 0.5 m wide with 1 m vertical gradations, was placed at plot center and a photograph was taken from plot edge at each cardinal direction towards the center with a T70h Android Quadcore Rugged Tablet. The photos were taken from eye-level, so camera height varied between 1.5 and 2 m. Figure 18A shows an example of one of these photos in an area with low ladder fuel density.

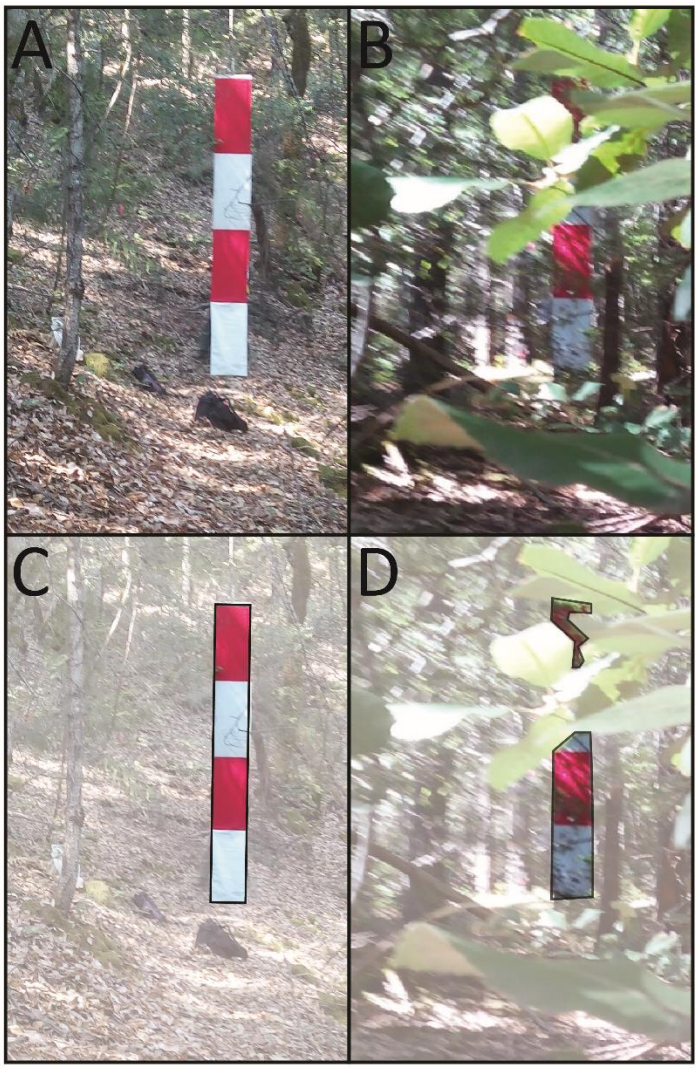

Figure 18. Examples of photos used to analyze ladder fuel density (18A and 18B) and their respective analysis boundaries (18C and 18D, respectively). Areas left out of analysis are faded out in 18C and 18D, whereas areas included in analysis are outlined in black. Figures 18A and 18B both show plots with low ladder fuels. 18A's banner is unobstructed, while the banner in 18B is partially obscured by tanoak leaves close to the camera lens, leading to only part of the banner being used for analysis, shown in 18D.

Ladder fuel density in each 1 m vertical segment of each photo was separately analyzed by four different technicians. I utilized a standard ocular estimation technique for estimating canopy cover as a proxy for estimating ladder fuel density. Cover estimates were binned into 6 classes between 0 and 100%, shown in Figure 19. One cover class was assigned to each 1 m vertical segment of banner that best approximated ladder fuel density as shown by the photo for that 1 m tall x 0.5 m wide section of banner.

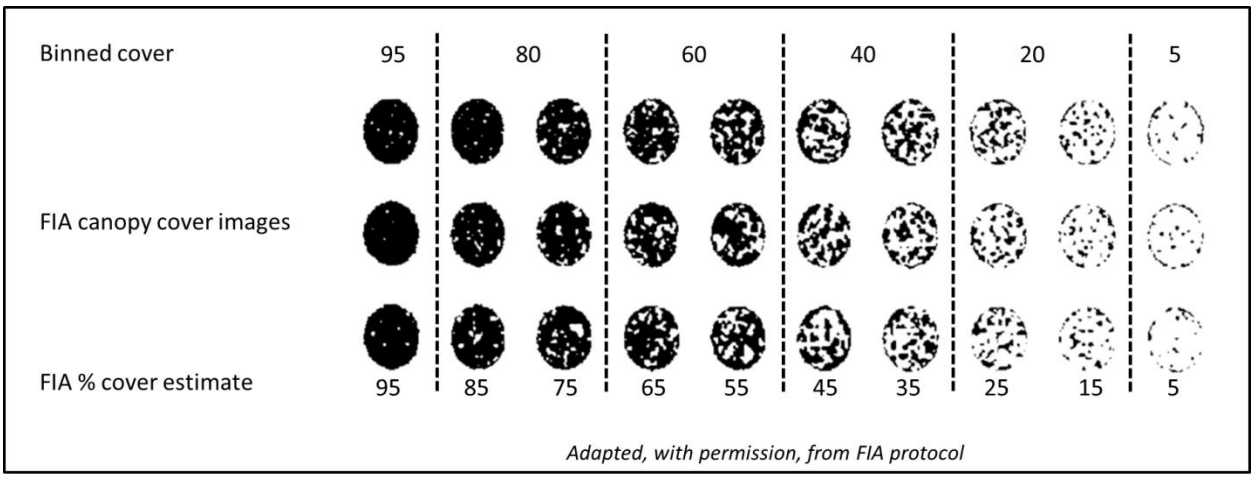

Figure 19. Binned cover estimates, used to approximate ladder fuel density. A canopy cover image series was adapted from Forest Inventory and Analysis (FIA) protocol (Schomaker et al. 2007), and binned into 6 cover classes. The cover estimates for each image set is shown at the bottom, and the average cover in each bin is shown at the top of each class. This was also the diagram used to assist technicians in assigning cover estimates.

To maintain consistency between estimates, photo-analysis periods were limited to 45 minutes. At the start of each session, technicians had to pass a cover estimation calibration test – scoring 5 correct estimates in a row. Correct classifications for analysts' tests were determined by an accurate assignment of a sample cover image, (one of the 30 shown in Figure 19), to a class designation (the 6 classes shown in Figure 19). To assist technicians with their estimates, they were provided with a printout of Figure 19, which served as a reference for their analysis.

To maintain a focus on ladder fuels and eliminate the complications of perspective (a leaf near the camera lens sometimes covered an entire 1 m section of the banner), a 10% rule was established, whereby, if the banner area covered by a single object was more than 10% of a 1 m banner section, that area was removed from analysis. This addressed potential error introduced by tree boles in front of the banner, as well as leaves and smaller branches that were close to the camera lens and thus took up a larger than appropriate area on the banner. One example of this rule is demonstrated by Figure 18B (the raw photo) and 18D (with unanalyzed area greyed out), where the banner is partially obscured by tanoak leaves close to the camera lens and the 10% rule was used. In this case, all large tanoak leaves were eliminated from analysis (shown in Figure 18D) because each leaf obscured over 10% of a banner 1 m segment. Ultimately, 18A was analyzed as having 5% cover (the lowest class) in all height bins; 18B was analyzed as having 20% cover from 0-1 m, 33% cover from 1-2 m, too little banner to determine cover from 2-3 m, and 27% cover from 3-4 m.

Because 4 independent technicians estimated the percent cover in each 1 m section of each photo, estimates often were not in perfect agreement. In cases where estimates differed

by more than 2 consecutive bins (15% of samples), photos were re-assessed by a pair of technicians, who added a 5th measure to the set of estimates. Estimates for each 1 m segment of each photo were then averaged and used for further analysis.

2.3 LiDAR Data and Processing

Quantum Spatial collected aerial LiDAR between May 23 and May 26, 2015. A Leica ALS70 laser system mounted on a Cessna was used to collect LiDAR points utilizing a scan angle of ± 15° from nadir. A pulse rate of 172 kHz, with unlimited returns per pulse (though often no more than 5) was used, averaging 8 pulses per m 2. IPAS TC v.3.1, ALS Post Processing Software v.2.75, Waypoint Inertial Explorer v.8.5, Leica Cloudpro v.1.2.1, and the TerraSolid software suite v.14&v.15 were used to calculate point positions, classify points, and test spatial accuracy of the point cloud by Quantum Spatial (Quantum Spatial 2015). The vendor reported that average vertical and horizontal accuracy were 5.7 cm and 0.9 cm, respectively, based on the mean divergence of points from ground survey point coordinates (60 ground survey points were collected and compared to measured LiDAR ground points across the study area).

LiDAR metrics were extracted for each 900 m^2 plot using LasTools (Isenburg 2011). Metrics included basic point statistics (9 metrics), percentile heights (8 metrics), and relative percent cover values (40 metrics), yielding a total of 57 LiDAR-derived metrics (see Appendix Table A.4 for a detailed breakdown). Relative percent cover values were calculated for a range of 20 strata each for first returns and all returns. A visual representation of this suite of values is shown in Figure 20. Rasters of each LiDAR-derived metric were also generated at a spatial resolution of 30 m to be used to make predictions across the landscape.

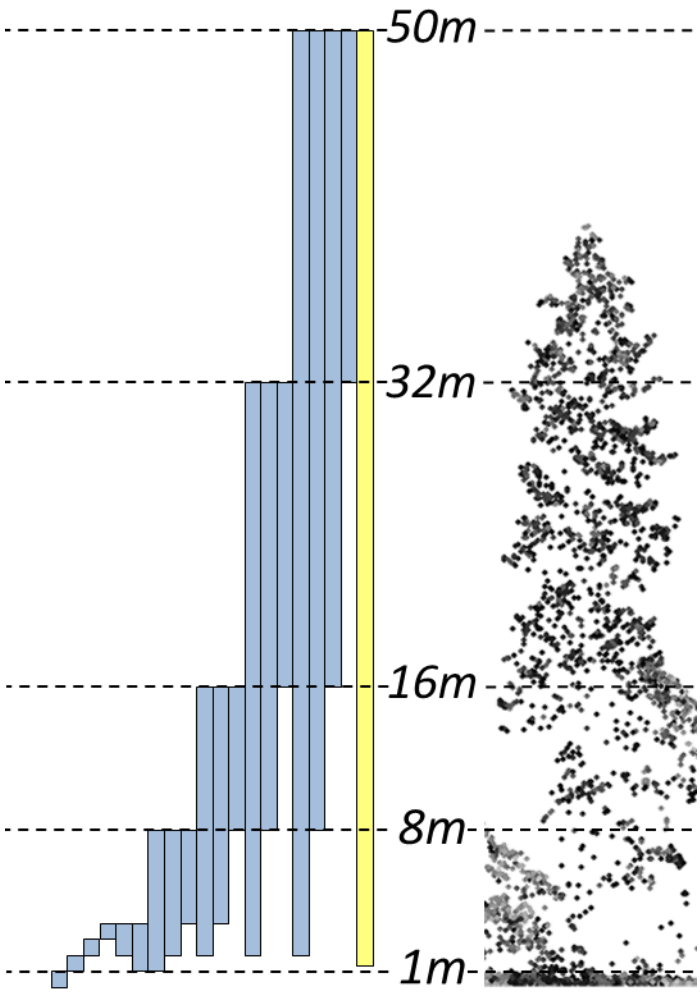

Figure 20. Relative percent cover strata are represented by each bar. For example, the most familiar metric is the percent cover, highlighted in the figure above. This metric is calculated as the number of LiDAR hits over breast height (1.37 m – 50 m) divided by the total number of LiDAR hits. These 20 metrics represent only a portion of LiDAR-derived metrics calculated, in addition to basic point statistics and percentile heights. These strata percent cover values were calculated for both first and all LiDAR returns (representing 40 of the 57 metrics calculated).

2.5 Statistical analysis

The workflow through plot and LiDAR processing is summarized in Figure 21. Average ladder fuel density was calculated for each 1 m height band in each photo by averaging the estimates of the four photo-interpretation technicians. To determine whether plots were sufficiently sampled, the R software program (R Development Core Team 2008) was used to calculate the standard error of ladder fuel density among the four photos for a given plot, for

each 1 m height stratum. This was done for a random sample of 2, 3, and 4 photo samples to examine whether repeated sampling per plot decreased standard error and increased the reliability of this measure.

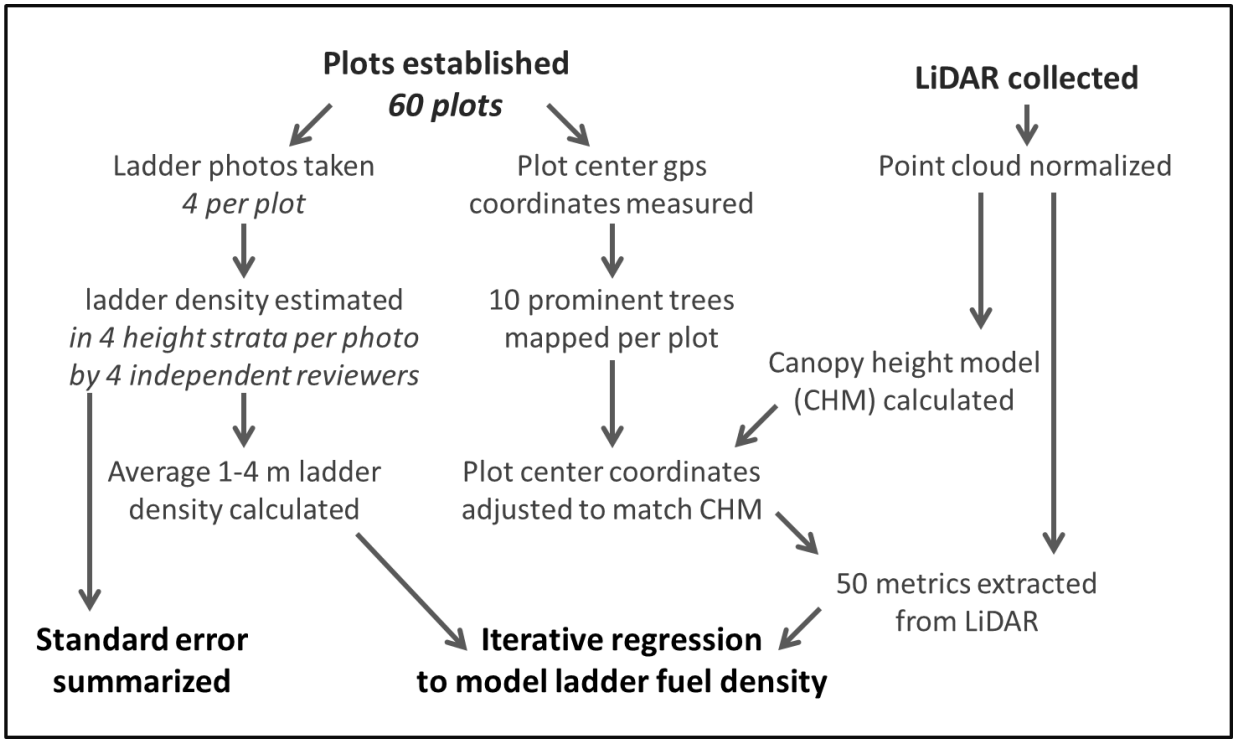

Figure 21. My detailed workflow illustrates how I used plots and LiDAR to answer my key questions.

For all subsequent analyses, the four estimates for each 1 m height band (one from each cardinal direction) were averaged to produce a single estimate of ladder cover for each 1 m height band in each plot. These data were used to examine the distribution of ladder fuels in each 1 m height band across the study area. Ladder fuel estimates between 1 and 4 m were then averaged for each plot to produce a dependent variable, upon which to build a regression model using LiDAR. Cover below 1 m was left out of this measure since fuels in this range are commonly defined as surface fuels. LiDAR is also less precise at differentiating ground points from low points within 1 m of the ground, and these points are often removed from analysis, though many different thresholds have been used (Hudak et al. 2006; Hudak et al. 2012; Kane et al. 2013; McGaughey 2012).

Because LiDAR-derived independent variables were highly correlated, an iterative model building approach was taken. 1) The best regression models using one to four independent variables were chosen using the leaps package in R (Lumley and Miller 2009). 2) Each model was evaluated for variable collinearity (correlation >0.6 in either Pearson or Spearman correlations was used to indicate collinear variables) and variable significance ($p<0.05$). Only models where all independent variables were significant and none were collinear with one

another were kept. 3) The leaps package was used to find the best non-collinear independent variable to add to each model. 4) The process was repeated for all potential models until independent variables were no longer all significant. 5) The model with the best adjusted R-squared value was chosen from these models. 6) This model was tested for heteroscedasticity (where the variability across the range of a regression is not consistent across the range of values) using the Breusch–Pagan test (Breusch and Pagan 1979). R-squared, root mean squared error (RMSE), and a 10-fold cross-validation error using the CVTools package in R (Alfons 2012) were calculated to evaluate the fit of the final model.

After a model was created, LiDAR-derived rasters of each independent variable used by the model were generated at 30 m resolution. This spatial resolution was chosen to match the plot size of 900 m^2. A new 30 m raster of predicted ladder fuel density was then generated for the entire study area.

3. Results

3.1 Assessment of photo-banner

To determine whether each plot had been sufficiently sampled, I calculated the standard error between 2, 3, and 4 photo-estimates of ladder fuels at the same height within a single plot. Table 7 shows the distribution of these standard error measures of increasing sampling density across all plots for each height band.

	2 photos		3 photos		4 photos	
Height bin	**Average**	**Maximum**	**Average**	**Maximum**	**Average**	**Maximum**
0 to 1 m	8.24	30.00	9.09	24.73	8.10	19.51
1 to 2 m	8.84	41.25	7.95	23.75	7.72	19.46
2 to 3 m	9.34	32.50	7.54	21.79	6.44	15.72
3 to 4 m	9.94	37.50	7.67	22.42	6.79	15.54

Table 7. Average standard error between measures of ladder fuel density within a given plot and height bin are shown. I report the average standard error for 2, 3, and 4 photo samples for each 1 m band in each plot.

The variability of samples in the lowest height class (0-1 m) did not change much with increased sampling. With the lowest sampling density of only 2 photos per plot, standard error was highest for the highest height class, at 9.94. However, for all but the height class within 1 m of the ground, standard error decreased with every subsequent photo-sample added. Since I do not have more than four photos per plot, it is difficult to speculate where standard errors level off. However, based on the decrease in standard error of less than 1% from 3 to 4 photos in all height strata above 1 m, it appears that four photos may be sufficient. Average standard error for plots over 1 m, with 4 photo samples per plot, was only 6.98%. Considering that the estimates of ladder fuel density were derived from 6 classes (shown in Figure 19), with most classes representing a range of 20%, the low standard error was encouraging. These low values

suggest reasonable consistency between measurements, even between only 2 samples per plot.

Average ladder fuel density is summarized in Figure 22 for each height class, as well as a combination of height classes from 1 to 4 m. Average 1-4 m ladder fuel density was used in subsequent analyses to build a predictive model from LiDAR-derived metrics. The majority of plots had 1-4 m ladder fuel density between 21 and 45%, with a maximum value of 91%, and minimum value of 7%, showing a good representation of sparse ladder fuels, and a weak, though still present, representation of dense ladder fuels.

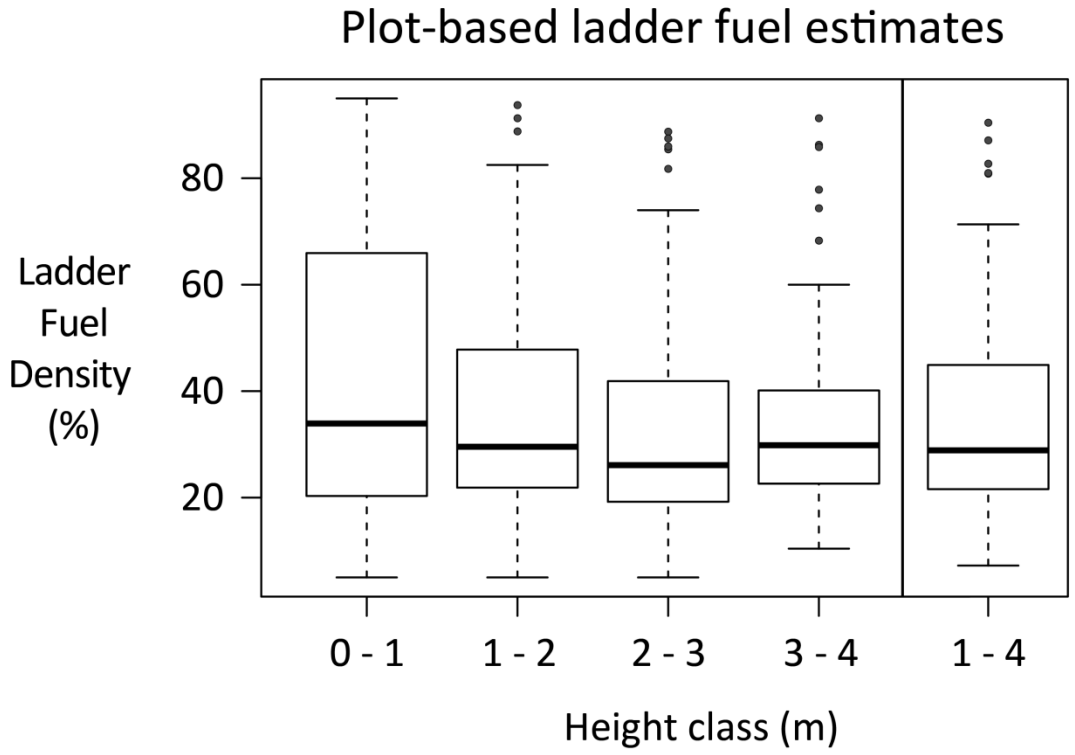

Figure 22. A box-and-whisker plot that displays the distribution of ladder fuel density within each 1 m class across all plots is shown. I also include the average ladder fuel density between 1 and 4 m in each plot.

3.2 Linking LiDAR to ground-based measures

Using the iterative model-building approach described, I built a multiple regression, shown in Equation 3, where independent variables included the percentage of all points between 1 and 8 m (COV1_8), the standard deviation of point heights above 2 meters (STD), and the percentage of first return points between 8 and 16 m (FCOV8_16). All model variables, as well as the model as a whole, were significant at $p<0.05$, with an R-squared value of 0.73, root mean squared error of 9.92, and 10-fold cross-validation error of 10.57. Figure 23 shows a scatterplot of the predicted versus measured values of ladder fuel density, using Equation 3.

Ladder fuels = 20.41 + 0.873*(COV1_8) - 1.73*(STD) - 0.189*(FCOV8_16) **Eqn. 3**

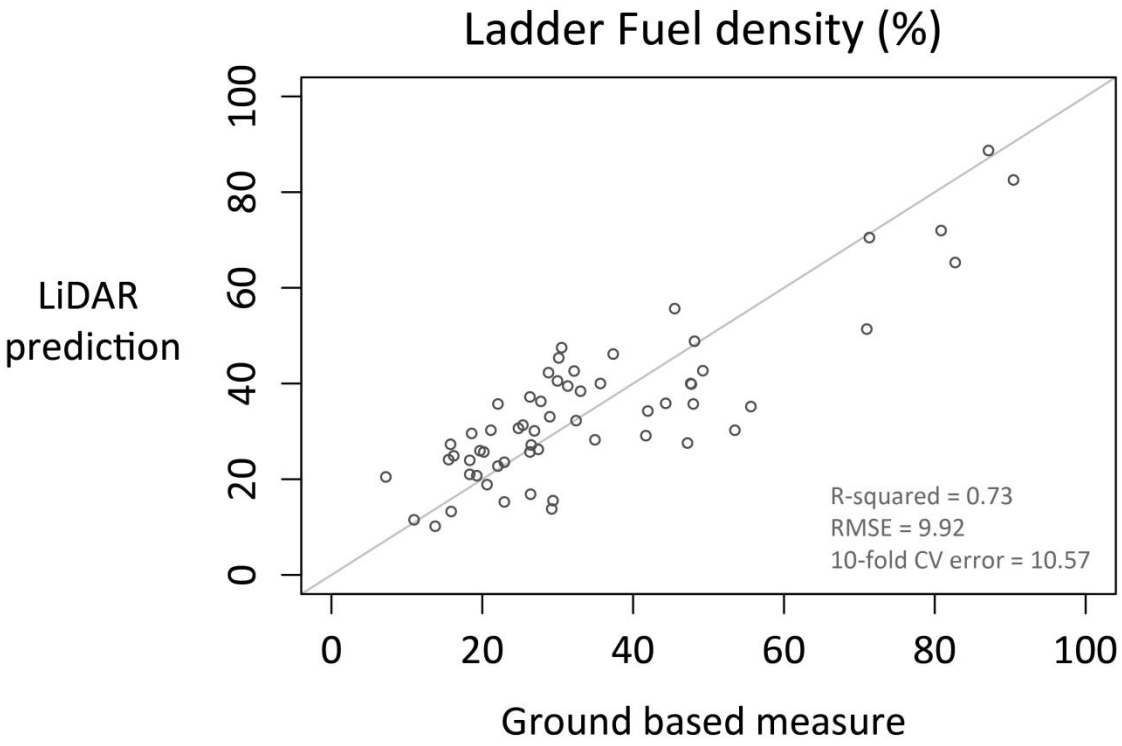

Figure 23. Ladder fuel density derived from the LiDAR point cloud is compared to ground-based measurements. This model is significant at the $p<0.05$ level, with an R-squared value of 0.73, root mean squared error of roughly 10%, and 10-fold cross-validation error of roughly 11%. The ground-based measurements range between 7% and 91% ladder fuel density.

Equation 3 was used to predict ladder fuel density across the entire study area, and is shown in Figure 24. Predicted ladder fuel density ranged from -8 to 99% across the four focal areas, with an average of 36.6% and standard deviation of 15.9%. Although some areas had predicted ladder fuel density under 0%, these only represented 0.12% of the total study area. While most areas have moderate to low densities of ladder fuels, a few areas have pockets with very high ladder fuel densities. The top 10% of ladder fuels in the study area encompassed predicted densities between 58% and 100%, and were concentrated in focal areas C and D. Table 8 displays the average ladder fuel density for each focal area, and the proportion of each focal area with exceptionally dense ladder fuels (in the top 10% of predicted values for the study area). Average ladder fuel density ranged between 31% and 40% across the 4 focal areas, but area D had, by far, the greatest proportion of dense ladder fuels, having over 4 times as much as area A where ladder fuel density was over the 90th percentile. Since area D has the highest human population density, it is especially critical to identify these pockets of dense ladder fuels for fire planning and mitigation.

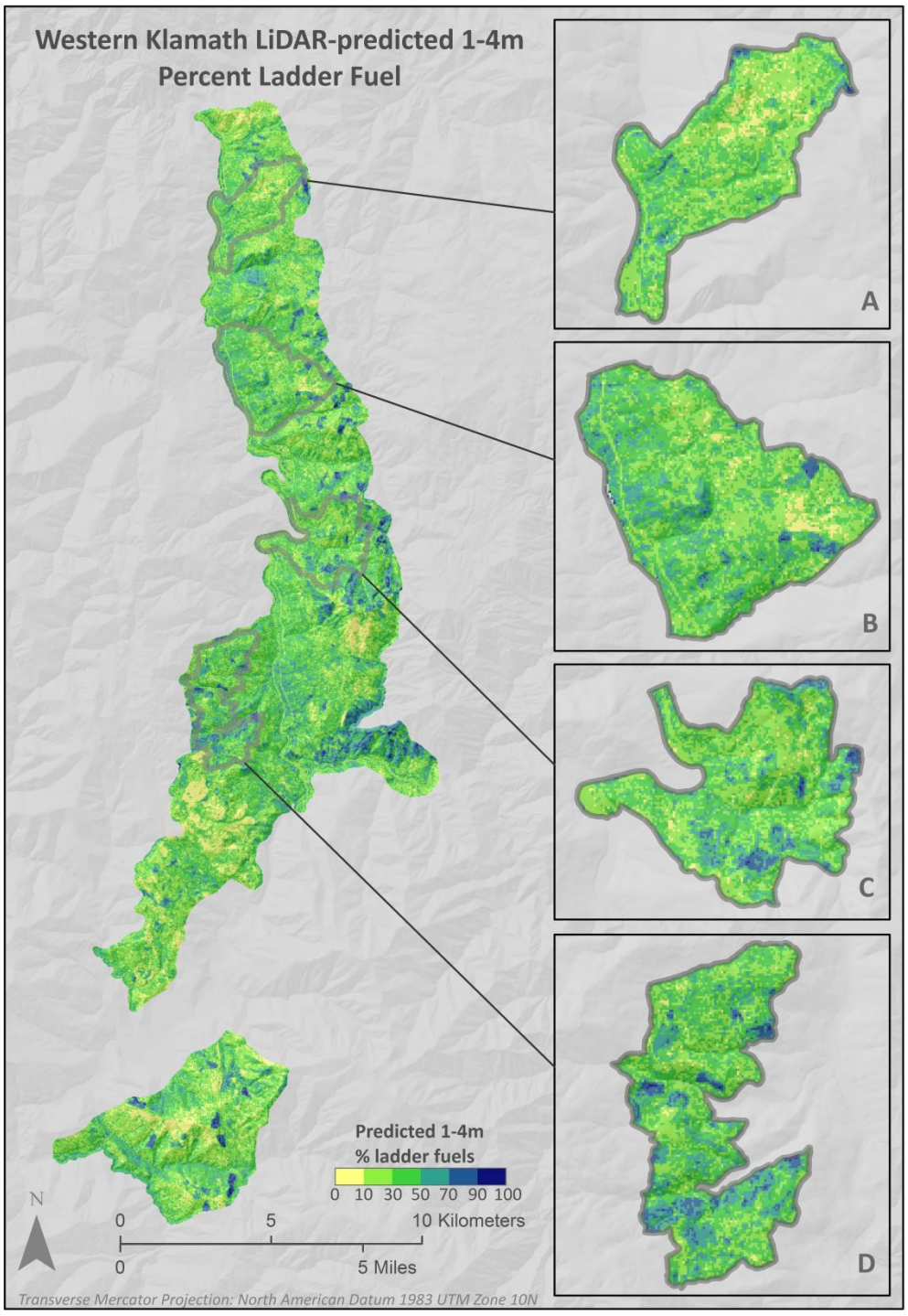

Figure 24. Ladder fuel density, as predicted from the LiDAR point cloud using Equation 3, is displayed across the study area.

Focal Area	Average ladder fuel density (%)	% area above 90th percentile ladder fuel density
A	31.53	3.89
B	36.27	6.59
C	36.61	10.23
D	40.99	16.02

Table 8. Average ladder fuel density in the four focal areas, as well as the proportion of each focal area with ladder fuel density in the top 10% (58 - 100% ladder fuel density) for the entire study area, are shown.

4. Discussion

I developed an improved ground-based method for quantifying ladder fuels using an ocular estimate of ladder fuel density. Not only is this method a more quantitative approach to ladder fuels measurement than the 5-class system developed by Menning et al. (2007), but it is also a promising method for change detection. Because my estimation relied on calibrated field photographs, my methods could be repeated in plots over time or after treatment or fire. The resulting series of photos taken in field plots could be utilized to record a quantitative change in ladder fuels, but could also serve as a visual indication of change, with a consistent and apparent measure of scale. In the study area ladder fuels were fairly consistent within most plots, with low standard error between estimates. However, to minimize standard error in all plots in the study area, my results suggested collecting at least 3 samples per plot to bring the average standard error in plots (for 1 m bands over 1 m) below 8% and bring the maximum standard error near 20% (the size of most of the ladder fuel bins).

Using the relative ladder fuel density derived from this ground-based measure, I built a robust model that predicted this value from the LiDAR point cloud with reasonable precision. This landscape-scale prediction also identified areas where there are pockets of uncharacteristically dense ladder fuels. Although it is out of the scope of this study to further investigate these areas, they indicate locations where efforts to mitigate ladder fuel hazard could be prioritized. While this measurement is not a direct input for current fire models, I believe that it holds much potential for landscape monitoring, fuels management, cultural resource identification and protection, and the evaluation of wildland fire risk. This method is robust, quantitative, repeatable, fairly inexpensive (10 person-minutes in the field plus 16 in the office per plot (assuming 4 independent assessments per photo)), and is based on direct observation (i.e., does not rely on allometry).

4.3 Immediate implications for managers

Managers can use these methods for ground-based ladder fuels characterization to establish a baseline for ladder fuels across their management area and return to these plots to remeasure ladder fuels after change, similar to photographic monitoring used for evaluating fuels treatment and wildland fire effects (Vaillant et al. 2013). Although these photographic methods require some analysis in the office, they are efficient to implement in the field, and

provide a visual reference for each plot for further analysis or evaluation of change over time. Mechanical and/or prescribed fire fuel reduction treatments are planned throughout this study area, likely including several areas that overlap the plots. Plot remeasurement is planned post-treatment to assist in evaluating treatment effectiveness. Not only is this a quantitative measure of change, but also a visual indication, since plot photos, with consistent scale, are byproducts of plot measurement. This will allow for robust quantification of change in ladder fuel density at the plot scale, and if LiDAR data collection is repeated, at the landscape scale as well.

Knowledge of the locations of areas with especially dense ladder fuels (such as those with ladder fuel density in the 90^{th} percentile for the study area) can be invaluable for prioritizing fuel reduction to facilitate community safety and fire preparedness. If areas of dense ladder fuels are near communities or evacuation routes (especially along routes that represent the only evacuation corridor for residents), these areas of dense ladder fuels could be targeted for fuel reduction or flagged as potentially hazardous for crown fire if a wildland fire were to occur in the area. Making these high-risk areas known to residents and fire managers could improve safety on large fires that threaten these communities in the wildland urban interface. Information about dense pockets of ladder fuels can also be useful to firefighters on the ground, for risk assessment of crown fire, ease of cutting fireline, and accessibility to and mobility through these areas, especially if they are to be traversed to get to a safety zone. My results directly inform land management, including treatment prioritization at the landscape scale within the Western Klamath Restoration Partnership Zones of Agreement (Harling and Tripp 2014).

For wildlife that require understory structural complexity such as fishers, these data could also be valuable (Zielinski et al. 2010). From a cultural perspective, which is especially important in the communities surrounding the study area, these results will be used to mitigate potential impacts from fire near valuable cultural resources, both historic and present (Hummel and Lake 2015; Lake 2013). These resources could include archaeological, heritage, and tribal sacred sites, as well as legacy oaks that provide a traditional food source, but are also critical habitat elements (Anderson 2005; Long et al. 2015). Thinning and prescribed fire treatments to enhance these cultural resources that are at elevated risk of intense wildland fire will be facilitated by my predictive map of ladder fuel density across the landscape. Because areas with lower densities of surface and ladder fuels facilitate enhanced accessibility, these areas are preferred by traditional gatherers, as suggested by Hummel and Lake (Hummel and Lake 2015). My work to predict the density of ladder fuels could be used to identify especially open understories that may be valuable for identifying gathering locations for (non-timber) forest products and associated ecological services for the community, tribes and public (Barbour et al. 2007; Burger et al. 2008).

Beyond the immediate implications of this work, this photographic technique, as well as the relationship I built between ground measures and the LiDAR point cloud, represents a new method to quantify an important fuel source that has been so elusive to previous fire behavior models that an allometric proxy was implemented in the place of a quantitative measure based on fuels actually present. Although Kane et al. (2015) were not able to find a significant

relationship between standard forest structure metrics and fire severity, I encourage further investigation into whether this estimation of ladder fuel density has any predictive power over fire behavior and effects. It will be particularly useful to test whether these methods for estimating ladder fuels can be used to explain observed fire severity in areas where pre-fire LiDAR data are available.

4.4 Study Limitations

While photo interpretation methods were robust, I did not show that the estimate relates to any specific measure on the ground, such as ladder fuel bulk density. Therefore, this model was only useful for predicting the relative amount of ladder fuels, and should not be used to predict specific quantities of fuel. Photo interpretation methods also contained numerous inherent sources of error, including 1) slope distorting the apparent height of ladder fuels, 2) objects in the foreground appearing disproportionately large, 3) using standard focal length settings, which could alter relative object sizes in the photo (Hoiem et al. 2008), and 4) photo interpreter error. I also noticed a moderate degree of inaccuracy, averaging 2.5 m (up to 15 m for some plots), between the LiDAR and the ground-based measures of tree locations. While I attempted to mitigate this error by shifting plot center GPS coordinates based on the mapped height of tall trees in relation to plot center, there are likely still inaccuracies between the plot measured on the ground and the LiDAR point cloud extracted from each plot perimeter. Furthermore, only a single study area was used, introducing the potential for locational bias in my analysis. Because my study area was a single sample of the landscape, results from this study should not be applied to other areas without first collecting ground reference data, testing the relationship, and adjusting where necessary to ensure accurate model estimates.

This research also emphasizes the need for better accuracy assessment of plot center coordinates for LiDAR-based studies. LiDAR vertical accuracy was reported to be 5.7 cm. Despite the use of a high-accuracy GPS with antenna, collecting at least 1,000 estimates per plot, using differential correction, and receiving an average horizontal precision of 87 cm, plot centers were still mis-aligned with the LiDAR data by an average of over 2.5 m, and up to at least 15 m. I urge those that work with LiDAR to assess how well recorded plot centers line up with the LiDAR point cloud and take measures to better match the plot to the LiDAR before undertaking further analyses. This is especially important when plots are located in heterogeneous landscapes or near roads, and when plot sizes are small (so a small shift in plot center equates to a dramatically different area of the LiDAR point cloud). While some LiDAR-derived metrics are not as sensitive to shifts in plot center location (Kramer et al. in review), many likely are, and plot accuracy should be better accounted for in all cases.

4.5 Future Research

This research demonstrated the importance of matching plot data to the LiDAR point cloud. I urge others to pursue further research into the best practices of measuring and addressing error when working with the LiDAR point cloud.

I am eager to further explore the ability of LiDAR to predict ladder fuel density, and plan to work more extensively with land managers and community members in this area to discuss ways to best utilize the products from these analyses. I urge others to experiment with these methods, not only as a way to estimate ladder fuels, which are important to the field of wildland fire, but also as a monitoring method for plot vegetation and fuel loading, as well as for the enhancement of access to and the quality of cultural resources.

I encourage others to test this metric against fire behavior to determine its influence on the likelihood of crown fire, and hope that fire behavior models will incorporate some version of this metric to further refine future wildland fire behavior and effects models.

5. Conclusions

Ladder fuels are an important piece of fire behavior and effects modeling. However, because they are difficult to quantify in the field, ladder fuels are indirectly measured through allometric equations that estimate canopy base height, leaving out the shrubs and small trees that are a large component of ladder fuels in many forests. This work presents a new ground-based method for estimating ladder fuels and establishes a strong predictive link with aerial LiDAR. I was able to predict the ground-based estimates of ladder fuel density from aerial LiDAR with an R-squared value of 0.73. I also demonstrate that plot center accuracy must be independently tested, and urge LiDAR users to critically compare their plot locations to the LiDAR point cloud.

Acknowledgements

Thanks to my co-authors Brandon Collins, Frank Lake, Marek Jakubowski, Scott Stephens, and Maggi Kelly. I thank the Western Klamath Restoration Partnership for sharing their LiDAR dataset and assisting with plot data collection, with specific thanks to Kenny Sauve, Jill Beckmann (Karuk Tribe, GIS analysts), and Mid Klamath Watershed Council plot crew (Chris Root, Skip Lowrey, Eric Nelson, Shan Davis, and Tony Dennis) for their hard work establishing and collecting plot data. I acknowledge Deer Creek GIS for helping get this project started. I also thank Alexis Bernal and Aseem Singh for their assistance with photo interpretation. Much thanks to Martin Isenburg and LAStools, as well as the LASmoons grant, for use of the software program, LAStools. Joan Canfield contributed comments that improved this paper. This work is supported by the Western Klamath Restoration Partnership, which is supported by Promoting Ecosystem Resiliency through Collaboration: Landscapes, Learning and Restoration, a cooperative agreement between The Nature Conservancy, USDA Forest Service and agencies of the Department of the Interior, as well as by the California Department of Fish and Wildlife and the US Fish and Wildlife Service. This material is also based upon work supported by the National Science Foundation Graduate Research Fellowship Program under Grant No. DGE 1106400.

Chapter 5: Conclusion

LiDAR is an important technology that is being utilized at an increasing rate by land managers and fire modelers. Despite this growth, there is still untapped potential in the LiDAR point cloud. My research explores some of these facets, making LiDAR-derived products more accessible to managers and exploring LiDAR's potential to estimate ladder fuels that contribute to extreme fire behavior and effects.

The contribution of my research is to:

1) Make LiDAR more accessible to managers by using creative metrics that do not rely on LiDAR processing beyond that completed by the vendor;
2) Utilize LiDAR to derive new metrics that elucidate forest structure in ways not possible with other forms of remote sensing.

To increase LiDAR accessibility for managers, my second chapter examines the utility of the canopy height model for calculating large tree density that is critical for mapping wildlife habitat, especially for species like the California spotted owl. The canopy height model is far more accessible to managers because it is a raster layer derived from LiDAR that is often derived by the LiDAR vendor and delivered alongside the raw point cloud data. This eliminates the need for LiDAR processing software and expertise, and allows managers with only basic GIS resources to derive valuable metrics from LiDAR-derived products. While resources such as the Remote Sensing Lab for the US Forest Service exist that can complete LiDAR processing requests, my methods eliminate this step entirely, and simplify the process for managers interested in estimating large tree density.

My third and fourth chapters dig into the LiDAR data to examine how well it is able to predict ladder fuels that carry fire from the surface of the ground into the canopy. These fuels are critical for fire behavior models, yet are not directly measured, either on the ground, or through remote sensing. Instead, allometric equations are utilized to estimate canopy base height as a surrogate for ladder fuel density, which, in turn, lead to a number of inaccuracies in fire behavior modeling. I investigate whether LiDAR can provide a more quantitative estimate that could augment fire models in the future.

My third chapter investigates the potential utility for LiDAR to differentiate between areas with high and low densities of ladder fuel. After showing this to be the case, my fourth chapter develops a field based method for quantifying ladder fuel density, then successfully relates those estimates with LiDAR. This work shows that LiDAR can be used to estimate ladder fuel density, which could improve the accuracy of fire models used in the US and abroad.

Not only are fire models important for studying fire itself, but they are also critical for planning fire prevention and suppression activities to protect life and property from wildland fire. My predictions of ladder fuel density will be utilized by managers to aid in

the planning of fuels reduction treatments around communities in the Klamath. In addition to aiding with wildland fire prevention and suppression, predictions of fire behavior and effects help facilitate managed wildfire and prescribed fires, allowing fires to reenter the forests where they are so critically needed, especially in the face of climate change.

My dissertation demonstrates some of the untapped potential of LiDAR. I show that metrics such as ladder fuel density can be successfully estimated across the landscape. I also show that an alternate (and much less technical) method for calculating large tree density from the canopy height model was equally accurate as a model built from a suite of LiDAR-derived metrics that require LiDAR software and expertise to extract.

Besides deriving the density of large trees and ladder fuels, I have also demonstrated the strengths and limitations of LiDAR data use for land managers, and suggested some novel methods for using historic datasets to make more plots available to managers, depending on the LiDAR product in which they are interested. My second chapter shows that older plots, which may not be ideal for traditional LiDAR-based derivations due to imprecise data or inaccurate plot center coordinates, can still be useful for other variable derivations, such as large tree density. By utilizing this data source, I show that more information is available to the land manager than what strictly meets LiDAR best-practices protocol. Conversely, my fourth chapter demonstrates that conventional methods for obtaining an accurate plot center may not be sufficient. I show that conventional methods do not always grant an exact match with the LiDAR point cloud, and can add a large degree of error to subsequent LiDAR analyses when plots are located near human-altered areas such as roads. I stress the importance of keeping these factors in mind when approaching a LiDAR analysis, and I encourage others to explore their plot data and think critically about what can be compared to available LiDAR data.

Moving forward, additional studies will be required to test these methods on different study areas and forest types. Because of the variable quality of LiDAR available to land managers, investigation of the necessary point density to make accurate predictions is also essential. For my work with both large tree density and ladder fuels, I encourage scientists and land managers to incorporate these methods and findings into habitat models for the California spotted owl (*Strix occidentalis occidentalis*) and other rare species for which large trees, low cover, mobility through the forest, and other factors associated with my derived metrics are important. For my work with ladder fuels, I urge others to experiment with my methods, not only as a way to estimate ladder fuels, which are important to the field of wildland fire, but also as a monitoring method for plot vegetation and fuel loading, as well as for the enhancement of access to and the quality of cultural resources. I hope that estimates of ladder fuels will be compared in burned areas to assess whether this metric could aid in fire modeling, and if so, it is my hope that wildland fire behavior and effects models will incorporate some version of this metric. LiDAR is a powerful technology that holds much promise, and I encourage future LiDAR users to explore this remotely sensed product to its fullest potential!

Appendices

Table A.1. details of each transformation applied to dependent and independent variables to normalize their distributions.

Variable group	Individual variable description	Transformation
Basic point statistics	Maximum point height	none
	Average point height above 2 m	none
	Skewness of point heights above 2 m	*(variable)^1/2*
	Standard deviation of point heights above 2 m	none
	Variance of point heights above 2 m	log*(variable+1)*
Percentile Heights	Height of 5th percentile of points above 2 m	1/*variable*
	Height of 10th percentile of points above 2 m	log*(variable+1)*
	Height of 25th percentile of points above 2 m	log*(variable+1)*
	Height of 50th percentile of points above 2 m	*(variable)^1/2*
	Height of 75th percentile of points above 2 m	none
	Height of 90th percentile of points above 2 m	none
	Height of 95th percentile of points above 2 m	none
	Height of 99th percentile of points above 2 m	none
Height Strata	Returns 0.5 to 1.37 m / returns below 1.37 m	log*(variable+1)*
	Returns 1.37 to 2 m / returns below 2 m	*(variable)^1/3*
	Returns 2 to 4 m / returns below 4 m	*(variable)^1/2*
	Returns 4 to 8 m / returns below 8 m	none
	Returns 8 to 16 m / returns below 16 m	none
	Returns 16 to 32 m / returns below 32 m	none
	Returns 32 to 48 m / returns below 48 m	*(variable)^1/2*
	Returns above 48 m / total returns	*(variable)^1/2*
Canopy Height Derived Cover	Percent area where CHM > 26 m	*(variable)^1/2*
	Percent area where CHM > 28 m	*(variable)^1/2*
	Percent area where CHM > 30 m	*(variable)^1/2*
	Percent area where CHM > 32 m	*(variable)^1/2*
	Percent area where CHM > 34 m	*(variable)^1/2*
	Percent area where CHM > 36 m	*(variable)^1/2*
	Percent area where CHM > 38 m	*(variable)^1/2*

Table A.2. Description of the 53 LiDAR-derived metrics used as explanatory variables for the classification tree analysis. All metrics were calculated on a 30 m raster grid using FUSION(McGaughey 2012).

Metric group	Individual metric description
Basic point statistics	Maximum point height
	Minimum point height above 2 meters
	Average point height above 2 meters
	Mode of point heights above 2 meters
	Coefficient of variation of point heights above 2 meters
	Interquartile distance of point heights above 2 meters
	Skewness of point heights above 2 meters
	Standard deviation of point heights above 2 meters
	Variance of point heights above 2 meters
	Kurtosis of point heights above 2 meters
	Average Absolute Deviation of point heights above 2 meters
Return ratios	Percentage of first return point heights above the mean point height
	Percentage of first return point heights above the mode of point height
	Percentage of first return point heights above 3 meters
	Number of returns greater than the mean point height / total number of first returns
	Number of returns greater than the mode of point height / total number of first returns
	Number of returns greater than 3 meters / total number of first returns
	Percentage of point heights above the mean point height
	Percentage of point heights above the mode of point height
	Percentage of point heights above 3 meters
L-moment statistics	1st L-moment of point heights above 2 meters
	2nd L-moment of point heights above 2 meters
	3rd L-moment of point heights above 2 meters
	4th L-moment of point heights above 2 meters
	Coefficient of variation of L-moments of point heights above 2 meters
	Kurtosis of L-moments of point heights above 2 meters
	Skewness of L-moments of point heights above 2 meters
Percentile Heights	Height of 1st percentile of points above 2 meters
	Height of 5th percentile of points above 2 meters
	Height of 10th percentile of points above 2 meters
	Height of 20th percentile of points above 2 meters
	Height of 25th percentile of points above 2 meters

	Height of 30th percentile of points above 2 meters Height of 40th percentile of points above 2 meters Height of 50th percentile of points above 2 meters Height of 60th percentile of points above 2 meters Height of 70th percentile of points above 2 meters Height of 75th percentile of points above 2 meters Height of 80th percentile of points above 2 meters Height of 90th percentile of points above 2 meters Height of 95th percentile of points above 2 meters Height of 99th percentile of points above 2 meters
Height strata	Number of points between 2 and 4 meters / number of points below 4 meters Number of points between 4 and 8 meters / number of points below 8 meters Number of points between 8 and 16 meters / number of points below 16 meters Number of points between 16 and 32 meters / number of points below 32 meters Number of points between 32 and 48 meters / number of points below 48 meters Number of points above 48 meters / total number of points
Topography	Aspect Slope in degrees Plan curvature Profile curvature Solar radiation index

Table A.3. Reported plot center precision and distance of plot shift when stem-mapped trees were compared to the LiDAR-derived canopy height model are presented for each plot.

Plot ID	Horizontal precision (m)	Distance shifted (m)
D001	0.7	3.2
D104	0.2	0
D105	0.6	0.9
D011	1.1	0
D116	0.8	1.6
D117	0.8	2.9
D118	0.6	0
D124	2.2	5.1
D126	0.8	0
D133	0.2	1.9
D136	1.3	26.4
D015	1	3.0
D151	1	0
D018	0.9	2.9
D204	1	0
D234	0.8	0
D235	1.3	2.7
D250	0.9	3.1
D255	0.9	2.6
D027	0.7	1.0
D039	2.5	2.5
D040	0.7	0.6
D005	0.9	0
B002	1.2	10.8
B020	1	3.3
B021	0.3	0
B022	0.9	1.7
B024	0.9	0
B026	0.8	0.8
B029	0.9	2.1
B034	1.1	3.3
B004	0.7	1.9
B041	0.9	1.5
B042	0.8	1.9

B045	0.9	3.2
B046	0.7	6.6
B049	0.8	0
B050	0.9	2.8
C033	0.8	0
C110	0.8	0
C114	0.8	2.8
C131	0.7	3.1
C132	1	1.3
C139	1	1.9
C036	0.8	1.2
C120	0.7	2.0
C130	1	1.7
C137	0.2	2.9
C152	0.7	1.4
A010	0.6	0.8
A017	0.9	4.0
A207	0.7	2.4
A216	0.8	3.0
A023	0.6	5.8
A236	0.6	1.6
A238	1	8.2
A043	1	2.8
A047	1.1	0
A007	0.9	2.8
A009	0.9	0

Table A.4. Each LiDAR-derived variable is described

Variable group	Individual variable description
Basic point statistics	Maximum point height
	Average of point height above 2 meters
	Quadratic average of point height above 2 meters
	Skewness of point heights above 2 meters
	Standard deviation of point heights above 2 meters
	Kurtosis of point heights above 2 meters
Cover by vertical strata *calculated for first **and** all returns* = $\frac{\text{\# points in strata}}{\text{\# points in \& below strata}}$	Percentage of points between 1-2 m
	Percentage of points between 2-3 m
	Percentage of points between 3-4 m
	Percentage of points between 2-4 m
	Percentage of points between 1-4 m
	Percentage of points between 1-8 m
	Percentage of points between 2-8 m
	Percentage of points between 4-8 m
	Percentage of points between 2-16 m
	Percentage of points between 4-16 m
	Percentage of points between 8-16 m
	Percentage of points between 2-32 m
	Percentage of points between 4-32 m
	Percentage of points between 8-32 m
	Percentage of points between 16-32 m
	Percentage of points over breast height (1.37 m)
	Percentage of points over 2 m
	Percentage of points over 8 m
	Percentage of points over 16 m
	Percentage of points over 32 m
Percentile Heights	Height of 5th percentile of points above 2 meters
	Height of 10th percentile of points above 2 meters
	Height of 25th percentile of points above 2 meters
	Height of 50th percentile of points above 2 meters
	Height of 75th percentile of points above 2 meters
	Height of 90th percentile of points above 2 meters
	Height of 95th percentile of points above 2 meters
	Height of 99th percentile of points above 2 meters

References

Ackers, S.H., Davis, R.J., Olsen, K.A., & Dugger, K.M. (2015). The evolution of mapping habitat for northern spotted owls (Strix occidentalis caurina): A comparison of photo-interpreted, Landsat-based, and lidar-based habitat maps. *Remote Sensing of Environment, 156*, 361-373

Agee, J.K., & Skinner, C.N. (2005). Basic principles of forest fuel reduction treatments. *Forest Ecology and Management, 211*, 83-96

Alfons, A. (2012). cvTools: cross-validation tools for regression models. R package version 0.3.2. *Online at https://cran.r-project.org/web/packages/cvTools/index.html*

Andersen, H.-E., McGaughey, R.J., & Reutebuch, S.E. (2005). Estimating forest canopy fuel parameters using LIDAR data. *Remote Sensing of Environment, 94*, 441-449

Anderson, K. (2005). *Tending the wild: Native American knowledge and the management of California's natural resources*. Univ of California Press

Ansley, J.S., & Battles, J.J. (1998). Forest composition, structure, and change in an old growth mixed conifer forest in the northern Sierra Nevada. *Journal of the Torrey Botanical Society, 125*, 297-308

Arroyo, L.A., Pascual, C., & Manzanera, J.A. (2008). Fire models and methods to map fuel types: The role of remote sensing. *Forest Ecology and Management, 256*, 1239-1252

Barbour, M.G., & Major, J. (1995). *Terrestrial Vegetation of California: New Expanded Edition*. Davis: California Native Plant Society

Barbour, R.J., Singleton, R., & Maguire, D.A. (2007). Evaluating forest product potential as part of planning ecological restoration treatments on forested landscapes. *Landscape and Urban Planning, 80*, 237-248

Beier, P., & Drennan, J.E. (1997). Forest structure and prey abundance in foraging areas of northern goshawks. *Ecological Applications, 7*, 564-571

Bergen, K., Goetz, S., Dubayah, R., Henebry, G., Hunsaker, C., Imhoff, M., Nelson, R., Parker, G., & Radeloff, V. (2009). Remote sensing of vegetation 3-D structure for biodiversity and habitat: Review and implications for lidar and radar spaceborne missions. *Journal of Geophysical Research: Biogeosciences, 114*

Bias, M.A., & Gutiérrez, R. (1992). Habitat associations of California spotted owls in the central Sierra Nevada. *The Journal of wildlife management, 56*, 584-595

Blakesley, J.A., Seamans, M.E., Conner, M.M., Franklin, A.B., White, G.C., Gutiérrez, R., Hines, J.E., Nichols, J.D., Munton, T.E., & Shaw, D.W. (2010). Population dynamics of spotted owls in the Sierra Nevada, California. *Wildlife Monographs, 174*, 1-36

Breusch, T.S., & Pagan, A.R. (1979). A simple test for heteroscedasticity and random coefficient variation. *Econometrica: Journal of the Econometric Society, 47*, 1287-1294

Brown, J.K. (1978). Weight and density of crowns of Rocky Mountain conifers. In. Ogden UT, USA: USDA Forest Service, Intermountain Forest and Range Experiment Station

Brown, J.K., & Johnston, C.M. (1976). Debris Prediction System. In. Missoula, MT, USA: USDA Forest Service, Intermountain Forest and Range Experiment Station

Burger, J., Gochfeld, M., Pletnikoff, K., Snigaroff, R., Snigaroff, D., & Stamm, T. (2008). Ecocultural attributes: evaluating ecological degradation in terms of ecological goods and services versus subsistence and tribal values. *Risk Analysis, 28*, 1261-1272

Chen, Q., Baldocchi, D., Gong, P., & Kelly, M. (2006). Isolating Individual Trees in a Savanna Woodland Using Small Footprint Lidar Data. *Photogrammetric Engineering & Remote Sensing, 72*, 923-932

Cheng, S. (2004). Forest Service research natural areas in California. *General Technical Report PSW-GTR-188. Pacific Southwest Research Station, Forest Service, U.S. Department of Agriculture, Albany, CA*

Chiono, L.A., O'Hara, K.L., De Lasaux, M.J., Nader, G.A., & Stephens, S.L. (2012). Development of Vegetation and Surface Fuels Following Fire Hazard Reduction Treatment. *Forests, 3*, 700-722

Clark, K.L., Skowronski, N., Hom, J., Duveneck, M., Pan, Y., Van Tuyl, S., Cole, J., Patterson, M., & Maurer, S. (2009). Decision support tools to improve the effectiveness of hazardous fuel reduction treatments in the New Jersey Pine Barrens. *International Journal of Wildland Fire, 18*, 268-277

Collins, B.M. (2013). personal communication. In. USFS Pacific Southwest Research Station

Collins, B.M., Kramer, H.A., Menning, K., Dillingham, C., Saah, D., Stine, P.A., & Stephens, S.L. (2013). Modeling hazardous fire potential within a completed fuel treatment network in the northern Sierra Nevada. *Forest Ecology and Management, 310*, 156-166

Collins, B.M., & Stephens, S.L. (2010). Stand-replacing patches within a 'mixed severity' fire regime: quantitative characterization using recent fires in a long-established natural fire area. *Landscape Ecology, 25*, 927-939

Coops, N.C., Hilker, T., Wulder, M.A., St-Onge, B., Newnham, G., Siggins, A., & Trofymow, J.A. (2007a). Estimating canopy structure of Douglas-fir forest stands from discrete-return LiDAR. *Trees, 21*, 295-310

Coops, N.C., Hilker, T., Wulder, M.A., St-Onge, B., Newnham, G., Siggins, A., & Trofymow, J.T. (2007b). Estimating canopy structure of Douglas-fir forest stands from discrete-return LiDAR. *Trees, 21*, 295-310

Cruz, M.G., & Alexander, M.E. (2010). Assessing crown fire potential in coniferous forests of western North America: a critique of current approaches and recent simulation studies. *International Journal of Wildland Fire, 19*, 377-398

Cruz, M.G., Alexander, M.E., & Wakimoto, R.H. (2003). Assessing canopy fuel stratum characteristics in crown fire prone fuel types of western North America. *International Journal of Wildland Fire, 12*, 39-50

Cruz, M.G., Alexander, M.E., & Wakimoto, R.H. (2004). Modeling the likelihood of crown fire occurrence in conifer forest stands. *Forest Science, 50*, 640-658

Davis, B., & Hendryx, M. (2004). *Plants and the people: the ethnobotany of the Karuk tribe*. Yreka, CA: Siskiyou County Museum

De'ath, G., & Fabricius, K. (2000). Classification and Regression Trees: A Powerful Yet Simple Technique for Ecological Data Analysis. *Ecology, 81*, 3178-3192

Dean, T.J., Cao, Q.V., Roberts, S.D., & Evans, D.L. (2009). Measuring heights to crown base and crown median with LiDAR in a mature, even-aged loblolly pine stand. *Forest Ecology and Management, 257*, 126-133

Department of Commerce (DOC), National Oceanic and Atmospheric Administration (NOAA), National Ocean Service (NOS), & (OCM), O.f.C.M. (2015). United States Interagency Elevation Inventory (USIEI). In. Charleston, SC: NOAA's Ocean Service, Office for Coastal Management (OCM)

Dixon, G.E. (2002). Essential FVS: A user's guide to the Forest Vegetation Simulator. In. Fort Collins, CO, USA: USDA-Forest Service, Forest Management Service Center

Dolanc, C.R., Safford, H.D., Thorne, J.H., & Dobrowski, S.Z. (2014). Changing forest structure across the landscape of the Sierra Nevada, CA, USA, since the 1930s. *Ecosphere, 5*, 1-26

Dubayah, R.O., & Drake, J.B. (2000). Lidar Remote Sensing for Forestry. *Journal of Forestry*

Ecological Restoration Institute (2013). The efficacy of hazardous fuel treatments: A rapid assessment of the economic and ecologic consequences of alternative hazardous fuel treatments: A summary document for policy makers. In. Northern Arizona University

Erdody, T.L., & Moskal, L.M. (2010). Fusion of LiDAR and imagery for estimating forest canopy fuels. *Remote Sensing of Environment, 114*, 725-737

Fernandes, P.M. (2009). Combining forest structure data and fuel modelling to classify fire hazard in Portugal. *Annals of Forest Science, 66*, 1-9

Finney, M.A., McHugh, C.W., & Grenfell, I.C. (2005). Stand- and landscape-level effects of prescribed burning on two Arizona wildfires. *Canadian Journal of Forest Research, 35*, 1714-1722

Forsman, E. (1995). Appendix A: Standardized protocols for gathering data on occupancy and reproduction in spotted owl demographic studies. 32-38 In: J. Lint, B. Noon, R. Anthony, E. Forsman, M. Raphael, M. Collopy, and E. Starkey. 1999. Northern spotted owl effectiveness monitoring plan for the Northwest Forest Plan. *U. S. Forest Service Gen. Tech. Rep. PNW-GTR-440*, 43p.

Fox, J., Bates, D., Firth, D., Friendly, M., Gorjanc, G., Graves, S., Heiberger, R., Monette, G., Nilsson, H., & Ogle, D. (2009). CAR: Companion to applied regression, R Package version 1.2-16. *Online at http://cran.r-project.org/web/packages/car/index.html*

Franklin, J.F., & Johnson, K.N. (2012). A restoration framework for federal forests in the Pacific Northwest. *Journal of Forestry, 110*, 429-439

Franklin, J.F., Spies, T.A., Van Pelt, R., Carey, A.B., Thornburgh, D.A., Berg, D.R., Lindenmayer, D.B., Harmon, M.E., Keeton, W.S., & Shaw, D.C. (2002). Disturbances and structural development of natural forest ecosystems with silvicultural implications, using Douglas-fir forests as an example. *Forest Ecology and Management, 155*, 399-423

Gallagher, C.V. (2010). Spotted Owl Home Range and Foraging Patterns Following Fuels-Reduction Treatments in the Northern Sierra Nevada, California. In: Masters thesis. University of California, Davis

García-Feced, C., Tempel, D.J., & Kelly, M. (2011). LiDAR as a tool to characterize wildlife habitat: California spotted owl nesting habitat as an example. *Journal of Forestry, 109*, 436-443

García, M., Danson, F.M., Riano, D., Chuvieco, E., Ramirez, F.A., & Bandugula, V. (2011a). Terrestrial laser scanning to estimate plot-level forest canopy fuel properties. *International Journal of Applied Earth Observation and Geoinformation, 13*, 636-645

García, M., Riaño, D., Chuvieco, E., Salas, J., & Danson, F.M. (2011b). Multispectral and LiDAR data fusion for fuel type mapping using Support Vector Machine and decision rules. *Remote Sensing of Environment, 115*, 1369-1379

González-Olabarria, J.-R., Rodríguez, F., Fernández-Landa, A., & Mola-Yudego, B. (2012). Mapping fire risk in the Model Forest of Urbión (Spain) based on airborne LiDAR measurements. *Forest Ecology and Management, 282*, 149-156

Greenwald, D.N., Crocker-Bedford, D.C., Broberg, L., Suckling, K.F., & Tibbitts, T. (2005). A review of northern goshawk habitat selection in the home range and implications for forest management in the western United States. *Wildlife Society Bulletin, 33*, 120-128

Gutiérrez, R., McKelvey, K., Noon, B., Steger, G., Call, D., LaHaye, W., Bingham, B., & Senser, J. (1992). Habitat relations of the California spotted owl, p. 79-98. In J. Verner, K. S. McKelvey, B. R. Noon, R. J. Gutiérrez, G. I. Gould Jr., and T W. Beck [tech. coordinators], The California Spotted Owl: a tech- nical assessment of its current status. In, *USDA For. Serv., Gen. Tech. Rep. PSW-GTR-133*. Albany, CA

Hall, S.A., & Burke, I.C. (2006). Considerations for characterizing fuels as inputs for fire behavior models. *Forest Ecology and Management, 227*, 102-114

Hall, S.A., Burke, I.C., Box, D.O., Kaufmann, M.R., & Stoker, J.M. (2005). Estimating stand structure using discrete-return lidar: an example from low density, fire prone ponderosa pine forests. *Forest Ecology and Management, 208*, 189-209

Harling, W., & Tripp, B. (2014). Western Klamath Restoration Partnership: A Plan for Restoring Fire Adapted Landscapes. *Western Klamath Restoration Partnership*, 57 pp.

Herger, W., & Feinstein, D. (1998). Herger-Feinstein Quincy Library Group forest recovery Act. In, *105th Congress 1st Session HR* (p. 1028). Washington, DC, USA: Department of the Interior and Related Agencies Appropriations Act, Section 401; U.S. Congress

Hessburg, P.F., Agee, J.K., & Franklin, J.F. (2005). Dry forests and wildland fires of the inland Northwest USA: Contrasting the landscape ecology of the pre-settlement and modern eras. *Forest Ecology and Management, 211*, 117-139

Hirsch, K., & Martell, D. (1996). A review of initial attack fire crew productivity and effectiveness. *International Journal of Wildland Fire, 6*, 199-215

Hoiem, D., Efros, A.A., & Hebert, M. (2008). Putting objects in perspective. *International Journal of Computer Vision, 80*, 3-15

Hollenbeck, J.P., Saab, V.A., & Frenzel, R.W. (2011). Habitat suitability and nest survival of white-headed woodpeckers in unburned forests of Oregon. *The Journal of wildlife management, 75*, 1061-1071

Hudak, A.T., Crookston, N.L., Evans, J.S., Falkowski, M.J., Smith, A.M.S., & Gessler, P. (2006). Regression modeling and mapping of coniferous forest basal area and tree density from discrete-return LiDAR and multispectral satellite data. *Canadian Journal of Remote Sensing, 32*, 126-138

Hudak, A.T., Crookston, N.L., Evans, J.S., Hall, D.E., & Falkowski, M.J. (2008). Nearest neighbor imputation of species-level, plot-scale forest structure attributes from LiDAR data. *Remote Sensing of Environment, 112*, 2232-2245

Hudak, A.T., Strand, E.K., Vierling, L.A., Byrne, J.C., Eitel, J.U., Martinuzzi, S., & Falkowski, M.J. (2012). Quantifying aboveground forest carbon pools and fluxes from repeat LiDAR surveys. *Remote Sensing of Environment, 123*, 25-40

Hummel, S., & Lake, F. (2015). Forest Site Classification for Cultural Plant Harvest by Tribal Weavers Can Inform Management. *Journal of Forestry, 113*, 30-39

Hunter, J.E., Gutiérrez, R.J., & Franklin, A.B. (1995). Habitat configuration around spotted owl sites in northwestern California. *The Condor, 97*, 684-693

Husari, S., Nichols, H.T., Sugihara, N.G., & Stephens, S.L. (2006a). Fire and fuel management. *Fire in California's Ecosystems* (pp. 444-465). Berkeley, CA: University of California Press

Husari, S., Nichols, T.H., Sugihara, N.G., & Stephens, S.L. (2006b). Fire and Fuel Management. (pp. 444-465). Berkeley: University of California Press

Hyyppa, H., Inkinen, M., & Engdahl, M. (2000). Accuracy comparison of various remote sensing data sources in the retrieval of forest stand attributes*, 128*, 109-120

Hyyppa, J., Kelle, O., Lehikoinen, M., & Inkinen, M. (2001). A segmentation-based method to retrieve stem volume estimates from 3-D tree height models produced by laser scanners. *IEEE Transactions on Geoscience and Remote Sensing, 39*, 969-975

Isenburg, M. (2011). LAStools—efficient tools for LiDAR processing. *Online at http://lastools.org*

Jakubowski, M., Li, W., Guo, Q., & Kelly, M. (2013a). Delineating Individual Trees from Lidar Data: A Comparison of Vector- and Raster-based Segmentation Approaches. *Remote Sensing, 5*, 4163-4186

Jakubowski, M.K., Guo, Q., Collins, B., Stephens, S., & Kelly, M. (2013b). Predicting Surface Fuel Models and Fuel Metrics Using Lidar and CIR Imagery in a Dense, Mountainous Forest. *Photogrammetric Engineering and Remote Sensing, 79*, 37-49

Jakubowski, M.K., Guo, Q., & Kelly, M. (2013c). Tradeoffs between lidar pulse density and forest measurement accuracy. *Remote Sensing of Environment, 130*, 245-253

Jensen, J., Humes, K., Vierling, L., & Hudak, A. (2008). Discrete return lidar-based prediction of leaf area index in two conifer forests. *Remote Sensing of Environment, 112*, 3947-3957

Johnson, M.C., Kennedy, M.C., & Peterson, D.L. (2011). Simulating fuel treatment effects in dry forests of the western United States: testing the principles of a fire-safe forest. *Canadian Journal of Forest Research, 41*, 1018-1030

Kane, V.R., Bakker, J.D., McGaughey, R.J., Lutz, J.A., Gersonde, R.F., & Franklin, J.F. (2010). Examining conifer canopy structural complexity across forest ages and elevations with LiDAR data. *Canadian Journal of Forest Research, 40*, 774-787

Kane, V.R., Cansler, C.A., Povak, N.A., Kane, J.T., McGaughey, R.J., Lutz, J.A., Churchill, D.J., & North, M.P. (2015). Mixed severity fire effects within the Rim fire: Relative importance of local climate, fire weather, topography, and forest structure. *Forest Ecology and Management, 358*, 62-79

Kane, V.R., Lutz, J.A., Roberts, S.L., Smith, D.F., McGaughey, R.J., Povak, N.A., & Brooks, M.L. (2013). Landscape-scale effects of fire severity on mixed-conifer and red fir forest structure in Yosemite National Park. *Forest Ecology and Management, 287*, 17-31

Kane, V.R., North, M.P., Lutz, J.A., Churchill, D.J., Roberts, S.L., Smith, D.F., McGaughey, R.J., Kane, J.T., & Brooks, M.L. Assessing fire effects on forest spatial structure using a fusion of Landsat and airborne LiDAR data in Yosemite National Park. *Remote Sensing of Environment*, In Press

Keane, J. (2015). personal communication. In. USFS Pacific Southwest Research Station

Keane, J.J. (2014). California spotted owl: Scientific considerations for forest planning. *Gen. Tech. Rep. PSW-GTR-247. Albany, CA: U.S. Department of Agriculture, Forest Service, Pacific Southwest Research Station, Chap. 7.2*, 437-467

Kelly, M., & Di Tommaso, S. (2015). Mapping forests with Lidar provides flexible, accurate data with many uses. *California Agriculture, 69*, 14-20

Kenward, R.E. (2000). *A manual for wildlife radio tagging*. Academic Press

Knapp, E.E., Skinner, C.N., North, M.P., & Estes, B.L. (2013). Long-term overstory and understory change following logging and fire exclusion in a Sierra Nevada mixed-conifer forest. *Forest Ecology and Management, 310*, 903-914

Kramer, H.A., Collins, B.M., Gallagher, C.V., Keane, J., Kelly, M., & Stephens, S.L. (in review). Accessible LiDAR: estimating large tree density for habitat identification. *Ecosphere: in review*

Kramer, H.A., Collins, B.M., Kelly, M., & Stephens, S.L. (2014). Quantifying Ladder Fuels: A New Approach Using LiDAR. *Forests, 5*, 1432-1453

Laes, D., Reutebuch, S., McGaughey, R., & Mitchell, B. (2011). Guidelines to estimate forest inventory parameters from lidar and field plot, companion document to the advanced lidar applications—forest inventory modeling class

Lake, F.K. (2013). Historical and cultural fires, tribal management and research issue in Northern California: Trails, fires and tribulations. *Interdisciplinary Studies in the Humanities, 5*, 22p

Larson, A.J., & Churchill, D. (2012). Tree spatial patterns in fire-frequent forests of western North America, including mechanisms of pattern formation and implications for designing fuel reduction and restoration treatments. *Forest Ecology and Management, 267*, 74-92

Lee, A.C., & Lucas, R.M. (2007). A LiDAR-derived canopy density model for tree stem and crown mapping in Australian forests. *Remote Sensing of Environment, 111*, 493-518

Lefsky, M.A., Cohen, W.B., Acker, S.A., Parker, G.G., Spies, T.A., & Harding, D. (1999). Lidar Remote Sensing of the Canopy Structure and Biophysical Properties of Douglas-Fir Western Hemlock Forests. *Remote Sensing of Environment, 70*, 339-361

Lefsky, M.A., Cohen, W.B., Parker, G.G., & Harding, D.J. (2002). Lidar Remote Sensing for Ecosystem Studies. *Bioscience, 52*, 19-30

Li, W., Guo, Q., Jakubowski, M.K., & Kelly, M. (2012). A New Method for Segmenting Individual Trees from the Lidar Point Cloud. *Photogrammetric Engineering & Remote Sensing, 78*, 75-84

Linn, R., Reisner, J., Colman, J.J., & Winterkamp, J. (2002). Studying wildfire behavior using FIRETEC. *International Journal of Wildland Fire, 11*, 233-246

Long, J.W., Quinn-Davidson, L., Goode, R.W., Lake, F.K., & Skinner, C.N. (2015). Restoring California black oak to support tribal values and wildlife. *Proceedings of the 7th California Oak Symposium: Managing Oak Woodlands in a Dynamic World. Gen. Tech. Rep. PSW-GTR-251. Albany, CA: U.S. Department of Agriculture, Forest Service, Pacific Southwest Research Station*, 113-122

Lumley, T., & Miller, A. (2009). Leaps: regression subset selection. R package version 2.9. *Online at http://CRAN.R-project.org/package=leaps*

Lutz, J., Van Wagtendonk, J., & Franklin, J. (2009). Twentieth-century decline of large-diameter trees in Yosemite National Park, California, USA. *Forest Ecology and Management, 257*, 2296-2307

Martinuzzi, S., Vierling, L.A., Gould, W.A., Falkowski, M.J., Evans, J.S., Hudak, A.T., & Vierling, K.T. (2009). Mapping snags and understory shrubs for a LiDAR-based assessment of wildlife habitat suitability. *Remote Sensing of Environment, 113*, 2533-2546

McAlpine, R., & Hobbs, M. (1994). Predicting the height to live crown base in plantations of four boreal forest species. *International Journal of Wildland Fire, 4*, 103-106

McDermid, G.J., Franklin, S.E., & LeDrew, E.F. (2005). Remote sensing for large-area habitat mapping. *Progress in Physical Geography, 29*, 449-474

McGaughey, R. (2012). FUSION/LDV: Software for LIDAR Data Analysis and Visualization, Version 3.01. In. Seattle, WA, USA: USDA Forest Service, Pacific Northwest Research Station, University of Washington

Menning, K.M., & Stephens, S.L. (2007). Fire climbing in the forest: a semiqualitative, semiquantitative approach to assessing ladder fuel hazards. *Western Journal of Applied Forestry, 22*, 88-93

Miller, J., Skinner, C., Safford, H., Knapp, E.E., & Ramirez, C. (2012). Trends and causes of severity, size, and number of fires in northwestern California, USA. *Ecological Applications, 22*, 184-203

Miller, J.D., Safford, H.D., Crimmins, M., & Thode, A.E. (2009). Quantitative Evidence for Increasing Forest Fire Severity in the Sierra Nevada and Southern Cascade Mountains, California and Nevada, USA. *Ecosystems, 12*, 16-32

Mitsopoulos, I., & Dimitrakopoulos, A. (2014). Estimation of canopy fuel characteristics of Aleppo pine (Pinus halepensis Mill.) forests in Greece based on common stand parameters. *European Journal of Forest Research, 133*, 73-79

Mitsopoulos, I.D., & Dimitrakopoulos, A.P. (2007). Canopy fuel characteristics and potential crown fire behavior in Aleppo pine (Pinus halepensis Mill.) forests. *Annals of Forest Science, 64*, 287-299

Moen, C.A., & Gutiérrez, R. (1997). California spotted owl habitat selection in the central Sierra Nevada. *The Journal of wildlife management, 61*, 1281-1287

Moghaddas, J.J., Collins, B.M., Menning, K., Moghaddas, E.E.Y., & Stephens, S.L. (2010). Fuel treatment effects on modeled landscape-level fire behavior in the northern Sierra Nevada. *Canadian Journal of Forest Research, 40*, 1751-1765

Moghaddas, J.J., & Craggs, L. (2007). A fuel treatment reduces fire severity and increases suppression efficiency in a mixed conifer forest. *International Journal of Wildland Fire, 16*, 673-678

Moody, T.J., Fites-Kaufman, J., & Stephens, S.L. (2006). Fire history and climate influences from forests in the northern Sierra Nevada, USA. *Fire Ecology, 2*, 115-141

Morsdorf, F., Kotz, B., Meier, E., Itten, K., & Allgower, B. (2006). Estimation of LAI and fractional cover from small footprint airborne laser scanning data based on gap fraction. *Remote Sensing of Environment, 104*, 50-61

Mutlu, M., Popescu, S., Stripling, C., & Spencer, T. (2008). Mapping surface fuel models using lidar and multispectral data fusion for fire behavior. *Remote Sensing of Environment, 112*, 274-285

Næsset, E., & Bjerknes, K.-O. (2001). Estimating tree heights and number of stems in young forest stands using airborne laser scanner data. *Remote Sensing of Environment, 78*, 328-340

Norgaard, K.M. (2014). The Politics of Fire and the Social Impacts of Fire Exclusion on the Klamath. *Humboldt Journal of Social Relations*, 77-101

OpenTopography (2016). OpenTopography: High-Resolution Topography Data and Tools. In. San Diego Supercomputer Center, University of California San Diego, La Jolla, CA

Ottmar, R.D., Vihnanek, R.E., & Wright, C.S. (1998). *Stereo Photo Series for Quantifying Natural Fuels, Volume 1: Mixed-conifer with Mortality, Western Juniper, Sagebrush, and Grassland Types in the Interior Pacific Northwest*. US National Wildfire Coordinating Group, National Interagency Fire Center

Pollet, J., & Omi, P.N. (2002). Effect of thinning and prescribed burning on crown fire severity in ponderosa pine forests. *International Journal of Wildland Fire, 11*, 1-10

Popescu, S.C. (2007). Estimating biomass of individual pine trees using airborne lidar. *Biomass and Bioenergy, 31*, 646-655

Popescu, S.C., Wynne, R.H., & Nelson, R.F. (2003). Measuring individual tree crown diameter with lidar and assessing its influence on estimating forest volume and biomass. *Canadian Journal of Remote Sensing, 29*, 564-577

Popescu, S.C., & Zhao, K. (2008). A voxel-based lidar method for estimating crown base height for deciduous and pine trees. *Remote Sensing of Environment, 112*, 767-781

Prichard, S.J., Sandberg, D.V., Ottmar, R.D., Eberhardt, E., Andreu, A., Eagle, P., & Swedin, K. (2013). Fuel Characteristic Classification System version 3.0: technical documentation

Quantum Spatial (2015). Lower Klamath Watersheds LiDAR & Digital Imagery: Technical Data Report Summary. In (p. 42pp.)

R Core Team (2014). R: A Language and Environment for Statistical Computing. In. Vienna, Austria: R Foundation for Statistical Computing

R Development Core Team (2008). R: A language and environment for statistical computing. In. Vienna, Austria: R Foundation for Statistical Computing

Raymond, C.L., & Peterson, D.L. (2005). Fuel treatments alter the effects of wildfire in a mixed-evergreen forest, Oregon, USA. *Canadian Journal of Forest Research, 35*, 2981-2995

Rebain, S.A. (2010 (revised December 18, 2012)). The Fire and Fuels Extension to the Forest Vegetation Simulator: Updated Model Documentation. In. Fort Collins, CO, USA: USDA Forest Service Internal Report, Forest Management Service Center

Reinhardt, E., Lutes, D., & Scott, J. (2006a). FuelCalc: A method for estimating fuel characteristics. *Fuels Management-How to Measure Success: Conference Proceedings. 2006 28-30 March; Portland, OR.* Fort Collins, CO: Proceedings RMRS-P-41; USDA Forest Service, Rocky Mountain Research Station

Reinhardt, E., Scott, J., Gray, K., & Keane, R. (2006b). Estimating canopy fuel characteristics in five conifer stands in the western United States using tree and stand measurements. *Canadian Journal of Forest Research, 36*, 2803-2814

Riaño, D. (2003). Modeling airborne laser scanning data for the spatial generation of critical forest parameters in fire behavior modeling. *Remote Sensing of Environment, 86*, 177-186

Riaño, D., Chuvieco, E., Condés, S., González-Matesanz, J., & Ustin, S.L. (2004a). Generation of crown bulk density for Pinus sylvestris L. from lidar. *Remote Sensing of Environment, 92*, 345-352

Riaño, D., Chuvieco, E., Ustin, S.L., Salas, J., Rodríguez-Pérez, J.R., Ribeiro, L.M., Viegas, D.X., Moreno, J.M., & Fernández, H. (2007). Estimation of shrub height for fuel-type mapping combining airborne LiDAR and simultaneous color infrared ortho imaging. *International Journal of Wildland Fire, 16*, 341-341

Riaño, D., Valladares, F., Condés, S., & Chuvieco, E. (2004b). Estimation of leaf area index and covered ground from airborne laser scanner (Lidar) in two contrasting forests. *Agricultural and Forest Meteorology, 124*, 269-275

Ruiz, L.A., Hermosilla, T., Mauro, F., & Godino, M. (2014). Analysis of the Influence of Plot Size and LiDAR Density on Forest Structure Attribute Estimates. *Forests, 5*, 936-951

Safford, H.D., Schmidt, D.A., & Carlson, C.H. (2009). Effects of fuel treatments on fire severity in an area of wildland–urban interface, Angora Fire, Lake Tahoe Basin, California. *Forest Ecology and Management, 258*, 773-787

Safford, H.D., Stevens, J.T., Merriam, K., Meyer, M.D., & Latimer, A.M. (2012). Fuel treatment effectiveness in California yellow pine and mixed conifer forests. *Forest Ecology and Management, 274*, 17-28

Sando, R.W., & Wick, C.H. (1972). A method of evaluating crown fuels in forest stands. In: USDA Forest Service

Schoenherr, A.A. (1992). *A Natural History of California*. Berkeley: University of California Press

Schomaker, M.E., Zarnoch, S.J., Bechtold, W.A., Latelle, D.J., Burkman, W.G., & Cox, S.M. (2007). Crown-condition classification: a guide to data collection and analysis. *Gen. Tech. Rep. SRS–102. Asheville, NC: U.S. Department of Agriculture, Forest Service, Southern Research Station*, 78 pp.

Scott, J.H., & Reinhardt, E.D. (2001). Assessing crown fire potential by linking models of surface and crown fire behavior. In. Fort Collins, CO: USDA Forest Service, Rocky Mountain Research Station

Seavy, N.E., Viers, J.H., & Wood, J.K. (2009). Riparian bird response to vegetation structure: a multiscale analysis using LiDAR measurements of canopy height. *Ecological applications : a publication of the Ecological Society of America, 19*, 1848-1857

Selvarajan, S., Mohamed, A., & White, T. (2009). Assessment of Geospatial Technologies for Natural Resource Management in Florida. *Journal of Forestry, 107*, 242-249

Shapiro, S.S., & Wilk, M.B. (1965). An analysis of variance test for normality (complete samples). *Biometrika*, 591-611

Skinner, C.N. (1995). Change in spatial characteristics of forest openings in the Klamath Mountains of northwestern California, USA. *Landscape Ecology, 10*, 219-228

Skinner, C.N., Taylor, A.H., & Agee, J.K. (2006). Klamath mountains bioregion. In N.S. Sugihara, J.W. Van Wagtendonk, J. Fites-Kaufman, K.E. Shaffer, & A. Thode (Eds.), *Fire in California ecosystems* (pp. 170-194). Berkeley, CA: University of California Press

Skowronski, N., Clark, K., Nelson, R., Hom, J., & Patterson, M. (2007). Remotely sensed measurements of forest structure and fuel loads in the Pinelands of New Jersey. *Remote Sensing of Environment, 108*, 123-129

Snider, G., Daugherty, P., & Wood, D. (2006). The irrationality of continued fire suppression: an avoided cost analysis of fire hazard reduction treatments versus no treatment. *Journal of Forestry, 104*, 431-437

Stephens, S.L., Bigelow, S.W., Burnett, R.D., Collins, B.M., Gallagher, C.V., Keane, J., Kelt, D.A., North, M.P., Roberts, L.J., & Stine, P.A. (2014). California spotted owl, songbird, and small mammal responses to landscape fuel treatments. *Bioscience, 64*, 893-906

Stephens, S.L., Collins, B.M., & Roller, G. (2012). Fuel treatment longevity in a Sierra Nevada mixed conifer forest. *Forest Ecology and Management, 285*, 204-212

Stephens, S.L., Fry, D.L., & Franco-Vizcaíno, E. (2008). Wildfire and spatial patterns in forests in northwestern Mexico: the United States wishes it had similar fire problems. *Ecology & Society, 13*

Stephens, S.L., Moghaddas, J.J., Edminster, C., Fiedler, C.E., Haase, S., Harrington, M., Keeley, J.E., Knapp, E.E., McIver, J.D., & Metlen, K. (2009). Fire treatment effects on vegetation structure, fuels, and potential fire severity in western US forests. *Ecological Applications, 19*, 305-320

Strom, B.A., & Fulé, P.Z. (2007). Pre-wildfire fuel treatments affect long-term ponderosa pine forest dynamics. *International Journal of Wildland Fire, 16*, 128-138

Taylor, A.H., & Skinner, C.N. (1998). Fire history and landscape dynamics in a late-successional reserve, Klamath Mountains, California, USA. *Forest Ecology and Management, 111*, 285-301

Team, H.I. (2011). Herger Feinstein Quincy Library Group Pilot Project: HFQLG Monitoring. In

Thompkins, R. (2013). personal communication. In. Plumas National Forest

U.S. Department of the Interior, U.S.G.S. (2016). EarthExplorer. In

US Forest Service (2001). Sierra Nevada Forest Plan Amendment: Final Environmental Impact Statement, Vol. 1–6. In: USDA Forest Service Pacific Southwest Region, Vallejo, California, USA

US Forest Service (2004). Sierra Nevada Forest Plan Amendment, Final Supplemental Environmental Impact Statement. In: US Department of Agriculture Forest Service Region 5, Vallejo, California, USA

US Forest Service (2015). The Rising Cost of Fire Operations: Effects on the Forest Service's Non-Fire Work. *US Department of Agriculture*, 16p.

USDA Forest Service - Pacific Southwest Region - Remote Sensing Lab (2010). CalvegTiles_Ecoregions07_4. In. McClellan, CA: Remote Sensing Lab

USDA Forest Service Plumas National Forest, M.H.R.D. (2003). Meadow Valley Defensible Fuel Profile Zone and Group Selection Project Environmental Assessment. In. Quincy, CA: USDA Forest Service Plumas National Forest, Mt. Hough Ranger District

Vaillant, N.M., Noonan-Wright, E., Dailey, S., Ewell, C., & Reiner, A. (2013). Effectiveness and longevity of fuel treatments in coniferous forests across California. *JFSP Research Project Reports, Paper 57*, 29p.

VESTRA (2003). HFQLG Vegetation Mapping Project Final Report. In. Redding, CA, USA: VESTRA Resources, Inc.

Vierling, K.T., Vierling, L.A., Gould, W.A., Martinuzzi, S., & Clawges, R.M. (2008). Lidar: shedding new light on habitat characterization and modeling. *Frontiers in Ecology and the Environment, 6*, 90-98

Wang, Y., Weinacker, H., & Koch, B. (2008). A lidar point cloud based procedure for vertical canopy structure analysis and 3D single tree modelling in forest. *Sensors, 8*, 3938-3951

White, G., & Garrott, R. (1990). *Analysis of wildlife radio-tracking data*. San Diego, California, USA: Academic Press

Whittaker, R.H. (1960). Vegetation of the Siskiyou mountains, Oregon and California. *Ecological Monographs, 30*, 279-338

Wilson, J., & Baker, P. (1998). Mitigating fire risk to late-successional forest reserves on the east slope of the Washington Cascade Range, USA. *Forest Ecology and Management, 110*, 59-75

Wing, B.M., Ritchie, M.W., Boston, K., Cohen, W.B., Gitelman, A., & Olsen, M.J. (2012). Prediction of understory vegetation cover with airborne lidar in an interior ponderosa pine forest. *Remote Sensing of Environment, 124*, 730-741

Wing, M.G., Eklund, A., & Sessions, J. (2010). Applying LiDAR technology for tree measurements in burned landscapes. *International Journal of Wildland Fire, 19*, 104-114

Wright, C.S., Ottmar, R.D., & Vihnanek, R.E. (2007). *Stereo photo series for quantifying natural fuels. Volume VIII: Hardwood, Pitch Pine, and Red Spruce/Balsam Fir types in the Northeastern United States*. US National Wildfire Coordinating Group, National Interagency Fire Center

Zhao, K., Popescu, S., Meng, X., Pang, Y., & Agca, M. (2011). Characterizing forest canopy structure with lidar composite metrics and machine learning. *Remote Sensing of Environment, 115*, 1978-1996

Zielinski, W.J. (2014). The forest carnivores: marten and fisher. *Gen. Tech. Rep. PSW-GTR-247. Albany, CA: U.S. Department of Agriculture, Forest Service, Pacific Southwest Research Station, Chap. 7.1*, 393-435

Zielinski, W.J., Dunk, J.R., Yaeger, J.S., & LaPlante, D.W. (2010). Developing and testing a landscape-scale habitat suitability model for fisher (Martes pennanti) in forests of interior northern California. *Forest Ecology and Management, 260*, 1579-1591